

**A physiological study on a commercial reef fish to quantify the relationship between exploitation and climate change resilience**



Dissertation submitted in fulfilment of the requirements for the degree of

DOCTOR OF PHILISOPHY

of

RHODES UNIVERSITY

By

**Murray Ian Duncan**

05/09/2018

Supervisors: Professor WM Potts, Dr NC James and Dr AE Bates

# Table of contents

Preface .....	v
Acknowledgements .....	viii
Declaration .....	ix
List of figures .....	x
List of tables .....	xviii
<b>Abstract .....</b>	<b>1</b>
<b>1 Chapter 1 General introduction: rationale behind this study.....</b>	<b>4</b>
1.1 Brief conceptual background.....	5
1.2 A conservation physiological approach .....	9
1.3 Climate change and fisheries exploitation .....	11
1.4 Aims of this thesis.....	12
<b>2 Chapter 2 Study area and species profile .....</b>	<b>15</b>
2.1 Study area .....	16
2.1.1 Climate change along the South African coastal zone .....	16
2.1.2 Sampling locations.....	18
2.2 Study species .....	24
<b>3 Chapter 3 Fishing targets high-performance metabolic phenotypes.....</b>	<b>29</b>
3.1 Introduction.....	30
3.2 Methods.....	32
3.2.1 Experimental set-up.....	32
3.2.2 Respirometers .....	33
3.2.3 Fish capture and husbandry.....	35
3.2.4 Experimental procedure.....	36

3.2.5	Data preparation .....	38
3.2.6	Statistical analysis .....	40
3.3	Results.....	41
3.3.1	Mass correcting $MO_2$ data.....	41
3.3.2	Standard Metabolic and Maximum Metabolic Rates (SMR and MMR) .....	43
3.3.3	Aerobic Scope (AS) .....	44
3.3.4	Aerobic Scope (AS) variability.....	45
3.3.5	Cold shock.....	46
3.4	Discussion .....	47
<b>4</b>	<b>Chapter 4 Upwelling intensity and post-spawning sea temperature drive the growth of <i>Chrysolephus laticeps</i>.....</b>	<b>51</b>
4.1	Introduction.....	52
4.2	Methods.....	55
4.2.1	Otolith collection and preparation.....	55
4.2.2	Otolith increment measurements .....	56
4.2.3	Environmental data.....	57
4.2.4	Modelling approach.....	59
4.3	Results.....	62
4.3.1	Data preparation .....	62
4.3.2	Protected population (TNP) mixed modelling results.....	65
4.3.3	Exploited (PE) mixed modelling results.....	67
4.3.4	Base model comparisons.....	69
4.3.5	Long-term trend in growth.....	70

4.4	Discussion .....	71
<b>5</b>	<b>Chapter 5 High temperatures and low oxygen availability constrain the edges of <i>C. laticeps</i> distribution by limiting metabolic potential .....</b>	<b>80</b>
5.1	Introduction .....	81
5.2	Methods.....	85
5.2.1	Metabolic index.....	85
5.2.2	Critical oxygen saturation.....	86
5.2.3	Data standardisation .....	87
5.2.4	Environmental and occurrence data.....	87
5.2.5	Distribution modelling.....	88
5.3	Results.....	89
5.3.1	Calibration of the metabolic index .....	89
5.3.2	Environmental and occurrence data.....	92
5.3.3	Species distribution modelling.....	93
5.4	Discussion .....	95
<b>6</b>	<b>Chapter 6 General discussion: synthesising research for current climate policy frameworks.....</b>	<b>102</b>
6.1	Overview.....	103
6.2	Incorporating physiological research to improve fisheries management in the Anthropocene.....	106
6.2.1	Background of marine climate policy in South Africa.....	106
6.2.2	Spatial plan of <i>C. laticeps</i> ' vulnerability to predicted climate change .....	108
6.2.3	Summary in management context.....	115
6.3	Caveats of this study.....	118

6.3.1	OCLTT critique .....	118
6.3.2	Plasticity and adaptability.....	119
6.3.3	Pseudoreplication .....	120
6.4	Future research .....	121
6.4.1	Recruitment .....	121
6.4.2	Multiple stressors .....	122
6.5	Conclusion .....	123
<b>7</b>	<b>Reference List .....</b>	<b>124</b>

## Preface

This thesis consists of a general introduction (Chapter 1); a study area and species profile chapter (Chapter 2) containing data analysis; three primary research chapters (Chapters 3, 4 and 5), and a general discussion chapter (Chapter 6) that contains further research and data analysis. The research chapters are written, where feasible, as stand-alone scientific publications. As such, there may be some overlap in ideas from chapter to chapter. Any repetition was limited by including the study area and species profile chapter (Chapter 2) and a single reference list at the end that represent all research chapters.

### **Additional outputs completed, or in the process of completion during this thesis:**

#### *Conference presentations:*

- Fisheries Society of British Isles, Exeter, UK – 2017
- Indo-Pacific Fish Conference, Tahiti, French Polynesia – 2017 – **Student prize winner**
- DIFS seminar series – 2016, 2017 – **Student prize winner x2**
- WIOMSA Symposium, Dar es Salaam, Tanzania – 2017 – **Student prize winner**

#### *Papers arising during this thesis either published, submitted, or in prep:*

- Bates AE, Helmuth B, Burrows MT, **Duncan MI** et al. 2018. Biologists ignore ocean weather at their peril. *NATURE*. 560: 299–301.
- Bates AE, **Duncan MI** et al. *in review*. Resilience in Marine Protected Areas and the ‘Protection Paradox’. *BIOLOGICAL CONSERVATION*.
- **Duncan MI**, Bates AE, James NC, Potts WM. *In prep*. Fisheries exploitation removes high-performance metabolic phenotypes.
- **Duncan MI**, Bates AE, James NC, Potts WM. *In prep*. Upwelling intensity and post-spawning sea temperature drives the growth of *Chrysolephus laticeps*.
- **Duncan MI**, Bates AE, James NC, Potts WM. *In prep*. High temperatures and low oxygen availability constrain the edges of *Chrysolephus laticeps*’ distribution by limiting metabolic potential.

*Students co-supervised:*

- Kyle Hewitt – BSc (Hons) – 2017 – Nelson Mandela University
- Mike Skeeles – BSc (Hons) – 2017 – Rhodes University
- Brett Pringle – BSc (Hons) – 2018 – Rhodes University
- Mike Skeeles – MSc – 2018 – Rhodes University

**Financial support was received from the following sources during this thesis:**

*Project funding*

- Rhodes University Sandisa Imbewu Fund

*Travel funding*

- Rhodes University PhD travel grant
- NRF KIC travel grant
- FSBI student bursary
- Indo-Pacific Fish Conference student bursary

*Personal funding*

- Rhodes University Prestigious Scholarship
- NRF Innovation PhD Scholarship
- Commonwealth Split-site Scholarship

**Institutional Support**

This thesis was submitted to fulfil the requirements for the degree of Doctor of Philosophy at Rhodes University. It formed part of the Aquatic Eco-Physiology Research Platform (AERP) at the South African Institute for Aquatic Biodiversity (SAIAB). Part of the thesis was supported by the University of Southampton and the National Oceanographic Centre (NOC) in the UK.

## **Contributions of others during this thesis:**

### *Construction, experiment preparation and technical support*

- Dave Drennan, Ndzaliseko Sangongo, Yusuf Ouardien, Judge Inglis, Alex Winkler, Justin Kemp

### *Fieldwork support*

- Dave Drennan, Richard Taylor, Judge Inglis, Didi

### *Laboratory experiments support*

- Jack Coupland

### *Otolith sectioning support*

- Dan Doran, Clive Trueman, Matthew Beverley-Smith

### *Statistical support*

- John Morrongiello, Ekaterina Popova, Horst Kaiser

### *Administrative support*

- Haroon Magera, Wendy Xibiya, Yvain Erasmus, Bulelwa Mangali

## **Ethics statement:**

All research activities were conducted under the Rhodes University Animal Ethics and Standards Council approval number: DIFS152015, and the Animal Use and Care Committee of the South African National Parks approval number: 004/16.

## Acknowledgements

I would like, foremost, to thank my supervisors, Dr Warren Potts, Dr Nikki James and Dr Amanda Bates for their support and guidance during this thesis. Warren, thank you for always taking the time to engage with my ideas; never saying no when I asked for something and the job. Nikki, thanks for sticking with me from my MSc, in 2011, up to now. Amanda, thank you so much for responding to that random email I sent two years ago, asking you to be my supervisor; you have made a huge impression on my research. I look forward to many future collaborations with all of you.

When doing research, one tends to ask for numerous favours from people often with nothing to offer in return. Thanks must therefore go to all the people mentioned in the preface for their contributions, which often involved going beyond their job profiles. I would also like to thank the South African National Parks and the Noordhoek Ski-boat Club for their assistance in facilitating fieldwork.

Thanks to my colleagues at the Department of Ichthyology and Fisheries Science for all the good times in between the work. Special mention must be made of Alex Winkler who has been on this journey with me from our first year, when we both came to Rhodes wanting to be abalone farmers.

This research would not be possible without funding. For financial contributions, I would like to thank Rhodes University, the NRF and the Commonwealth Scholarship Commission. It has been an amazing journey that literally took me all over the world, from Grahamstown to the National Oceanographic Centre in the UK and to conferences from Tanzania to French Polynesia.

Lastly, but most importantly, I would like to thank my mom, Michele, and my dad, Rob, for their support and encouragement over the years and for allowing me to study for ten years. Also, of course, my brother, Andrew, for always keeping things in perspective during the challenging times.

## Declaration

I, Murray Ian Duncan, hereby declare that the work described in this thesis was carried out in the Department of Ichthyology and Fisheries Science, Rhodes University, under the supervision of Professor WM Potts, Associate Professor AE Bates and Dr NC James. The components of this thesis comprise original work by the author and have not been submitted to any other university.

Signed:  \_\_\_\_\_

Date: 05/09/2018

## List of figures

- Figure 1.1:** Broad schematic diagram of how climate change can affect marine fish populations, the thought process behind the design of the research chapters (red arrows and boxes), and the questions (blue and green question marks) it hopes to answer: 1) assess climate resilience (green arrow and box) and 2) elucidate how exploitation and physiology may interact to influence climate change resilience (blue arrows and boxes)..... 13
- Figure 2.1:** Hourly sea temperature thermistor string data (19 m depth) (black points) from within the Tsitsikamma National Park Marine Protected Area during January 2003 with major upwelling/downwelling events indicated with black arrows, highlighting the range and rate of temperature change, and anomalous cold (blue arrow) and hot (red arrow) spells indicated..... 17
- Figure 2.2:** Map depicting the location of sampling areas (black arrows): Tsitsikamma National Park (TNP) Marine Protected Area (black outline) and Port Elizabeth (PE) in South Africa. Colours are MODIS Terra satellite sea surface temperatures depicting an upwelling event on 04-03-2010 taken from Smit et al. (2013). ..... 19
- Figure 2.3:** Daily sea temperature data from underwater temperature recorders at exploited (PE) (5 m depth) and protected (TNP) (10 m depth) sampling areas from December 2002–March 2003 indicating extreme thermal variability and synchrony between areas. .... 20
- Figure 2.4:** Monthly mean SST (a), yearly mean SST (b), year-to-year difference in mean SST (c) and modelled SST trend splines including the difference in SST trend spline (dashed black line with 95% confidence intervals shaded in grey) (d) for the AVHRR SST time series data for exploited (PE, red) and protected (TNP MPA, blue) sampling areas. .... 22
- Figure 2.5:** Standard deviation of monthly mean UTR sea temperature data (mean monthly SST stdev) for exploited (PE, red) and protected (TNP, blue) sampling areas..... 23

**Figure 2.6:** Time series of the random component of UTR data (random ts component (°C)) for exploited (PE, red) and protected (TNP, blue) sampling areas. .... 24

**Figure 2.7:** Adult and juvenile roman seabream *Chrysoblephus laticeps* (Valenciennes 1830). Photo credit: Coastal Fishes of southern Africa - Phil and Elaine Heemstra (South African Institute for Aquatic Biodiversity). .... 26

**Figure 2.8:** Spatial distribution of total commercial *C. laticeps* catch from 1985–present in relation to protected (TNP, black outline) and exploited (PE) sampling locations. Data obtained from the national marine linefish system (NMLS) at DAFF. .... 27

**Figure 3.1:** Experimental room housing four respirometers with each circulation loop connected to a peristaltic pump from where oxygen concentrations were measured. .... 33

**Figure 3.2:** Design of intermittent flow respirometers. Flush pump inlet was connected to a pump set on a 15 min flush/5 min wait protocol. The recirculation pump continuously moved water through the recirculation loop via a peristaltic pump connected in line to an oxygen sensor and maintained mixing in the chamber. Check valves ensured no oxygen leakage during measurement periods. .... 34

**Figure 3.3:** Test specimen housed within a respirometer during an experimental trial. .... 37

**Figure 3.4:** Example of an intermittent flow respirometry dataset. Each decline in oxygen concentration ( $O_2(\text{mg. L}^{-1})$ ) represents the five-minute measurement period and increases in oxygen concentration represent the fifteen-minute flushing period over a time period measured in seconds (sec). The steep decline in oxygen concentration represents the measurement period directly after maximum metabolic rate elicitation. .... 38

**Figure 3.5:** Mass correcting SMR data process showing raw SMR data ( $\text{SMR } (O_2.\text{min}^{-1})$ ) per temperature (a) regression of the natural logarithm of temperature-corrected SMR ( $\ln(\text{SMR} \cdot e^{E/kT})$ ) against the natural logarithm of mass ( $\ln(\text{Mass}(\text{kg}))$ ) (b) and mass-corrected SMR data ( $\text{SMR } (O_2.\text{min}^{-1})$ ) per temperature used for the analysis (c)... 41

- Figure 3.6:** Mass correcting MMR data process showing raw MMR data (MMR (O<sub>2</sub>.min<sup>-1</sup>)) per temperature (a) regression of the natural logarithm of temperature-corrected MMR (ln(MMR.e<sup>E/kT</sup>)) against the natural logarithm of mass (ln(Mass(kg)) (b) and mass-corrected MMR data (MMR (O<sub>2</sub>.min<sup>-1</sup>)) per temperature used for the analysis (c).. 42
- Figure 3.7:** GLS model fits per exploited (red) and protected (blue) sampling populations for standard metabolic rate (SMR) (a) and maximum metabolic rate (MMR) (b) across test temperatures with shaded areas representing 95% confidence interval..... 44
- Figure 3.8:** GLS model fits per exploited (red) and protected (blue) sampling populations for absolute aerobic scope (AS) across test temperatures with shaded areas representing 95% confidence interval..... 45
- Figure 3.9:** Variance structure of the absolute aerobic scope generalised least squares model (AS variance str) partitioned by temperature and population for exploited (red) and protected (blue) populations. .... 45
- Figure 3.10:** Linear temperature dependence of the natural logarithm of mass-corrected standard metabolic rate (*lnSMR*) and temperature (*1/kT*), where temperature (*T*) is measured in Kelvin and *k* is the Boltzmann constant, for exploited (red) and protected (blue) sampling populations. Corresponding test temperature in °Celsius is indicated in brackets. The regression line was derived using temperatures 39.05 to 40.70 (24 to 12 °C) and predicted towards 41.28 (8 °C) for the exploited population as no breakpoint relationship was measurable..... 46
- Figure 4.1:** Sectioned *C. laticeps* otolith showing opaque (light) and translucent (dark) annual growth bands marked with dots between which increment widths were measured.56
- Figure 4.2:** Example of how integrated cooling (IC, light grey shading) and integrated anomaly (IA, dark grey shading) were calculated (area of shaded regions) for extreme (> 2 °C) upwelling anomalies following (Tapia et al. 2009). Points represent daily temperature anomalies calculated as departures from a 30-day moving average..... 58
- Figure 4.3:** Raw otolith increment width measurement (mm) per exploited (red, PE) and protected (blue, TNP) sampling populations across all years (a) and ages (b). Each

point represents a single width measurement and successive width measurements from the same individual are connected with a solid line. ....	62
<b>Figure 4.4:</b> Relationship between otolith length (mm) along the measurement plane for 4+ year olds and fish fork length (cm) from the 62 <i>C. laticeps</i> otoliths used in this study. ....	63
<b>Figure 4.5:</b> Linear relationship (black line) between monthly (black dot) <i>in situ</i> sea surface temperatures on the surface (SANParks data) and temperatures at 12 m (a), 19 m (b), 27 m (c) and 35 m (d) depths (thermistor string data) (1994–2004). The 95% confidence intervals shaded grey .....	64
<b>Figure 4.6:</b> Time series of daily sea temperature measurements (dots) per depth from thermistor string data (12–37 m depths) and SANParks <i>in situ</i> data (0 m) from December 2002.....	65
<b>Figure 4.7:</b> Predicted growth of the protected (TNP) population of <i>C. laticeps</i> otolith increment (mm) at each age (solid blue line) with 95% confidence intervals shaded in blue (a) and annual growth variation after accounting for intrinsic effects represented by the Year random-effect conditional modes (solid blue line) +/- SE (shaded blue) for <i>C. laticeps</i> from 1962–2015 (b).....	67
<b>Figure 4.8:</b> Predicted growth (solid blue line) and 95% confidence intervals (shaded blue) of <i>C. laticeps</i> from protected (TNP) population across the sum of integrated cooling index per calendar growth year (CGY) (a), autumn temperature (b) and mean calendar growth year (CGY) temperature(c).....	67
<b>Figure 4.9:</b> Predicted growth of the exploited (PE) population of <i>C. laticeps</i> otolith increment (mm) at each age (solid red line) with 95% confidence intervals shaded in red (a) and annual growth variation after accounting for intrinsic effects represented by the Year random-effect conditional modes (solid red line) +/- SE (shaded red) for <i>C. laticeps</i> from 1999–2015 (b).....	68
<b>Figure 4.10:</b> Comparison of the ontogenetic decline in growth with age of <i>Chrysoblephus laticeps</i> (a) and the inter-annual variability in growth response (b) between exploited	

(red, PE) and protected (blue, TNP) sampling populations. Data was extracted from the best base model with no extrinsic fixed effects. .... 69

**Figure 4.11:** Predicted growth over time for *C. laticeps* otolith increment (mm) (solid blue line) with 95% confidence intervals shaded in blue for the protected (TNP) population. 70

**Figure 4.12:** Cumulative integrated cooling (IC) per calendar growth year (black points) with best-fit linear equation (black line) and 95% confidence intervals (shaded grey) depicting an increase in IC over time. .... 73

**Figure 4.13:** TNP annual mean autumn (Mar–May) *in situ* sea surface temperature time series (a) (block dots and solid line) and TNP cumulative integrated cooling (IC) time series (b) (black dots and solid line). Overall mean autumn sea temperature of 17.11 °C and cumulative IC of 81.4 (dashed lines) and years spanning protected (TNP, blue line) and exploited (PE, red line) biochronologies are indicated. .... 75

**Figure 4.14:** Predicted annual growth (solid dots) after accounting for intrinsic effects per mean autumn temperature of CGY for protected (a, blue) and exploited (b, red) populations. Curved lines represent aerobic scope from Chapter 3, dashed line is the temperature where aerobic scope is maximised, and the solid linear blue line is the fixed mean autumn temperature effect from model t4p. No extrinsic effect was identified for the exploited population. .... 77

**Figure 5.1:** Dataset demonstrating the determination of  $O_{2crit}$  for an individual specimen at a set temperature. Each circle represents a metabolic rate at an  $O_2$  saturation. The solid black line is SMR calculated as the 0.2 percentile of metabolic rates in normoxia (>70%). The solid red line is the linear relationship between metabolic rate and  $O_2$  saturation for MR below SMR. The intersection of both solid lines is the critical oxygen saturation (dotted blue line). .... 86

**Figure 5.2:** Power law relationship (black line) between mass (kg) and temperature normalised  $pO_{2crit}$  (Torr), indicating a mass scaling exponent of 0.155 for combined exploited (red points) and protected (blue points) populations. .... 90

**Figure 5.3:** Temperature effect on mass normalised critical oxygen partial pressure ( $pO_{2crit}$ ) per exploited (red) and protected (blue) populations. Points represent individual data points fit with the linear relationship (solid line) and 95% confidence interval (shaded) for each sampling population..... 90

**Figure 5.4:** Piecewise (12 °C) relationship between the natural logarithm of standardised mass-specific hypoxia tolerance ( $\ln(B^n \cdot pO_{2crit})$ ) and the inverse product of temperature (T in kelvin) and the Boltzmann constant ( $k_B$  in ev) for combined exploited and protected data. .... 91

**Figure 5.5:** Graphical representation of the metabolic index for *C. laticeps* across a matrix of temperature and oxygen saturations. .... 91

**Figure 5.6:** Spatial representation of *C. laticeps* occurrence data (blue dots) from 2000–2010 (a), mean bottom temperature (°C) between 2005–2010 (b), mean bottom oxygen concentration ( $mmol \cdot m^{-3}$ ) between 2005–2010 (c) and the mean metabolic index ( $\phi$ ) for *C. laticeps* between 2005–2010 (d) at depths less than -100 m below seas level. .... 93

**Figure 5.7:** Feature contribution (black dots) of depth cells (a) and minimum  $\phi$  cells (b) for all ten random forest reduced models. Depth thresholds for occurrence were between -72 and -15 metres below sea level (red dashed lines in (a)) taken as the x intercepts for  $y = 0$  of the quadratic relationship (solid red line) and minimum metabolic  $\phi$  threshold of 2.9 (red dashed lines (b)) taken as the 0.5 threshold of the logistic regression (solid blue line)..... 94

**Figure 5.8:** Modelled current (a) and future (b) distribution of *C. laticeps* based on the probability of occurrence among ten random forest projections on current and future changes in minimum metabolic index and predicted change in *C. laticeps* distribution (c) between current (2005–2010) and future (2095–2099) binary projections taken with 0.5 as the probability threshold of occurrence. .... 95

**Figure 5.9:** Current distribution from ten random forest models added together and occurrence threshold taken at 50% agreement between all ten models (a), minimum monthly  $\phi$

from ocean model 2005–2010 (b) and the historical and contemporary (1970–2016) occurrence data for *C. laticeps* from the NMLS of South Africa housed at DAFF (c).  
 ..... 98

**Figure 6.1:** Temperature range where 20% (grey shaded) and 10% (red shaded) of maximum (black dotted line) aerobic scope (red line) is maintained (a), and spatial representation of these metabolic thresholds applied to temperature data up to 2100 for minimum (b), maximum (c) and mean (d). ..... 109

**Figure 6.2:** Spatial representation of mean change in autumn temperature (March–May) from 2005–2010 to 2095–2100, indicating that autumn temperatures will increase by a minimum of 0.5 °C up to 4.43 °C around the coast of southern Africa. .... 110

**Figure 6.3:** Predicted distribution of *C. laticeps* for 2100 based on a 0.5 threshold of occurrence from the future ten random forest model runs (see Chapter 5). ..... 111

**Figure 6.4:** Total historical spatial commercial catch of *C. laticeps* against corresponding spatial mean current metabolic index ( $\phi$ ) calibrated for *C. laticeps* (a). Each point represents a grid location. Areas where the spatial mean of  $\phi$  is greater than the 3.5 threshold for 2095–2100 are indicated in blue (b). ..... 112

**Figure 6.5:** Conceptual diagram of the *GDMP* index showing the future (2100) spatial layers multiplied together to produce a final value. From top to bottom, binary transformed minimum monthly temperature (orange), binary transformed maximum monthly temperature (purple), binary transformed mean monthly temperature (green), change in mean autumn temperature (viridis colour scale), binary transformed predicted distribution (red) and binary transformed metabolic index production threshold (blue).  
 ..... 113

**Figure 6.6:** Predicted areas for optimum *C. laticeps* resilience up to 2100 based on growth, distribution, and metabolic responses (*GDMP*). ..... 114

**Figure 6.7:** Total commercial catch of *C. laticeps* from 1985–present in kg (a) and areas where *C. laticeps* is least likely to be affected by predicted climate change (dark blue) based on this research (b). ..... 116

**Figure 6.8:** Location of major Marine Protected Areas (shaded orange) in relation to areas where *C. laticeps* is predicted to be resilient to climate change (blue scale). MPAs not indicated through *C. laticeps*' distribution are Helderberg, Stilbaai and Sardinia Bay, which are small and/or unenforced. .... 118

## List of tables

- Table 2.1:** Approximate significance of spline functions for a single explanatory variable (Smooth term) of the GAMM model indicating the estimated degrees of freedom (edf), F-statistic (F-stat) with significant  $p$ -values highlighted in bold. .... 23
- Table 2.2:** Checklist of species considered and attributes deemed important for this research. Ticks indicate attribute present in species, crosses indicate attribute not present and N.A. indicates no data was available. .... 25
- Table 3.1:** Mean condition factor (CF) and standard error (SE), mean weight (weight (g)) and standard error (SE), and weight range in grams (g) for number of specimens (n) per sampling population used in this study. There was no significant difference in condition factor or mass of specimens between populations (one-tailed T-test,  $p$ -value > 0.05). .... 36
- Table 3.2:** Generalised least squares modelling results for SMR of *Chrysoblephus laticeps* from an exploited and a protected population, presented as a quadratic function of temperature (Temp), with exploitation/protection (population) as an interaction term. SE is standard error, AIC is Akaike information criterion, and significant  $p$ -values are highlighted in bold. .... 43
- Table 3.3:** Generalised least squares modelling results for MMR of *Chrysoblephus laticeps* from an exploited and a protected population, presented as a quadratic function of temperature (Temp), with exploitation/protection (Population) as an interaction term. SE is standard error, AIC is Akaike information criterion and significant  $p$ -values are highlighted in bold. .... 43
- Table 3.4:** Generalised least squares modelling results for aerobic scope (AS) of *Chrysoblephus laticeps* from an exploited and protected population, presented as a quadratic function of temperature (Temp), with exploitation/protection (Population) as an interaction term. SE is standard error, AIC is Akaike information criterion and significant  $p$ -values are highlighted in bold. .... 44

**Table 4.1:** Description of intrinsic, extrinsic and random effects used in the mixed modelling approach of *C. laticeps* growth biochronology. .... 60

**Table 4.2:** Summary of considered models for optimal random effects (1a–2h), intrinsic effects (I. effects) (3a–b) and extrinsic effects (4a–l) models for fish growth in the protected (TNP) population. Each model (M) and its associated degrees of freedom (df), fixed intrinsic effects structure, fixed extrinsic effects structure, random effects structure, Akaike’s information criterion corrected for small sample size (AICc), change in AIC ( $\Delta$ AIC), AIC weight (AICwt) and restricted (models 1a–3b) or maximum (models 4a–l) log likelihood (LL) ranked based on lowest AIC at each modelling step with the most parsimonious model highlighted in bold. .... 66

**Table 4.3:** Summary of the most parsimonious mixed effects models (t4k, t4a and t4e) for growth of *C. laticeps* from the protected (TNP) population showing extrinsic fixed effects parameter estimates, standard errors (Std. Error), parameter upper and lower confidence intervals (CI), t statistic (*t*) and parameter p-values. IC is cumulative integrated cooling, autumn temp is mean autumn temperature and CGY temp is mean calendar growth year temperature. .... 67

**Table 4.4:** Summary of considered models for optimal random effects (p1a–p2h), intrinsic effects (I. effects) (p3a–b) and extrinsic effects (4a–l) models for fish growth from the exploited, Port Elizabeth population. Each model (M) and its associated degrees of freedom (df), intrinsic effects structure, extrinsic effects structure, random effects structure, Akaike’s information criterion corrected for small sample size (AICc) change in AIC ( $\Delta$ AIC), AIC weight (AICwt) and restricted (models 1a–3b) or maximum (models 4a–l) log likelihood (LL) ranked based on lowest AIC at each modelling step with the optimum model highlighted in bold. .... 68

**Table 4.5:** Summary of the most parsimonious mixed effect model (p3a) for growth of *C. laticeps* from Port Elizabeth showing parameter estimates, standard errors (Std. Error) and t statistic (t-stat). Number of obs. Is total number of increments, ID is

unique fish identifier, AICc is Akaike’s information criterion corrected for small sample sizes,  $R^2_{(m)}$  is marginal  $R^2$  and  $R^2_{(c)}$  is conditional  $R^2$ ..... 69

**Table 4.6:** Modelling results for testing the temporal trend in growth over time for the protected (TNP) population. Each model (M) and its associated degrees of freedom (df), fixed intrinsic effects structure, fixed extrinsic effects structure, random effects structure, Akaike’s information criterion corrected for small sample size (AICc), change in AIC ( $\Delta$ AIC), AIC weight (AICwt) and maximum log likelihood (LL) ranked based on lowest AIC with the most parsimonious model highlighted in bold. .... 70

**Table 4.7:** Summary of the mixed effects model (t5a) revealing the temporal trend of growth based on otolith increment (mm) for protected (TNP) population showing parameter estimates, standard errors (Std. Error) and t statistic (t-stat). Number of obs. Is total number of increments, ID is unique fish identifier, AICc is Akaike’s information criterion corrected for small sample sizes,  $R^2_{(m)}$  is marginal  $R^2$ ,  $R^2_{(c)}$  is conditional  $R^2$  and Year is the continuous year predictor..... 70

**Table 4.8:** Modelling results for testing the temporal trend in growth over time for PE. Each model (M) and its associated degrees of freedom (df), fixed intrinsic effects structure, fixed extrinsic effects structure, random effects structure, Akaike’s information criterion corrected for small sample size (AICc), change in AIC ( $\Delta$ AIC), AIC weight (AICwt) and maximum log likelihood (LL) ranked based on lowest AIC with the most parsimonious model highlighted in bold..... 71

**Table 5.1:** Model parameters of calibrated piecewise metabolic index model.  $k_B$  Is the Boltzmann constant, n is the mass scaling exponent,  $-E_o$  is the temperature dependence, and  $A_o$  is the ratio of oxygen supply and demand rate coefficients. . 91

**Table 5.2:** Mean model predictive accuracy based on ten runs for full  $\phi$  model (a) and reduced  $\phi$  model (b). .... 94

## Abstract

The persistence of harvested fish populations in the Anthropocene will be determined, above all, by how they respond to the interacting effects of climate change and fisheries exploitation. Predicting how populations will respond to both these threats is essential for any adaptive and sustainable management strategy. The response of fish populations to climate change is underpinned by physiological rates and tolerances, and emerging evidence suggests there may be physiological-based selection in capture fisheries. By quantifying important physiological rates of a model species, the endemic seabream, *Chrysoblephus laticeps*, across ecologically relevant thermal gradients and from populations subjected to varying intensities of commercial exploitation, this thesis aimed to 1) provide the first physiologically grounded climate resilience assessment for a South African linefish species, and 2) elucidate whether exploitation can drive populations to less physiologically resilient states in response to climate change.

To identify physiologically limiting sea temperatures and to determine if exploitation alters physiological trait distributions, an intermittent flow respirometry experiment was used to test the metabolic response of spatially protected and exploited populations of *C. laticeps* to acute thermal variability. Exploited populations showed reduced metabolic phenotype diversity, fewer high-performance aerobic scope phenotypes, and a significantly lower aerobic scope curve across all test temperatures. Although both populations maintained a relatively high aerobic scope across a wide thermal range, their metabolic rates were compromised when extreme cold events were simulated (8 °C), suggesting that predicted future increases in upwelling frequency and intensity may be the primary limiting factor in a more thermally variable future ocean.

The increment widths of annuli in the otoliths of *C. laticeps* from contemporary and historic collections were measured, as a proxy for the annual growth rate of exploited and protected populations. Hierarchical mixed models were used to partition growth variation within and

among individuals and ascribe growth to intrinsic and extrinsic effects. The best model for the protected population indicated that the growth response of *C. laticeps* was poorer during years characterised by a high cumulative upwelling intensity, and better during years characterised by higher mean autumn sea surface temperatures. The exploited population growth chronology was too short to identify an extrinsic growth driver. The growth results again highlight the role of thermal variability in modulating the response of *C. laticeps* to its ambient environment and indicate that the predicted increases in upwelling frequency and intensity may constrain future growth rates of this species.

A metabolic index ( $\phi$ ), representing the ratio of O<sub>2</sub> supply to demand at various temperatures and oxygen concentrations, was estimated for exploited and protected populations of *C. laticeps* and used to predict future distribution responses. There was no difference in the laboratory calibrations of  $\phi$  between populations, and all data was subsequently combined into a single piecewise (12 °C) calibrated  $\phi$  model. To predict the distribution of *C. laticeps*,  $\phi$  was projected across a high-resolution ocean model of the South African coastal zone, and a species distribution model implemented using the random forest algorithm and *C. laticeps* occurrence points. The future distribution of *C. laticeps* was estimated by predicting trained models across ocean model projections up to 2100. The best predictor of *C. laticeps*' current distribution was minimum monthly  $\phi$  and future predictions indicated only a slight range contraction on either edge of *C. laticeps*' distribution by 2100.

In order to provide policy makers, currently developing climate change management frameworks for South Africa's ocean, with a usable output, the results of all research chapters were combined into a marine spatial model. The spatial model identified areas where *C. laticeps* is predicted to be resilient to climate change in terms of physiology, growth and distribution responses, which can then be prioritised for adaptation measures, such as spatial protection from exploitation. While these results are specific to *C. laticeps*, the methodology developed to identify areas of climate resilience has broad applications across taxa.

From a global perspective, perhaps the most salient points to consider from this case study are the evidence of selective exploitation on physiological traits and the importance of environmental variability, rather than long-term mean climate changes, in affecting organism performance. These ideas are congruent with the current paradigm shift in how we think of the ocean, selective fisheries, and how they relate to organism climate resilience.



Thesis word cloud representing most used words scaled by size

# 1 Chapter 1

## General introduction: rationale behind this study



A typical scene on a South African temperate reef (photo credit: Steven Benjamin)

## 1.1 Brief conceptual background

It is now accepted that anthropogenic-induced climate change is resulting in unprecedented rates of change in long-term trends and the short-term variability of the physical ocean environment (Diaz & Rosenberg 2008, Hoegh-guldberg & Bruno 2010, Howes et al. 2015, Frölicher et al. 2018, Oliver et al. 2018). Evidence is accumulating that these environmental changes are affecting patterns and processes of biodiversity at rates higher than historically documented (Parmesan 2006, Wernberg et al. 2011). Responses of populations of organisms to climate change are, however, variable across space and time and can result in populations that are “winners” or “losers” through multiple interacting mechanisms (Somero 2010, Fulton 2011). For exploited fishery populations, it is therefore vital to assess the resilience of exploited resources to anticipated climate change, given the variable potential impact of climate change on them and the value of goods and services they provide to humans (Cheung et al. 2010, Sumaila et al. 2011).

In South Africa, commercial linefisheries form an important component of marine ecosystem goods and services, supporting 27% of all fishers (~455 commercial boats) and generating around R2.2 billion per annum (DAFF 2014). Linefisheries also support parts of large recreational (~750 000 participants) and subsistence (~29 000 participants) sectors that increasingly rely on the abundance of linefish for their livelihoods (Branch & Clark 2006). As elsewhere, the persistence of South Africa’s linefish is threatened by impacts of climate change with the south coast of South Africa considered a global marine “hot spot”, where the rate of ocean change is relatively rapid (Hobday & Pecl 2014, Popova et al. 2016). The effects of localised, accelerated climate change on linefish resources in South Africa is predicted to vary according to species-specific tolerances and life history, but this prediction is based largely on evidence from other regions owing to a lack of long-term monitoring and process-based research in South Africa (Potts et al. 2015). It is therefore important to quantify species-specific climate change resilience and the localised climate drivers on linefish persistence in

South Africa to inform adaptive management and prioritise species most at risk (Huey et al. 2012).

The effects of climate change on fish populations can be either direct or indirect (Breeggemann et al. 2016). Indirect effects influence fish populations via changes in the productivity or structure of ecosystem processes that have cascading effects throughout ecosystem networks (Brander 2010). For example, climate warming is predicted to change the abundance and spatial distribution of zooplankton species in the North Sea (Helaouët & Beaugrand 2007), which in turn will exert a bottom-up control on Atlantic cod (*Gadus morhua*) recruitment within the same area (Beaugrand et al. 2003). Direct effects of climate change on fish populations are physical changes in the ocean environment that influence internal patterns and processes which can modulate behaviour, reproductive output, or distribution responses (Rijnsdorp et al. 2009, Brander 2010). Changes in ocean temperature, oxygenation, and acidification are considered the three most important direct physical environmental drivers on fish populations, and responses to these stressors will determine resilience to future climate change (Gruber 2011, Pörtner 2012).

Studies investigating the effects of ocean acidification on fish suggest that the early life stages may be the most vulnerable to ocean acidification (Melzner et al. 2009b, Baumann et al. 2012), although some species are more tolerant than others and can emerge as “winners” (Ishimatsu et al. 2004, Munday et al. 2011). Deleterious ocean acidification responses manifest through the negative effects on growth, development, metabolism, behaviour, and ultimately, mortality and recruitment (Ishimatsu et al. 2008, Munday et al. 2010). In a pioneering ocean acidification study on a South African linefish, Erasmus (2017) and Edworthy (2017) found reduced growth, development, metabolism, and survival of post-flexion dusky kob (*Argyrosomus japonicas*) larvae at low pH levels of 7.78 predicted for the end of the century (2100). This reduced larval performance could ultimately result in complete recruitment failure of the species if no evolutionary adaptation towards an acidified ocean occurs. Direct effects of ocean acidification on sub-adult and adult fishes are, however, believed to be minimal as compensatory

mechanisms can maintain balanced acid-base levels in an acidic environment (e.g., Melzner et al. 2009a, Haigh et al. 2015).

Low oxygen zones can also affect fish populations through reductions in available habitat or altered metabolic/physiological processes, that can ultimately result in increased mortality (Stramma et al. 2010). Temperature and oxygen are intrinsically linked in the ocean as rising temperatures can reduce the supply of oxygen while simultaneously increasing oxygen demand in organism tissues (Deutsch et al. 2015). Although direct effects of physical environmental drivers on fish populations can often interact (e.g., Munday et al. 2009), the overarching environmental driver is considered to be temperature because of the pervasive effect of temperature on ectotherm physiological rates which regulate performance (Holt & Jørgensen 2014, Potts et al. 2015, Hoey et al. 2016).

The response of fish populations to changes in ocean temperature can be broken down into four broad components of behaviour, phenology, distribution, and demography (Rijnsdorp et al. 2009, Potts et al. 2015, Poloczanska et al. 2016). Behavioural modifications are often a first response to ocean temperature changes as fish may seek to avoid unfavourable temperatures (Rijnsdorp et al. 2009). Behaviours such as swimming style or foraging behaviour are temperature sensitive (Brownscombe et al. 2014, Johansen et al. 2014) and fish may thus seek temperatures that maximise these behavioural processes or adjust behaviours when temperatures are sub-optimal (Freitas et al. 2015). Temperature-induced behavioural modifications can affect fish population phenology (the timing of cyclical events), as temperature is often a cue for seasonal migrations (Sousa et al. 2016), diel migrations (Keyser et al. 2016) and spawning migrations (Sims et al. 2004). A global analysis of sea temperature trends by Lima & Wetthey (2012) identifies the coast off South Africa as having some of the highest advances in seasonal warming. When temperature stressors are chronic over time, these short-term behavioural and phenology responses can manifest into negative impacts on the abundance and productivity of fish populations (Crozier et al. 2008).

Over longer timescales, changing ocean temperatures can drive distributional shifts in fish populations across latitudes or depths (Pecl et al. 2017). For example, Perry et al. (2005) show that nearly two-thirds of North Sea fishes responded to warming temperatures by shifting their distribution either deeper or to higher latitudes. In South Africa, James et al. (2008) report that the ranges of certain tropical fish species have extended to higher latitudes, most probably due to the warming of the Agulhas Current and the subsequent extension of suitable habitat for tropical species. Temperature also affects demographic processes like growth, mortality and recruitment, such that even small changes in temperature can have big impacts on population biomass and abundance (Brander 2010, Poloczanska et al. 2016). For example, temperatures that exceed the narrow thermal tolerance of fertilised eggs may lead to faster larval development, resulting in increased mortality and reduced recruitment into fisheries (Pankhurst & Munday 2011). Warming temperatures can also result in faster juvenile and adult growth rates, which alter fish production (Audzijonyte et al. 2016). Ultimately these behavioural, phenological, demographic, and distributional changes affect the abundance, productivity, and persistence of fish populations that the human population relies on for goods and services (Brander 2007). With a myriad of potential changes likely, an assessment of climate resilience, defined as the ability to resist or recover from a climate-related stressor (Côté & Darling 2010, Hodgson et al. 2015), of commercially important fish populations is a research priority in South Africa.

Most previous research quantifying the resilience of marine species to environmental stressors has specifically focused on the effects of future (normally up to 2100) mean changes in temperature, oxygen, or ocean acidification on contemporary performance (Bates et al. 2018). Experimental approaches that employ such techniques, however, overestimate negative responses when there is potential for evolutionary adaptation (Hoffmann & Sgró 2011) or acclimation (Donelson et al. 2011). Furthermore, experimental approaches that quantify organism responses to predicted future mean environmental changes may be better suited to tropical species in relatively stable environments, as their ecological applicability for

temperate species in dynamic environments, may be limited (Morash et al. 2018). There is a growing paradigm shift among researchers that the effects of environmental variability may be more important for species performance than long-term mean changes in the environment (Dillon et al. 2016, Bates et al. 2018, Vasseur et al. 2018). This environmental variability is particularly important for South Africa's marine resources as the coastal zone is characterised by extreme thermal fluctuations that are linked to global weather patterns such as the El Niño-Southern Oscillation (ENSO), and the magnitude and frequency of this variability is predicted to increase with climate change (Rouault et al. 2010). For South Africa, and probably most temperate regions globally, quantifying organism responses to acute thermal variability will be an important and ecologically relevant measure, in addition to long-term experiments over multiple generations, to assess species climate change resilience.

## **1.2 A conservation physiological approach**

Determining species resilience to climate change has generally been studied through correlations between environmental variables and historical population responses (Horodysky et al. 2015). Correlative studies mostly take a "black box" approach and do not consider the underlying mechanisms that govern population responses (Helmuth 2009), which can make forecasting responses unreliable (Horodysky et al. 2015). Furthermore, assigning biological responses of populations to climate change is challenging, given the complexity of interacting mechanisms, variable species responses, and the potential of cascading effects (Poloczanska et al. 2016). While it is still useful to assess past responses to climate change, incorporating experimentally derived information on the sensitivity of underlying processes can improve inference and forecasting accuracy (Wernberg et al. 2011).

The field of conservation physiology is a relatively newly established discipline in marine science that can improve understanding and predictive accuracy of species responses to climate change (Wikelski & Cooke 2006). Conservation physiology goes beyond describing correlative patterns by evaluating underlying physiological processes, their response to

environmental stressors, and ultimately predicting future responses based on experimentally deduced physiological thresholds and capacities (Cooke et al. 2013). Through this mechanistic understanding, on an individual level, of the underlying cause of environment-related responses, one is able to scale up and forecast how a population will be affected, given a set of future environmental scenarios (Wikelski & Cooke 2006, Helmuth 2009, Somero 2010, Cooke et al. 2013, Ward et al. 2016).

Because fish are ectotherms, their physiological rates are governed by external temperatures (Brown et al. 2004, Whitney et al. 2016) and these physiological rates underpin many behaviour, phenology, demographic or distribution responses (Rijnsdorp et al. 2009, Hofmann & Todgham 2010, Bozinovic & Pörtner 2015). Physiological rates and tolerances are thus the processes that mechanistically link fish populations to their ambient environment (Horodysky et al. 2015). From a climate change perspective, eco-physiological research can therefore identify environmental stressors and their consequence on physiological performance and thus contribute to informed, process-based predictions of how animals will respond to future environmental change (Horodysky et al. 2015). This approach allows for the classification of vulnerable species as well as an assessment and implementation of more appropriate adaptation strategies (Huey et al. 2012, McKenzie et al. 2016).

The incorporation of physiology into the assessment of vulnerability or resilience of fishes to climate change is relatively new, but holds great promise as a method to develop a suite of more appropriate management tools (McKenzie et al. 2016). For example, in Papua New Guinea, Rummer et al. (2014) used metabolic physiology to identify fish species vulnerable to climate change, while Fitzgibbon et al. (2014) used metabolic physiology to identify the most vulnerable life history stage of spiny lobster (*Sagmariasus verreauxi*). A recent fisheries example of the incorporation of physiological research into adaptive management plans is the Fraser River sockeye salmon (*Oncorhynchus nerka*) (Patterson et al. 2016). Physiological research involved identifying the impacts of high water temperature and high river discharge in terms of thermal tolerance, energy metabolism and respiratory capacity, which among other

factors, influence successful spawning migrations, and adjusting catch limits when appropriate (Clark et al. 2010, Eliason et al. 2011, 2013a).

### **1.3 Climate change and fisheries exploitation**

Assessing the resilience of fish populations to climate change must be done in the context of other anthropogenic stressors, such as exploitation, for research to be more applicable to real-world scenarios (Brander 2010). On a population level, fisheries exploitation, together with climate change, are considered the two primary threats to the persistence of fish populations into the future (Brander 2007, 2010, Perry et al. 2010). Exploitation and climate change effects can interact synergistically or additively, such that the response of a population to environmental stressors is amplified, or nearer to critical threshold levels, in the presence of exploitation (Perry et al. 2010, Poloczanska et al. 2016). A mechanistic understanding of why exploited populations of fish may be more sensitive to environmental stressors is thus fundamental for eco-physiological research to be appropriate.

Research into why fisheries exploitation may render populations less resilient to environmental stressors has largely focused on fisheries-induced alterations to population demographic process and life history traits, and the resultant effect on recruitment and growth dynamics (Hsieh et al. 2006, Ottersen et al. 2006, Anderson et al. 2008). By selecting individuals based on certain characteristics (e.g., size), exploitation alters the frequency distribution of certain traits, which can lead to truncated populations and fisheries-induced evolution (FIE) towards faster growing, earlier maturing populations (Jørgensen et al. 2007). Exploited populations thus lose the buffering capacity provided by the highly fecund large/old individuals and tend to track environmental variability more closely (Anderson et al. 2008, Rijnsdorp et al. 2009, Perry et al. 2010).

Our understanding of the impact of fisheries selection on population-scale physiological processes which can underpin climate change responses is limited. Increasing evidence suggests that certain fisheries gear types (passive gears) select individuals on characteristics

other than size (Klefoth et al. 2017, Lennox et al. 2017, Hollins et al. 2018). Bold or aggressive individuals can be more vulnerable to capture in passive-gear fisheries, ultimately resulting in more timid and less behaviourally diverse exploited populations (Biro & Post 2008, Arlinghaus et al. 2017, Cooke et al. 2017). These vulnerable behavioural types are often associated with certain physiological phenotypes (Killen et al. 2014, Binder et al. 2016, Rupia et al. 2016). For example, Hessenauer et al. (2015) demonstrate that exploited populations of largemouth bass (*Micropterus salmoides*) have a lower resting metabolic rate compared to unexploited populations. Emerging evidence suggests that there may be physiological-based fisheries-induced evolution at a population level (Hollins et al. 2018). Indeed, Auer et al. (2018) recently showed that metabolic phenotypes evolve rapidly and in tandem with life history traits under evolutionary selection, through the additional mortality imposed by increased predation.

When combining evidence highlighting the importance of physiological rates and tolerances for maintaining climate change resilience with emerging information on the potential physiological effects of passive-gear fisheries selection, research into whether fisheries exploitation is driving populations to less or more physiologically resilient states is necessary. In order to achieve this, baseline physiological data on commercial fish populations (pre-exploitation) is required, but such baseline data is often not available (Wikelski & Cooke 2006). The South African coastline, however, has some of the oldest marine protected areas (MPAs) globally, where ecosystems have been unaffected by the impact of human exploitation for as long as 50 years. These MPAs are home to many exploited linefish species with characteristics (such as high residency) that allow them to maximise the benefit of spatial protection and behaviour types that suit the rigours of experimental biology, making it an ideal “natural laboratory” to explore some of these questions.

#### **1.4 Aims of this thesis**

The broad aims of this thesis are to conduct the first physiologically-based research on the resilience of a commercially important linefish species to predicted thermal climate change off

the coast of South Africa (Figure 1.1 green question mark) and to elucidate how fisheries exploitation and physiological traits may interact to shape the resilience of fish populations to climate change (Figure 1.1 blue question mark). To achieve this, the thesis is broken down into an exploratory research chapter (Chapter 2), three primary research chapters (Chapters 3, 4 and 5) and a final synthesis chapter (Chapter 6) that addresses these questions as follows:

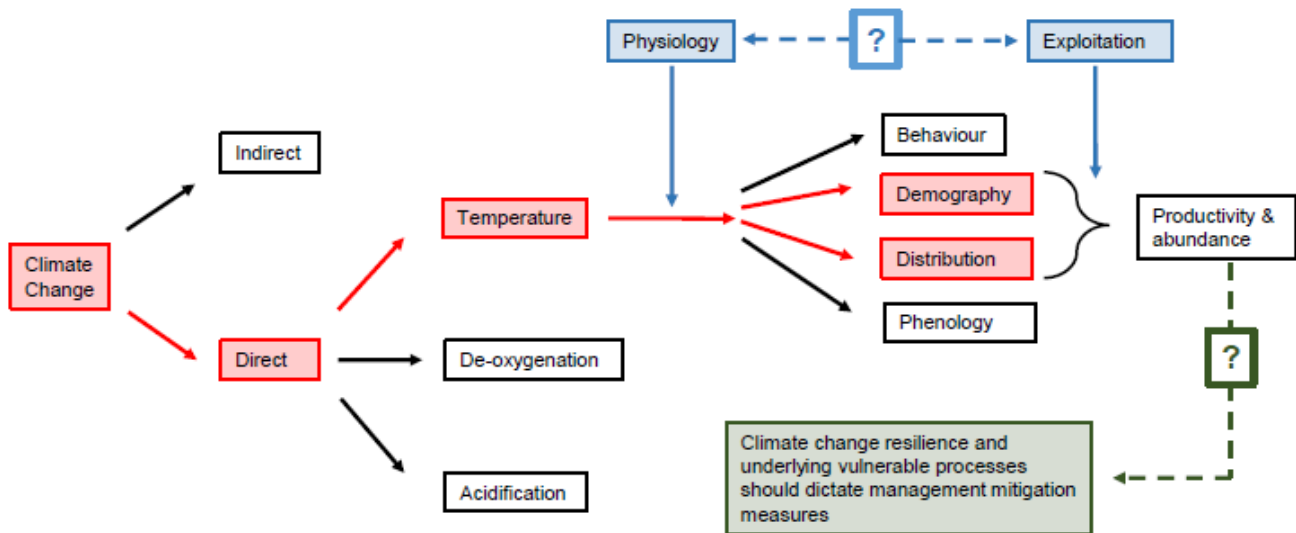


**Figure 1.1:** Broad schematic diagram of how climate change can affect marine fish populations, the thought process behind the design of the research chapters (red arrows and boxes), and the questions (blue and green question marks) it hopes to answer: 1) assess climate resilience (green arrow and box) and 2) elucidate how exploitation and physiology may interact to influence climate change resilience (blue arrows and boxes).

The first, Chapter 2, identifies suitable areas and a model species to answer the research questions of this thesis. The thermal regimes of proposed areas are explored to account for temperature as a covariate and elucidate the thermal characteristics of the South African coast. A review of climate change literature for the South African coast and global ocean trends is carried out to justify quantifying fish population responses to acute variability rather than long-term mean changes in sea temperature.

The second, Chapter 3, assesses the relationship between temperature and metabolic phenotypic traits of protected and exploited populations of *Chrysolephus laticeps* (an endemic, commercial linefish species, see Chapter 2). This allowed exploration of the potential

of fisheries exploitation to shape how fish populations respond to climate change on a physiological level (Figure 1.1 green question mark) and the interaction between physiological traits and exploitation (Figure 1.1 blue question mark).

The third, Chapter 4, quantifies the environmental drivers on somatic growth of *C. laticeps* by developing otolith-based growth biochronologies for exploited and protected populations. This enabled discernment of the growth sensitivity of *C. laticeps* to environmental variability between different levels of exploitation and in the context of population physiological capacity (Figure 1.1 demographic response, red box).

The fourth, Chapter 5, models the distribution response of *C. laticeps* to the predicted future environmental seascape around South Africa based on how temperature and oxygen affect a metabolic index (Deutsch et al. 2015), which was calibrated with data from protected and exploited populations. This provided physiological insight into whether commercial exploitation may affect the sensitivity of distribution response of marine fish to climate perturbations (Figure 1.1 distribution response, red box).

The final chapter, Chapter 6, synthesises all the research chapters into a spatial model, which aims to predict areas where *C. laticeps* would be most resilient to anticipated climate change in terms of physiology, growth and distribution responses. This spatial inference on the resilience of *C. laticeps* to localised climate change (Figure 1.1 green question mark) can be incorporated into the climate management framework and policy currently being developed by the South African government.

## 2 Chapter 2

### Study area and species profile



The rugged shoreline of the Tsitsikamma Marine Protected Area

## 2.1 Study area

### 2.1.1 Climate change along the South African coastal zone

This thesis broadly aims to quantify aspects of the physiological resilience of linefish to climate change. It was therefore important to understand what aspects of ocean climate are predicted to change along South Africa's coast because testing ecologically relevant rates of environmental change ensures results are ecologically meaningful (Farrell 2016).

While mean increases in sea temperature dominate global literature, areas of cooling are also reported, particularly around coastal upwelling zones (Lima & Wethey 2012). Schlegel & Smit (2016) report an overall warming trend of between 0 °C to 0.2 °C per decade since the 1970's around coastal South Africa, but localised areas of cooling have also been recorded (Rouault et al. 2010). Long-term trends of sea temperature in South Africa are, however, a function of substantial short-term thermal variability (Goschen & Schumann 1995, Schumann 1999, Goschen & Schumann 2011) (Figure 2.1). Furthermore, this anomalously warm or cold temperature variability can persist for a number of days, termed, Marine Heat Waves (MHW) and Marine Cold Spells (MCS) (Hobday et al. 2016, Schlegel et al. 2017). Research by Schlegel et al. (2017) shows that MHW and MCS occur at least once a year along South Africa's coast, and an analysis of temporal trends shows that the occurrence of MHW has increased over time, consistent with global trends (Frölicher et al. 2018, Oliver et al. 2018). Extreme temperature variability associated within mean temperature changes is emerging as an important component of climate change and is speculated to have a greater biological impact than long-term mean changes (Dillon et al. 2016, Bates et al. 2018, Vasseur et al. 2018), particularly in South Africa (Schlegel & Smit 2016, Schlegel et al. 2017).

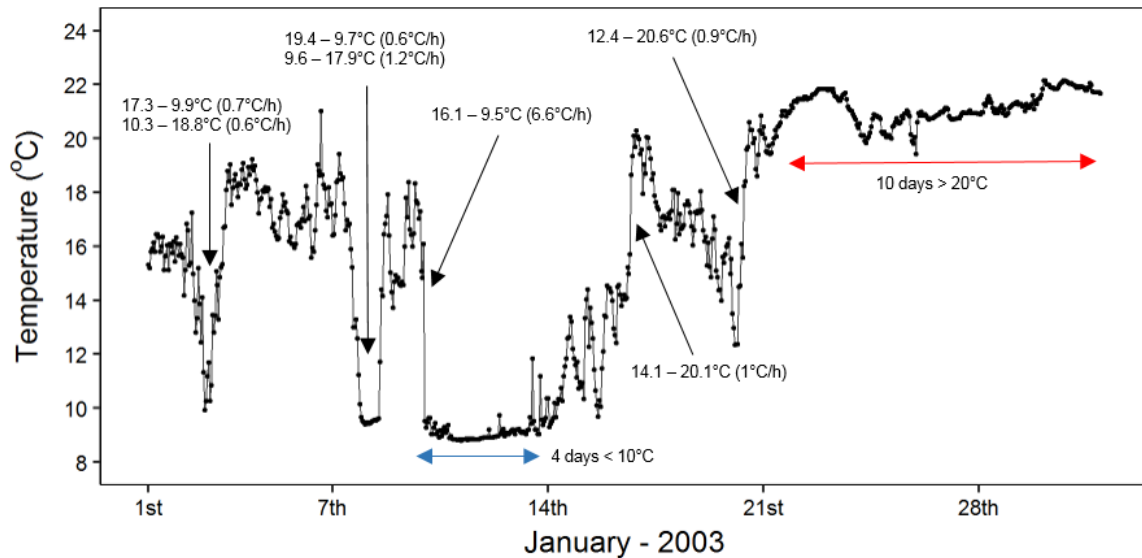


**Figure 2.1:** Hourly sea temperature thermistor string data (19 m depth) (black points) from within the Tsitsikamma National Park Marine Protected Area during January 2003 with major upwelling/downwelling events indicated with black arrows, highlighting the range and rate of temperature change, and anomalous cold (blue arrow) and hot (red arrow) spells indicated.

Temperature variability patterns along South Africa’s coast are driven by intermittent wind-induced upwelling and downwelling. Upwelling primarily occurs off prominent capes along the south coast of South Africa (Goschen & Schumann 1995) and is driven by easterly component winds (Goschen & Schumann 2011) which generate offshore surface Ekman transport (Schumann 1999). The offshore bathymetry is abrupt, allowing upwelling to occur right up to the coast (Schumann 1999), and the summer thermocline permits sharp changes in sea temperature of more than 10 °C within a few hours (Schumann et al. 1995); changes that normally last one to two days (Schumann 1999) (Figure 2.1 blue arrow). Occasionally, downwelling can result in abnormally high sea temperatures in deeper waters off the coast of South Africa (Schumann 1999) (Figure 2.1 red arrow). Upwelling and the associated variability of the sea surface temperature is largely a summer occurrence because easterly winds are more prevalent in summer than winter (Goschen & Schumann 1995, Schumann et al. 1995).

The frequency and intensity of upwelling and downwelling along South Africa’s coast is also partly driven by the ENSO, where easterly winds driving upwelling strengthen during La Niña and weaken during El Niño (Rouault et al. 2010, Dufois & Rouault 2012). Recent climate

modelling consensus predicts an increase in the frequency and intensity of ENSO events, even if the Paris Agreements global mean temperature increase targets are met (Cai et al. 2014, 2015, Wang et al. 2017). This future increase in ENSO strength is predicted to drive increases in associated sea temperature variability trends in South Africa further. Increased upwelling through intensification of easterly winds has already been reported in South Africa (Rouault et al. 2010) and there is high confidence that ENSO will remain one of the dominant drivers of natural climate variability in the future (Christensen et al. 2013).

For studies exploring the response of organisms to environmental stressors in South Africa, and many temperate regions globally, to be ecologically appropriate, the response of organisms to acute thermal variability is proposed as more suitable than research into organism responses to long-term mean changes in temperature.

### 2.1.2 Sampling locations

In order to explain the effect of commercial exploitation on linefish physiology, baseline reference physiological information was required from within South Africa's MPAs, which could be referenced against exploited areas. Sampling multiple MPAs and exploited areas was not feasible. For this reason, it made sense to choose the Tsitsikamma National Park (TNP) MPA, the largest and oldest protected area in South Africa, as a study site (Figure 2.2). The TNP MPA was proclaimed a no-take marine reserve in 1964 and the status of the resident fish stocks within its boundaries is considered at pre-exploitation levels (Kyle Smith pers. comm.). The MPA runs along the exposed side of a cape headland for approximately 60 km, extends 5.6 km offshore (Buxton 1987) and forms part of the greater Garden Route National Park. Although parts of the shore have recently been opened to shore-based exploitation, no boat-based exploitation is permitted. There is limited evidence for illegal boat fishing in the park, suggesting that compliance is high in this MPA (WWF-SA 2014).

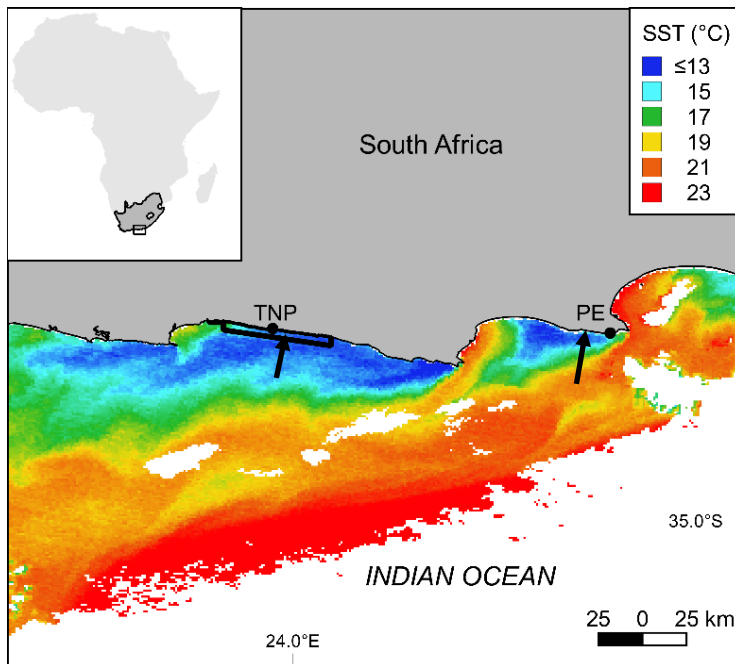


**Figure 2.2:** Map depicting the location of sampling areas (black arrows): Tsitsikamma National Park (TNP) Marine Protected Area (black outline) and Port Elizabeth (PE) in South Africa. Colours are MODIS Terra satellite sea surface temperatures depicting an upwelling event on 04-03-2010 taken from Smit et al. (2013).

Because of the limited replication of treatment effects (protection/exploitation), it was important to choose an exploited area with similar ecological conditions to the TNP MPA. This is particularly important for studies exploring thermal physiology as contemporary thermal performance curves are influenced by historical thermal regimes (Norin et al. 2014, McKenzie et al. 2016). The area offshore of Noordhoek Ski-boat Club, just outside the Port Elizabeth (PE) metropolitan and approximately 140 km east of the TNP (Figure 2.2), was chosen as the exploited area because previous studies have highlighted the ecological similarity of the marine habitat between both areas (Buxton & Smale 1989, Buxton 1993). Like the protected area (TNP MPA), the area of the exploited location (PE) is along the exposed side of a cape headland and, since localised sea temperature variability is reported in waters around headlands compared to bays in South Africa (Beckley 1983), it was hypothesised that the thermal regimes would be similar (Figure 2.3).

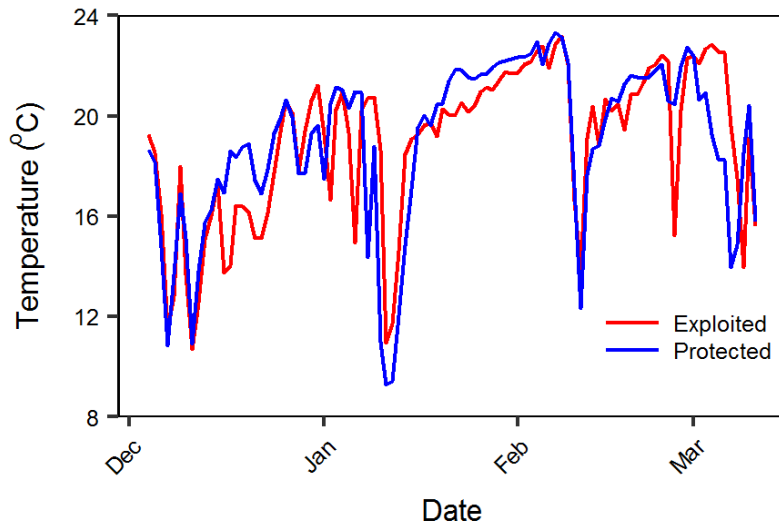


**Figure 2.3:** Daily sea temperature data from underwater temperature recorders at exploited (PE) (5 m depth) and protected (TNP) (10 m depth) sampling areas from December 2002–March 2003 indicating extreme thermal variability and synchrony between areas.

To test this hypothesis, long-term (1981–2015) REYNOLDS AVHRR V2 high precision 0.25° OI daily sea surface temperature (SST) data for protected (TNP) and exploited (PE) areas were obtained from the National Oceanic and Atmospheric Administration’s National Climate Data Centre website: <https://www.ncdc.noaa.gov> (Reynolds et al. 2002). Level-2 MODIS Terra data for 04-03-2010 around the South African coast were obtained from the Ocean Colour website: <http://oceancolor.gsfc.nasa.gov> (NASA Goddard Space Flight Center). MODIS Terra data were reprocessed at a 4 km resolution and masked with the CLDICE flag using the Data Analysis System (SeaDAS) (Baith et al. 2001).

To compare long-term sea temperature trends between protected (TNP) and exploited (PE) sampling areas, the daily AVHRR SST data were modelled using a generalised additive mixed effects model (GAMM), including a seasonal cyclical smoothing spline and a trend smoothing spline for each area with an autoregressive moving average (1,0) correlation structure to remove autocorrelation, in the mgcv package (Wood 2011). The difference between the protected and exploited area trend smoothing splines was tested for significance from zero using ordered factors within the GAMM. While remotely sensed SST data can be useful when exploring large-scale, long-term, temporal patterns, it can sometimes fail to capture localised

SST variability on shorter time scales (e.g., upwellings), particularly when data points are located close to shore (Smit et al. 2013).

Because the South African south coast is characterised by localised variability in sea temperature, it was important to quantify the similarity of this variability between sampling areas. This was done using higher resolution, daily underwater temperature recorder (UTR) sea temperature data. Underwater temperature data were obtained from the Southern African Data Centre for Oceanography (SADCO) for the TNP (10 m depth) and Mangolds Pool (PE) (5 m depth) deployments collected by the Department of Environmental Affairs (DEA) Oceans and Coasts. Only concurrent data from both UTRs were included in the analysis, resulting in a daily time series from January 1992–November 2005 per area.

Each time series was decomposed into its trend, seasonal, and random components using the `tseries` package (Trapletti & Hornik 2017). The random component of each UTR time series is irregular variance that represents intermittent sea temperature variability, such as upwelling or downwelling events (Goela et al. 2016). The similarity in direction and magnitude of irregular sea temperature variability between sampling areas was tested for significant synchrony using the `meancorr` function in the `synchrony` package (Gouhier & Guichard 2014). Spatial and temporal correlation were removed by a naïve randomisation procedure and tests for significant correlations were performed using 999 Monte Carlo randomisations.

A visual inspection of the AVHRR SST time series data indicated similar seasonal (Figure 2.4 a) and yearly (Figure 2.4 b) patterns between the sampling areas. Year-to-year differences in mean annual SST were similar in direction and magnitude, indicating a similar long-term trend between sampling areas (Figure 2.4 c). The difference between the area-specific trend splines of the GAMM model (Figure 2.4 d, dashed black line with 95% CI shaded grey) were not significantly different to zero ( $p$ -value > 0.05, Table 2.1), further suggesting that the long-term SST trends between sampling areas were similar.

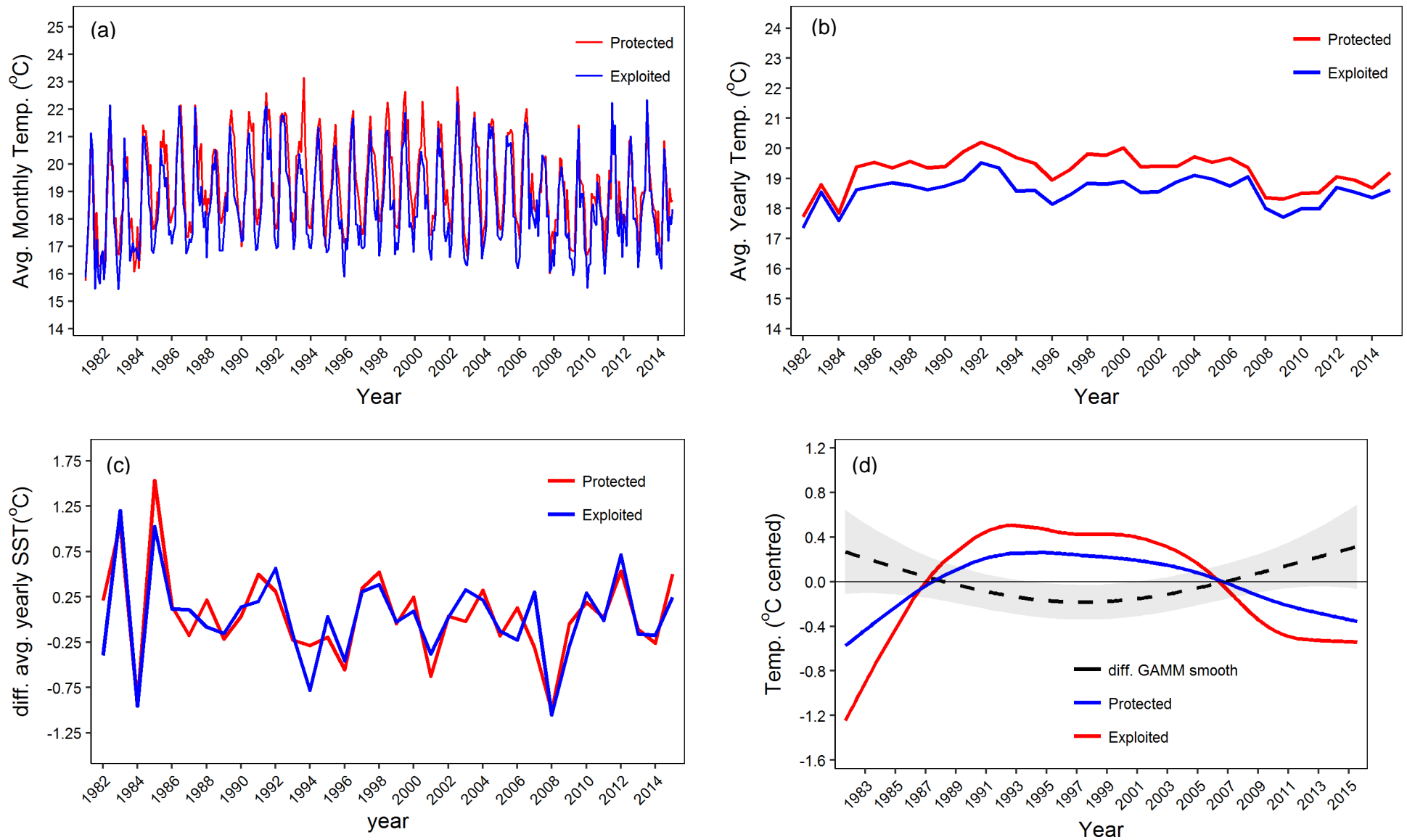


**Figure 2.4:** Monthly mean SST (a), yearly mean SST (b), year-to-year difference in mean SST (c) and modelled SST trend splines including the difference in SST trend spline (dashed black line with 95% confidence intervals shaded in grey) (d) for the AVHRR SST time series data for exploited (PE, red) and protected (TNP MPA, blue) sampling areas.

**Table 2.1:** Approximate significance of spline functions for a single explanatory variable (Smooth term) of the GAMM model indicating the estimated degrees of freedom (edf), F-statistic (F-stat) with significant  $p$ -values highlighted in bold.

Smooth term	edf	F-stat	$p$ -value
Seasonal spline exploited	7.792	61.869	<b>&lt;0.001</b>
Seasonal spline protected	8.724	86.036	<b>&lt;0.001</b>
Reference trend spline	12.099	11.243	<b>&lt;0.001</b>
Difference trend spline	2.082	3.077	0.052

The UTR data revealed distinct seasonal patterns of sea temperature variability, with higher standard deviations during summer months and more stable sea temperatures during winter months (Figure 2.5). A plot of the random component of the UTR time series data indicated that this sea temperature variability occurred at similar times at both sampling areas (Figure 2.6). The synchrony in thermal variability was statistically significant (mean Pearson's correlation: 0.572,  $p$ -value < 0.001), indicating a similar direction and magnitude of abrupt departures from mean sea temperatures at sampling locations.

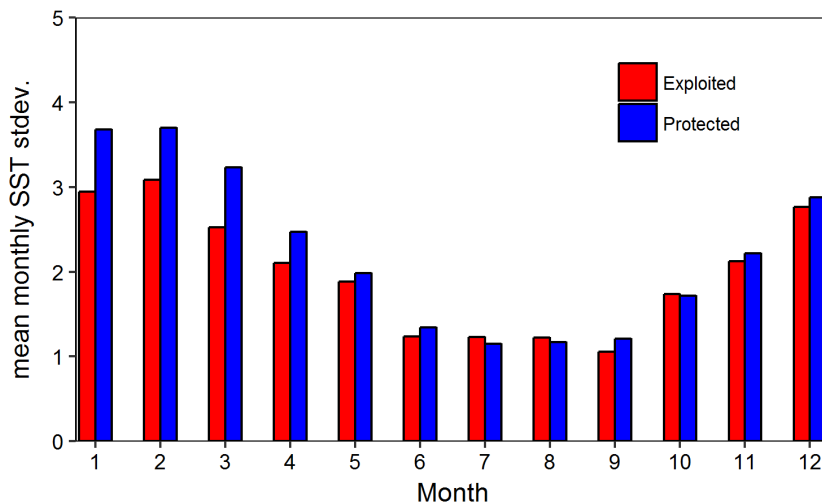


**Figure 2.5:** Standard deviation of monthly mean UTR sea temperature data (mean monthly SST stdev) for exploited (PE, red) and protected (TNP, blue) sampling areas.

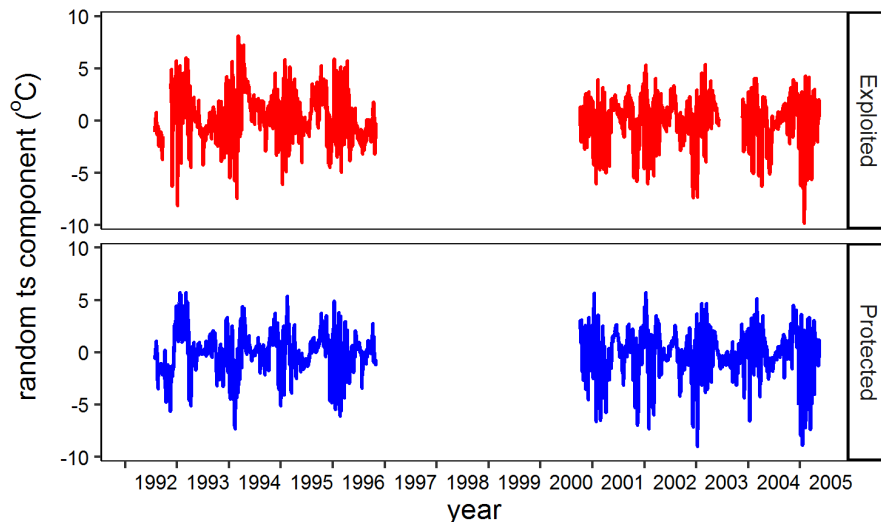


**Figure 2.6:** Time series of the random component of UTR data (random ts component (°C)) for exploited (PE, red) and protected (TNP, blue) sampling areas.

The similarity in long-term trend and short-term variability of sea temperature patterns between the two sampling areas indicates they are appropriate for this research. While using satellite-derived SST data can underestimate localised variability and can have warm biases along the South African coast (Smit et al. 2013, Schlegel et al. 2017), it was the only dataset of sufficient length to analyse any long-term trends between both areas. Any disproportionate biases of satellite SST between sampling areas were considered by the GAMM, as trend splines are centred around 0 °C. Furthermore, satellite-derived SST were not used to analyse any localised high-frequency variability patterns between areas. The slight higher standard deviation of sea temperature at the protected area (TNP) (Figure 2.5) was likely due to the UTR being positioned 5 metres deeper than at the exploited area (PE) deployment.

## 2.2 Study species

To ensure that physiological data adequately represented exploited and unexploited fish populations, identifying a study species that had behavioural traits which maximised the benefits of spatial protection (Gell & Roberts 2003) and suited the rigours experimental physiology (Clark et al. 2013) was important. This limited the potential study species to resident linefishes, that form a component of commercial and recreational linefishery catch in

South Africa (DAFF 2014). The South African small-scale, boat-based commercial and recreational boat linefisheries are multi-species fisheries that operate off ski-boats using hook and line as a capture method, and target multiple species (DAFF 2014). To determine the most appropriate species, a thorough suitability assessment of potential species was performed.

Multiple attributes were considered, derived from the South African marine linefish species profiles book (Mann 2013), publications, and expert knowledge, to select an applicable model species for this thesis' research. Key attributes of species required to answer the overarching research question were a core distribution through the proposed sampling areas, and commercial exploitation by the South African linefisheries, together with the other, following attributes: site fidelity, so the benefit of spatial protection was maximised (Palumbi 2004); hardiness, to ensure specimens could handle the stress of translocation and laboratory experimentation; shallow habitat depth, because of the positive relationship between depth and discard mortality (Kerwath et al. 2013a); intra-specific competitiveness, which was thought to act as an added selection pressure on the physiological attributes of the species; panmixia to ensure that sampling areas did not represent a locally adapted population. All species considered were from the family Sparidae. The roman seabream, *Chrysoblephus laticeps* (Valenciennes, 1830) (Figure 2.7), fulfilled every attribute deemed important (Table 2.2) and was chosen as the model species for this thesis' research.

**Table 2.2:** Checklist of species considered and attributes deemed important for this research. Ticks indicate attribute present in species, crosses indicate attribute not present and N.A. indicates no data was available.

	Argyrozona argyrozona	Chrysoblephus laticeps	Cheimerius nufar	Chrysoblephus gibbiceps	Chrysoblephus cristiceps
Distribution	✓	✓	✓	✓	✓
Residency	✓	✓	✗	N.A.	✓
Exploited	✓	✓	✓	✓	✓
Panmictic	N.A.	✓	N.A.	N.A.	N.A.
Hardy	✓	✓	✓	✓	✓
Competitive	✗	✓	✗	N.A.	N.A.
Depth	✗	✓	✓	✓	✓



**Figure 2.7:** Adult and juvenile roman seabream; *Chrysolephus laticeps* (Valenciennes 1830). Photo credit: Coastal Fishes of southern Africa - Phil and Elaine Heemstra (South African Institute for Aquatic Biodiversity).

*Chrysolephus laticeps* (Figure 2.7) is an endemic seabream of the South African coast, with a core distribution throughout the Western and Eastern Cape in South Africa (Götz & Kerwath 2013). The selected protected (TNP MPA) and exploited (PE) sampling areas, lie towards the centre of this distribution. Importantly, *C. laticeps* is heavily exploited by both the commercial and recreational ski-boat linefisheries in South Africa (Brouwer & Buxton 2002). Catch estimates of between 10 000–100 000 kg have been recorded from locations (5 by 5 nautical mile grid cells) west of PE between 1985–2000 with no reported catch from within the TNP MPA (Kerwath et al. 2013b, Figure 2.8). Total catch per unit effort (CPUE) of *C. laticeps* has fallen from historical highs in the early 20<sup>th</sup> century to between 4.7 and 17.4% of those levels up to 1998 (Griffiths 2000) and has remained relatively stable at these levels since (Götz & Kerwath 2013, Kerwath et al. 2013b).

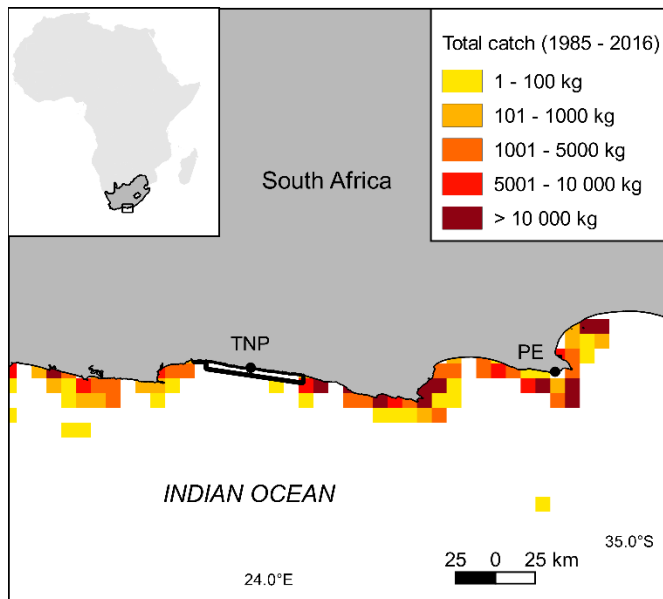


**Figure 2.8:** Spatial distribution of total commercial *C. laticeps* catch from 1985–present in relation to protected (TNP, black outline) and exploited (PE) sampling locations. Data obtained from the national marine linefish system (NMLS) at DAFF.

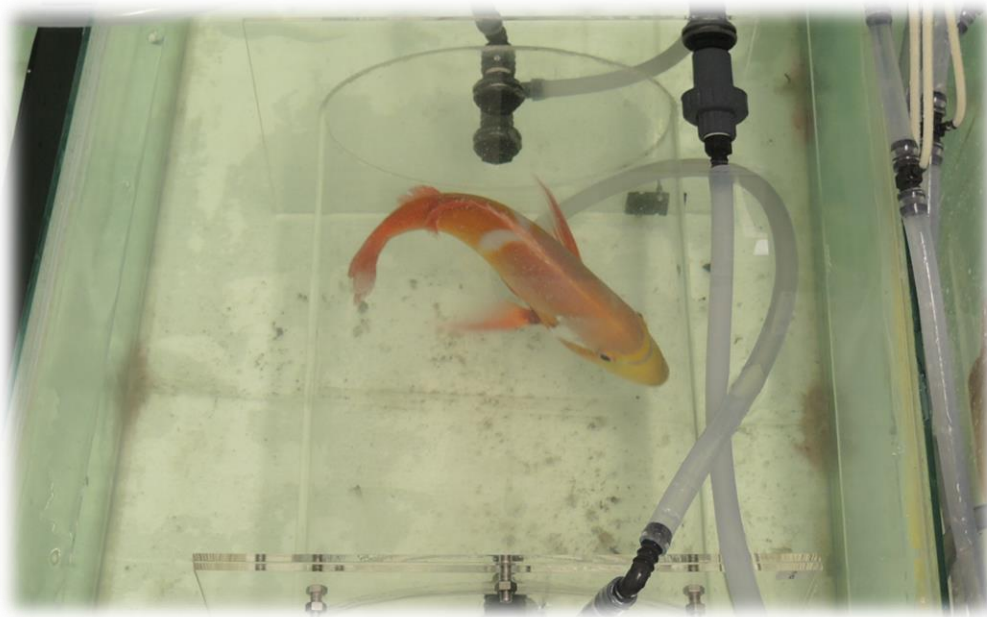
Based on catch-tag-recapture data, *C. laticeps* is considered highly resident, with the probability of being recaptured within the TNP MPA estimated at 0.94 (Kerwath et al. 2007a) and using acoustic telemetry data, *C. laticeps*' home range size was estimated to be small; between 1000–3000 m<sup>2</sup> (Kerwath et al. 2007b). The few studies that have kept *C. laticeps* in captivity have reported that it is extremely hardy, will begin feeding soon after capture, and has a low mortality rate of 0.03 in captivity (Davis 1996, Kerwath et al. 2006). Behavioural observations indicate intra-specific competition, as dominant males have been seen defending territories during the summer breeding season (Buxton 1987), and aggressive behaviour during foraging and spawning has been observed (Kerwath et al. 2007b). The species can be caught from relatively shallow depths and is reported to recover from any effects of barotrauma following capture and swim bladder deflation (Kerwath et al. 2007b). Population genetics indicate a single, well-mixed population of *C. laticeps* in South Africa with genetic connectivity patterns throughout its distribution (Teske et al. 2010).

Life history traits of *Chrysolephus laticeps* render the species particularly vulnerable to selective exploitation. The species reaches 50% maturity as a female between 2.5–4.27 years

old, or 167–190 mm fork length (FL) (Buxton 1987, 1990, Götz et al. 2008), and undergo a protogynous sex change (Buxton 1990). Sex change from female to male is 50% complete between ages of 8–10.25 (Götz et al. 2008) or between 275–350 mm FL (Buxton 1993). Spawning occurs in the summer months between October to January (Buxton 1990). The species is considered fairly slow growing, reaching a maximum recorded age of 19 years (Götz et al. 2008). Overall, *C. laticeps*' behavioural traits, commercial vulnerability and distribution make it an ideal model species to answer this thesis' research questions.

### 3 Chapter 3

## Fishing targets high-performance metabolic phenotypes



A roman seabream inside a respirometer

### 3.1 Introduction

The persistence of fish populations in the Anthropocene is determined, above all, by the intensity of fisheries exploitation, through direct effects on population characteristics or indirectly through habitat degradation, and human-induced climate change (Brander 2010, Planque et al. 2010). These threats can interact synergistically or additively, such that the response of a population to climate change is enhanced in the presence of exploitation (Perry et al. 2010). The relationship between these two threats will thus determine population and community resilience to climate change/variability (Horodysky et al. 2015) where resilience is defined as the ability to resist or recover from environmental disturbance (Hodgson et al. 2015).

Fishing often targets the biggest individuals within populations; which tend to have life history traits such as high fecundity (Hixon et al. 2014) or excess body reserves (Sogard & Olla 2000) that can provide a buffer to climatic disturbances and thus enhance population climate resilience (Planque et al. 2010, Bates et al. 2014). Because these life history traits are often heritable, fishing – through the selective removal of specific phenotypic traits – can shape the evolutionary trajectory of exploited populations termed “fisheries-induced evolution” (Law 2000, Jørgensen et al. 2007, Allendorf & Hard 2009). Fisheries-induced evolution research has primarily focused on how selection can alter aspects of fish life history, such as growth rates (Enberg et al. 2012), or size at maturity, and fecundity (Kuparinen & Merilä 2007). The physiological consequences of fisheries-induced evolution have only been considered from a theoretical perspective (Hollins et al. 2018), yet it is alterations to physiological trait distributions that may have the greatest potential to move populations towards states associated with less resilience to climate change (Rijnsdorp et al. 2009, Hofmann & Todgham 2010, Bozinovic & Pörtner 2015).

How populations perform under a range of environmental conditions is fundamentally determined by their physiological rates and tolerances (Hofmann & Todgham 2010, Bernhardt & Leslie 2013, Bozinovic & Pörtner 2015). Temperature is the primary climate variable that

governs the physiological rates of ectothermic organisms such as fish (Schulte 2015). Consequently, an understanding of the relationship between temperature and physiological performance of fishes is paramount for predicting their capacity to persist in a future ocean environment (Cooke et al. 2013). Physiological concepts such as the metabolic theory of ecology (MTE) (Brown et al. 2004) and the dynamic energy budget (DEB) (Kooijman 2009) are examples of energetic, process-based approaches that can explain the relationship between the organism and its environment. Fry's (1947, 1971) concept of aerobic scope is, however, considered the most practical, unifying physiological concept as it links behaviour processes to energy metabolism constraints modulated by environments (Horodysky et al. 2015).

Extending on Fry's aerobic scope paradigm, the oxygen and capacity limited thermal tolerance (OCLTT) theory (Pörtner & Knust 2007), suggests that a mismatch between oxygen demand and oxygen supply across environmental gradients is the first mechanism to restrict animal performance. Absolute aerobic scope (AS), defined as the difference between standard (SMR) and maximum (MMR) metabolic rates, conceptually represents an approximation of the available energy budget for various energetic process (e.g., growth, reproduction, digestion) across various environmental gradients (e.g., temperature, oxygen saturation) above that required for the processes required to stay alive (e.g., respiration, osmoregulation, acid-base regulation) (Auer et al. 2015b, Metcalfe et al. 2016, Pörtner et al. 2017).

Under the aerobic scope paradigm, considerable variation in metabolic phenotypes among individuals (2–3 fold) has been reported (Metcalfe et al. 2016). Despite this, our knowledge of the potential consequences of low or high metabolic phenotypes is limited, but was recently found to be context dependent in terms of other environmental factors, such as food availability (Auer et al. 2015b). Understanding the diversity of metabolic phenotypes and their associated plasticity is a key consideration when evaluating the influence of environment stressors on fish populations in changing climates (Norin et al. 2016). Ward et al. (2016) suggest that the magnitude and variability of individual metabolic phenotypes influence the response of fish

populations to environmental stressors and have significant consequences for fisheries management. For example, the broader aerobic scope of pink salmon (*Oncorhynchus gorbuscha*), is thought to have facilitated successful spawning during warming conditions compared with other Pacific salmon species (Clark et al. 2011).

Although desirable fish population traits (life history, behavioural, physiological) are often reduced by fisheries exploitation (Pauly et al. 2002, Planque et al. 2010), it is surprising that the consequences of exploitation on physiological traits, that may promote climate resilience, has only recently been considered (Hollins et al. 2018). The aim of this chapter was therefore to discern the influence of fisheries exploitation in shaping the physiological trait distribution of *C. laticeps* and to elucidate how that may relate to climate change resilience. By quantifying physiological indices of individuals from protected populations (TNP MPA), an estimate of baseline (no exploitation) physiological trait distributions was obtained and compared with individuals from exploited populations. By simulating environmental temperature variability, the physiological response of the exploited and unexploited populations of *C. laticeps* populations was compared in an ecologically meaningful context.

## **3.2 Methods**

### **3.2.1 Experimental set-up**

A marine fish physiology laboratory was purpose-built at the Department of Ichthyology and Fisheries Science (DIFS), Rhodes University, for this experiment. The laboratory consisted of two controlled environment rooms (holding and experimental), and a workroom. The holding room contained a recirculating aquaculture system supporting two 5900 L cylindrical tanks with a filtration system comprising a sump (750 L slimline), protein skimmer (UltraZap with submerged Red Devil DC 5000s pump), bubble bead filter (BBF-200-COMP, Wilpet Koi Products), fluidised bed biological filter (750 L slimline tank with SuperActiFlo Media) and UV sterilisers (UVS-30, Wilpet Koi Products). Water was recirculated through the system via a pool pump (Speck Porpoise 0.75 kW) and air was supplied to the fluidised bed filter and tanks

using a 2.2 kW blower housed outside. Water temperature was maintained by a submerged heating element (1.5 kW titanium hotrod) and wall-mounted air conditioner, which were both connected to temperature controllers (STC-1000).

The experimental room contained a recirculating system, that comprised a single 2100 L cylindrical tank, with a filtration system consisting of a protein skimmer, bubble bead filter (BBF-100-COMP), fluidised bed biological filter and UV steriliser. The water temperature was manipulated using a heat pump (Aquaheat SF020P), which was connected in line to the filtration system, allowing water temperature to be closely manipulated. Air supplied from the same blower to the cylindrical tank and fluidised bed filter maintained 100% O<sub>2</sub> concentration. A separate recirculation loop continuously pumped cleaned water from the cylindrical tank into four glass tanks used to house the respirometers for the experiment (Figure 3.1).

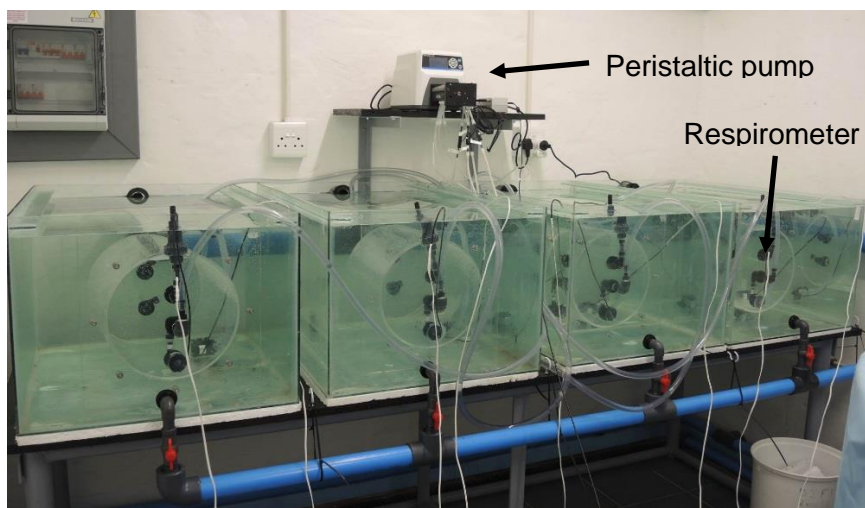


**Figure 3.1:** Experimental room housing four respirometers with each circulation loop connected to a peristaltic pump from where oxygen concentrations were measured.

### 3.2.2 Respirometers

Appropriate respirometer design is crucial for accurate metabolic rate measurements and varies depending on species lifestyle and organism size (Clark et al. 2013, Svendsen et al. 2016). Purpose-built intermittent flow respirometers (Figure 3.2) were developed following the guidelines of Clark et al. (2013) and Svendsen et al. (2016), as detailed below.

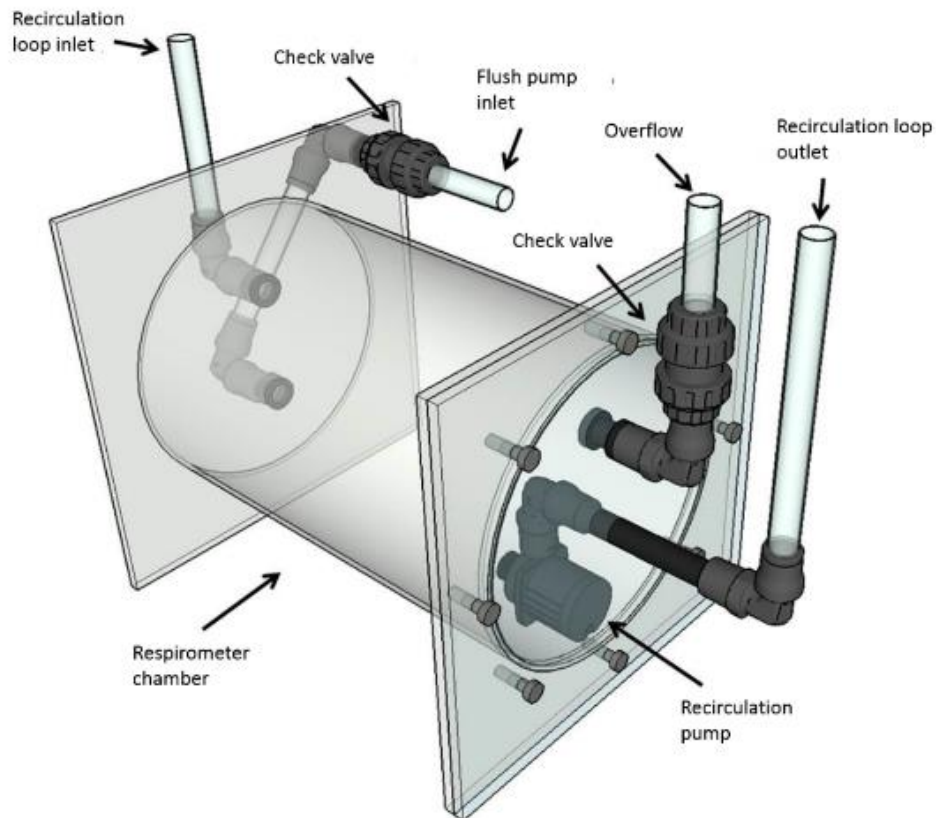


**Figure 3.2:** Design of intermittent flow respirometers. Flush pump inlet was connected to a pump set on a 15 min flush/5 min wait protocol. The recirculation pump continuously moved water through the recirculation loop via a peristaltic pump connected in line to an oxygen sensor and maintained mixing in the chamber. Check valves ensured no oxygen leakage during measurement periods.

Cylindrical respirometer chambers (29 cm internal diameter and a length of 45 cm) were used (Figure 3.2). These corresponded to g:ml ratio of between 20 and 70, depending on fish size, allowed for reasonable rates of O<sub>2</sub> decline, accommodated a specimen comfortably, but also limited potential movement. These chambers were small enough to measure a drop in O<sub>2</sub> concentration within a short time period that could yield sufficiently high  $R^2$  values, but not so small that oxygen levels depleted too quickly, resulting in hypoxic conditions. To reduce water stratification or localised variability in O<sub>2</sub> levels, water in the respirometers was mixed continuously using an internally mounted pump (800 L.h<sup>-1</sup> 12V DC pump), which was mounted onto the back of the respirometer with a recirculation loop plumbed in a non-contouring way (Figure 3.2). A flush pump (Red Devil DC 10000s) was used to introduce fresh seawater into the respirometer after the closed measurement period to replenish oxygen and wash out waste

products. The flush pump was regulated with a digital on/off timer (Eliro VODDTS) and split four ways into the respirometers, ensuring at least a four times flush volume ratio. To reduce oxygen leaks, the flush pump and overflow lines were fitted with one-way check valves (Figure 3.2). The recirculation loop was made from oxygen-impermeable thick-wall PVC tubing; the respirometer chamber was constructed from thick-wall Perspex, and the respirometer opening was bolted closed and sealed with a silicon O-ring.

Dissolved O<sub>2</sub> concentration readings (mg.L<sup>-1</sup>) were taken from the water in the recirculation loop using a four-channel peristaltic pump (Masterflex HV-07522 L/S standard drive with 4 multi-channel F/S pump head). Oxygen concentration was determined by passing this water through a cell with an optical oxygen sensor (OXFTC, Pyro Science GmbH) connected to a FireStingO2 fibre optic oxygen meter (FSO2-4, Pyro Science GmbH) with bare optical fibres (SPFIB-BARE, Pyro Science GmbH). Oxygen concentration levels were recorded using Pyro Oxygen Logger Software (Pyro science GmbH).

### 3.2.3 Fish capture and husbandry

Live *C. laticeps* specimens were collected from both the exploited and protected areas in September 2016 on the 20<sup>th</sup> and 23<sup>rd</sup>, respectively. Fish were caught using hook and line with standard boat angling tackle off a ski-boat in water between ~12 m and ~25 m depth. Once landed fish were vented using a hypodermic needle and placed into a 1000 L tank filled with fresh seawater, transported back to the shore and transferred to a large, circular holding tank, which was continuously supplied with fresh seawater using a submersible pump. Fish were retained in this tank for approximately five hours before being transported to the laboratory at DIFS in a 1000 L tank, with a constant supply of 100% O<sub>2</sub> for the duration of the journey. Fish were then transferred into the holding system tanks according to sampling area, where they remained until experimented on. There was no significant difference in weight or condition factor between fish caught from exploited/protected populations (Table 3.1).

**Table 3.1:** Mean condition factor (CF) and standard error (SE), mean weight (weight (g)) and standard error (SE), and weight range in grams (g) for number of specimens (n) per sampling population used in this study. There was no significant difference in condition factor or mass of specimens between populations (one-tailed T-test,  $p$ -value > 0.05).

Population	n	CF (SE)	weight (g) (SE)	weight range (g)
Exploited	25	2.86 (0.04)	879 (63.30)	402–1500
protected	25	2.84 (0.05)	946 (77.21)	320.9–1794

Fish were acclimated for six weeks in the holding tanks prior to the start of the experiment. During this time, the temperature was kept constant at 16 °C and a photoperiod was set to 9.5 h of light and 14.5 h dark. Oxygen, salinity, pH and ammonia were measured once daily and adjusted if necessary. Fish were fed a diet of frozen sardine (*Sardinops sagax*) and squid (*Loligo reynaudii*) every other day. Because of the positive relationship between food availability and standard metabolic rate (SMR) (Auer et al. 2016), it was important to control feeding rates. To ensure every fish was fed, food was cut into large chunks and fed to fish individually (<https://www.youtube.com/watch?v=SJ2hedCXiMY>).

#### 3.2.4 Experimental procedure

After a 36-hour fasting period, a single fish was placed into each of the four respirometers (two from each population) at 16 °C and given 12 hours to acclimate prior to experimentation (Figure 3.3). In order to mimic the natural temperature variability that fish experience in the wild, the temperature was either increased or decreased by one degree per hour to temperatures of 8, 12, 20 and 24 °C or maintained at 16 °C, simulating upwellings or downwelling of various intensities.

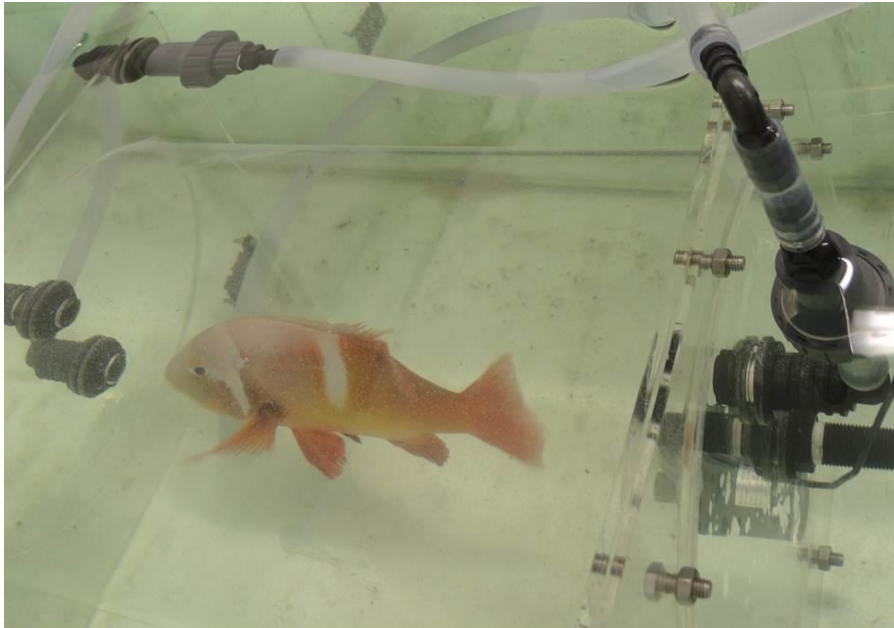


**Figure 3.3:** Test specimen housed within a respirometer during an experimental trial.

Once the final test temperature had stabilised, SMR measurements were immediately recorded using intermittent flow respirometry with a five-minute measurement period followed by a fifteen-minute flushing period. The measurement cycle was adjusted to a three-minute measurement and seventeen-minute flushing period at the 24 °C test temperature to account for the increase in metabolic rate. The SMR measurements were taken for a minimum of 20 hours to account for diel variability in metabolic rates (Chabot et al. 2016).

To elicit MMR, individuals were transferred alone to the small cylindrical tank in the experimental room, chased to exhaustion for ten minutes, exposed to air for 30 seconds and placed back into the respirometer. Oxygen concentration was recorded within 20 seconds of the fish being returned to the chamber. This was assumed to be the most appropriate method to induce MMR because of the reef-associated lifestyle of the species (Roche et al. 2013, Norin & Clark 2016). This protocol also ensured that MMR was elicited across the test temperature range (8 to 24 °C). The intermittent flow respirometry experiment was terminated once the decline in oxygen consumption appeared to stabilise at levels near SMR measurement periods. Background respiration data was subsequently recorded by measuring oxygen concentration within closed and empty respirometers for approximately three hours.

### 3.2.5 Data preparation

Data generated throughout the experimental protocol consisted of a series of measurement and flushing periods (Figure 3.4). These were used to create a dataset of numerous independent rates of oxygen consumption for each specimen. A quality threshold  $R^2 > 0.9$  was implemented to filter the linear decline in oxygen during measurement periods, except for the 8 °C test temperature, where a threshold of 0.8 was used to maintain sample sizes as rates of decline were low.

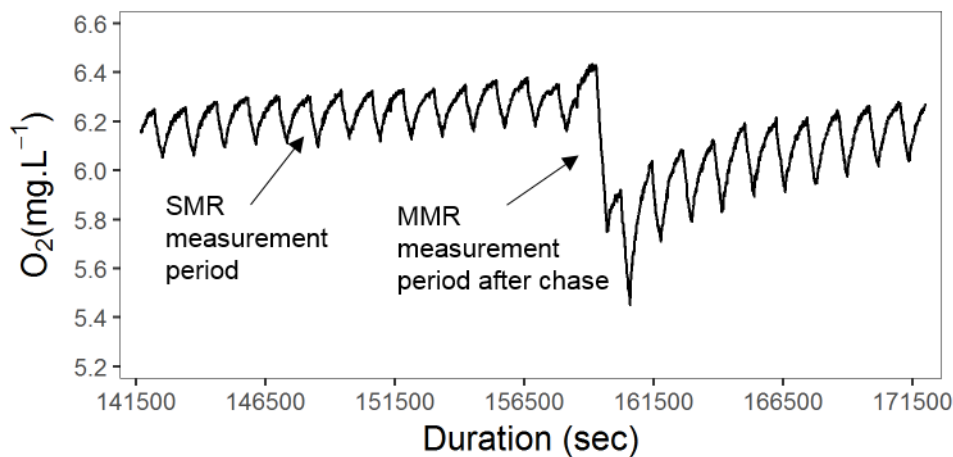


**Figure 3.4:** Example of an intermittent flow respirometry dataset. Each decline in oxygen concentration ( $O_2(\text{mg. L}^{-1})$ ) represents the five-minute measurement period and increases in oxygen concentration represent the fifteen-minute flushing period over a time period measured in seconds (sec). The steep decline in oxygen concentration represents the measurement period directly after maximum metabolic rate elicitation.

The rate of oxygen consumption ( $\text{mg.kg}^{-1}.\text{h}^{-1}$ ) for each measurement period ( $RO_2$ ), excluding the first minute as wait time, was calculated using Equation 3.1 which was adapted from Svendsen et al. (2016).

$$RO_2 = \left( \left( \frac{V_{re} - M}{W} \right) \left( \frac{\Delta[O_{2a}]}{\Delta t} \times 60 \right) \right) - \left( \left( \frac{V_{re} - M}{W} \right) \left( \frac{\Delta[O_{2b}]}{\Delta t} \times 60 \right) \left( \frac{V_{re}}{V_{re} - M} \right) \right) \quad (\text{Equation 3.1})$$

where  $V_{re}$  is the total volume of the respirometer in litres;  $M$  is the mass of the specimen in kg expressed as l;  $W$  is mass of the specimen in kg,  $\frac{\Delta[O_{2a}]}{\Delta t}$  is the slope of the linear decrease in oxygen concentration during the measurement period and  $\frac{\Delta[O_{2b}]}{\Delta t}$  is the slope of the linear decrease in oxygen concentration when no specimen was in the chamber (background respiration).

A number of different techniques have been used to estimate SMR from intermittent flow respirometry data of fishes that yield variable results when applied to the same dataset (Chabot et al. 2016). Following the recommendations of Chabot et al. (2016), the quantile that assigned the bottom 20% of the data was used as an estimate of SMR for all measurement periods at test temperatures, prior to elicitation of MMR, as the coefficient of variation between readings was generally above the proposed 5.4% threshold. Maximum metabolic rate was estimated as the single biggest rate of oxygen consumption following the post-exhaustive recovery period (Killen et al. 2016).

Metabolic rates are well approximated when their major influences, temperature, and mass, are accounted for (Gillooly et al. 2001). Typically, metabolic rates scale with mass as a power function and temperature as a function of the Boltzmann factor (Brown et al. 2004). In order to determine the effect of mass on metabolic rates, data was temperature corrected ( $RO_{2(\text{temp corrected})}$ ) following Equation 3.2.

$$RO_{2(\text{temp corrected})} = RO_2 \times e^{\frac{-E}{kT}} \quad (\text{Equation 3.2})$$

where  $E$  is the average activation energy of ectotherms  $\sim 0.63$  eV (Gillooly et al. 2001),  $k$  is the Boltzmann constant  $8.617 \ 3303 \times 10^{-5}$  eV.K<sup>-1</sup> and  $T$  is the absolute temperature in kelvin.

The slope of the linear regression between the natural logarithm of  $RO_{2(\text{temp corrected})}$  and the natural logarithm of mass was used to estimate the allometric exponent ( $\alpha$ ) of the mass scaling relationship with both SMR and MMR data.  $RO_2$  data was then mass corrected ( $MO_2$ ) using the mass scaling relationship following Equation 3.3.

$$MO_2 = \frac{RO_2}{M^\alpha} \quad (\text{Equation 3.3})$$

where  $MO_2$  is mass normalised SMR or MMR,  $RO_2$  is standard or maximum oxygen consumption rate,  $M$  is the mass of the organism and  $\alpha$  is the allometric mass scaling exponent.

Absolute aerobic scope (AS) was calculated using mass normalised metabolic rates following Equation 3.4.

$$AS = MMR - SMR \quad (\text{Equation 3.4})$$

Where MMR is mass normalised maximum metabolic rate and SMR is mass normalised standard metabolic rate

### 3.2.6 Statistical analysis

A generalised least squares (GLS) modelling approach was implemented using the nlme package (Pinheiro et al. 2017) to account for data heteroscedasticity in R version 3.3.3 (R Core Team 2017). Differences in mass-corrected metabolic rate data between sampling populations were tested by modelling a second order polynomial relationship between metabolic data and temperature, including population (exploited/protected) as an interaction term, and a variance structure weighted by temperature and population (exploited/protected). Orthogonal polynomials were used for statistical inference to reduce the effect of collinearity among explanatory polynomial terms (Rawlings et al. 1998). Metabolic phenotype variability per exploited/protected populations was compared using a paired (by test temperature) student's T-test on the variance structure of the aerobic scope GLS model. A piecewise linear breakpoint relationship was estimated on an Arrhenius plot of standard metabolic rate against temperature for each population to determine the point of departure from linearity, using the segmented package (Muggeo 2003, 2008).

### 3.3 Results

#### 3.3.1 Mass correcting $MO_2$ data

Considerable variation in non-mass-corrected SMR data, which could obscure any clear trend with temperature, was recorded (Figure 3.5 a). The natural logarithm of temperature-corrected SMR scaled linearly with the natural logarithm of mass with a mass scaling exponent estimated as 0.97 (Figure 3.5 b). Mass-corrected SMR reduced the variability among the data but showed conditional heteroscedasticity as variances increased with temperature (Figure 3.5 c).

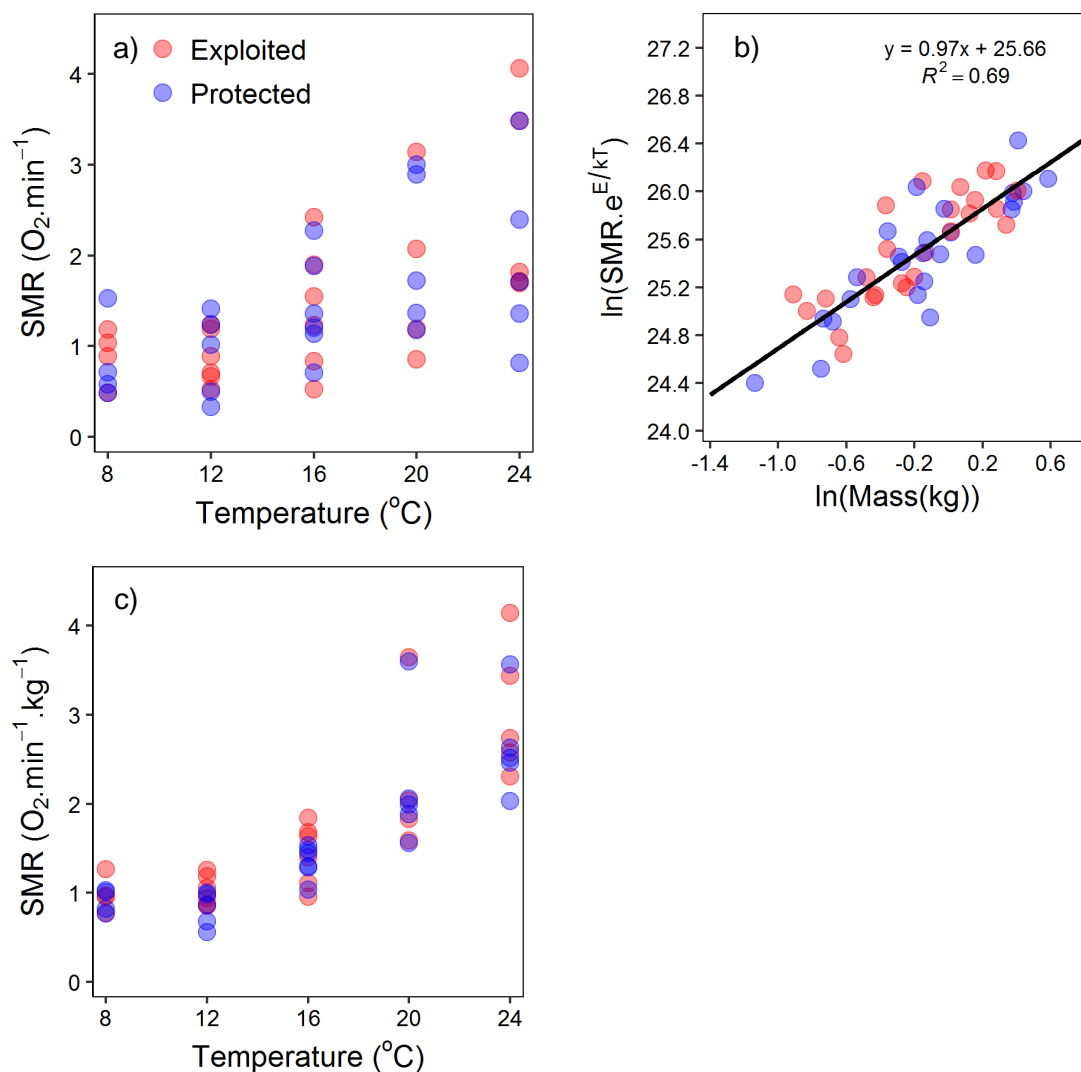


**Figure 3.5:** Mass correcting SMR data process showing raw SMR data ( $\text{SMR } (O_2 \cdot \text{min}^{-1})$ ) per temperature (a) regression of the natural logarithm of temperature-corrected SMR ( $\ln(\text{SMR} \cdot e^{E/kT})$ ) against the natural logarithm of mass ( $\ln(\text{Mass}(\text{kg}))$ ) (b) and mass-corrected SMR data ( $\text{SMR } (O_2 \cdot \text{min}^{-1} \cdot \text{kg}^{-1})$ ) per temperature used for the analysis (c).

Non-mass-corrected MMR data also showed variability, which again obscured any clear trend with temperature (Figure 3.6 a). The allometric mass scaling exponent of MMR was taken as 0.82 (Figure 3.6 b). Mass-corrected MMR showed no trend in variance with temperature (Figure 3.6 c).

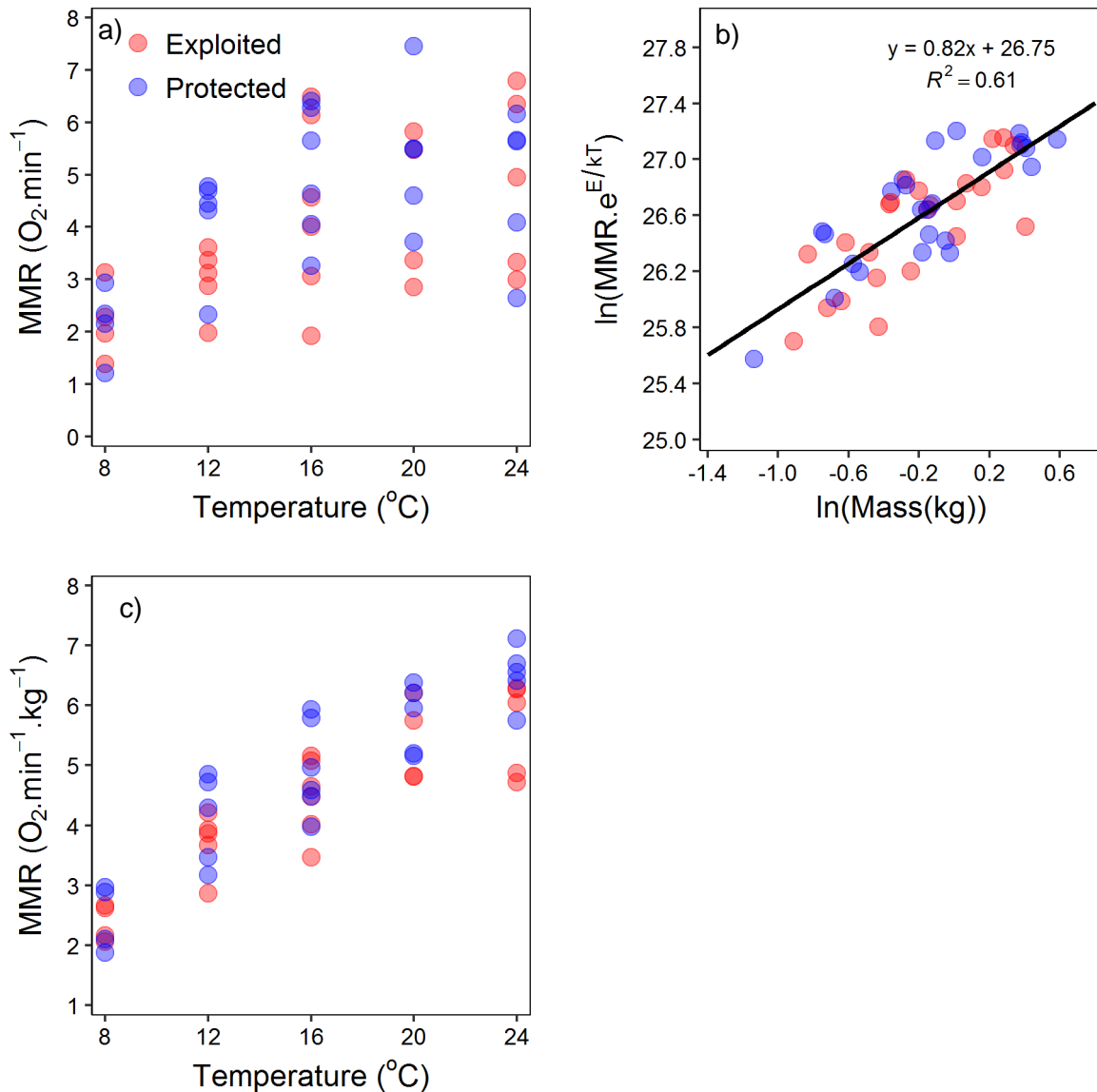


**Figure 3.6:** Mass correcting MMR data process showing raw MMR data ( $\text{MMR} (\text{O}_2 \cdot \text{min}^{-1})$ ) per temperature (a) regression of the natural logarithm of temperature-corrected MMR ( $\ln(\text{MMR} \cdot e^{E/kT})$ ) against the natural logarithm of mass ( $\ln(\text{Mass}(\text{kg}))$ ) (b) and mass-corrected MMR data ( $\text{MMR} (\text{O}_2 \cdot \text{min}^{-1})$ ) per temperature used for the analysis (c).

### 3.3.2 Standard Metabolic and Maximum Metabolic Rates (SMR and MMR)

There was no significant influence of exploitation/protection (population) on the relationship between SMR and temperature ( $p$ -value = 0.214, Table 3.2). Population did, however, have a significant influence on the relationship between MMR and temperature ( $p$ -value = 0.015,

Table 3.3).

**Table 3.2:** Generalised least squares modelling results for SMR of *Chrysoblephus laticeps* from an exploited and a protected population, presented as a quadratic function of temperature (Temp), with exploitation/protection (population) as an interaction term. SE is standard error, AIC is Akaike information criterion, and significant  $p$ -values are highlighted in bold.

Effect	Estimate	SE	t-value	$p$ -value
Intercept	1.744	0.100	17.440	<b>0.000</b>
Population	-0.157	0.125	-1.263	0.214
Temp	5.250	0.756	6.946	<b>0.000</b>
Temp <sup>2</sup>	1.854	0.510	3.637	<b>0.001</b>
Population: temp	-0.489	0.976	-0.501	0.619
Population: temp <sup>2</sup>	-0.236	0.655	-0.360	0.721
AIC	65.639			
Residual SE	0.201			

**Table 3.3:** Generalised least squares modelling results for MMR of *Chrysoblephus laticeps* from an exploited and a protected population, presented as a quadratic function of temperature (Temp), with exploitation/protection (Population) as an interaction term. SE is standard error, AIC is Akaike information criterion and significant  $p$ -values are highlighted in bold.

Effect	Estimate	SE	t-value	$p$ -value
Intercept	4.390	0.122	36.092	<b>0.000</b>
Population	0.440	0.174	2.530	<b>0.015</b>
Temp	7.696	0.836	9.205	<b>0.000</b>
Temp <sup>2</sup>	-1.684	0.772	-2.180	<b>0.035</b>
Population: temp	1.587	1.140	1.392	0.171
Population: temp <sup>2</sup>	0.232	1.114	0.203	0.840
AIC	111.989			
Residual SE	0.306			

Overall, both SMR and MMR increased with temperature (Figure 3.7 a, b). However, the rate of change in metabolic rate increased logarithmically with temperature for SMR, but decreased with temperature for MMR.

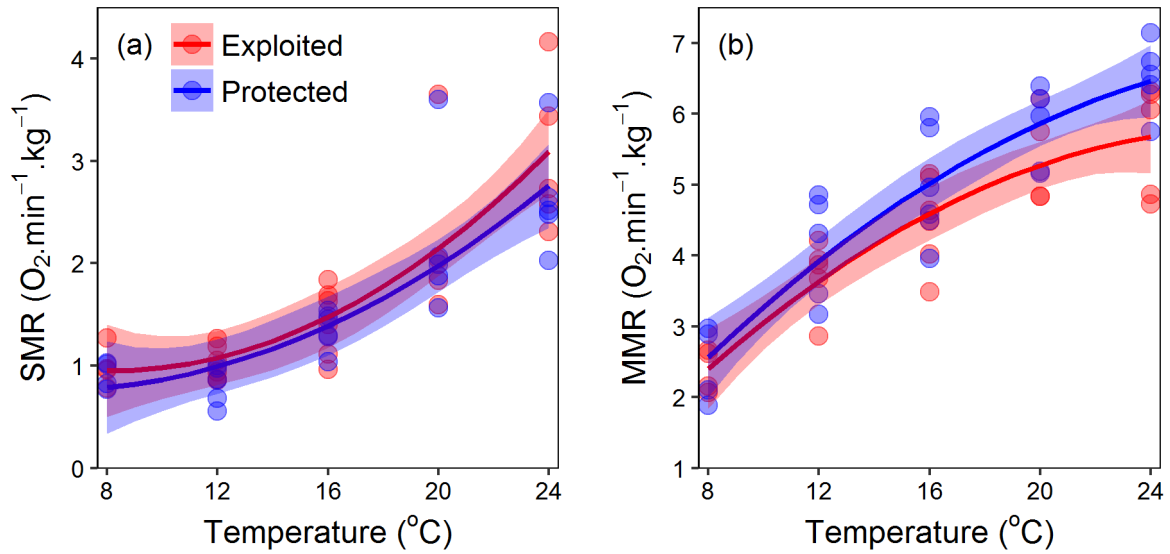


**Figure 3.7:** GLS model fits per exploited (red) and protected (blue) sampling populations for standard metabolic rate (SMR) (a) and maximum metabolic rate (MMR) (b) across test temperatures with shaded areas representing 95% confidence interval.

### 3.3.3 Aerobic Scope (AS)

Population (exploited/protected) had a significant effect on the relationship between AS and temperature ( $p$ -value = 0.007,

Table 3.4). Modelled AS was greater across all temperatures for protected populations (Figure 3.8) and differences in AS increased as temperature increased (Figure 3.8).

**Table 3.4:** Generalised least squares modelling results for aerobic scope (AS) of *Chrysolephus laticeps* from an exploited and protected population, presented as a quadratic function of temperature (Temp), with exploitation/protection (Population) as an interaction term. SE is standard error, AIC is Akaike information criterion and significant  $p$ -values are highlighted in bold.

Effect	Estimate	SE	t-value	$p$ -value
Intercept	2.630	0.108	24.272	<b>0.000</b>
Population	0.515	0.180	2.858	<b>0.007</b>
Temp	2.465	0.721	3.417	<b>0.001</b>
Temp <sup>2</sup>	-3.488	0.745	-4.682	<b>0.000</b>
Population: Temp	1.731	1.341	1.291	0.204
Population: Temp <sup>2</sup>	0.708	1.324	0.535	0.597
AIC	117.094			
Residual SE	0.203			

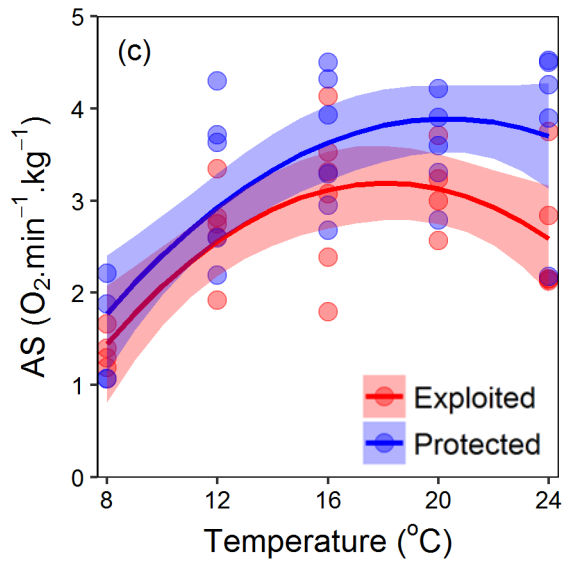


**Figure 3.8:** GLS model fits per exploited (red) and protected (blue) sampling populations for absolute aerobic scope (AS) across test temperatures with shaded areas representing 95% confidence interval.

### 3.3.4 Aerobic Scope (AS) variability

Variability in AS was greater for protected than exploited populations at all temperatures following an acute temperature change (8, 12, 20, 24 °C) (Figure 3.9). However, variability in AS was similar at 16 °C, which corresponded to the same temperature as the holding environment and hence, no acute change. This disparity between populations in AS variability was significant when tested using a paired one-way T-test ( $p$ -value = 0.0326,  $t$ -stat = -2.5224,  $df = 4$ ).

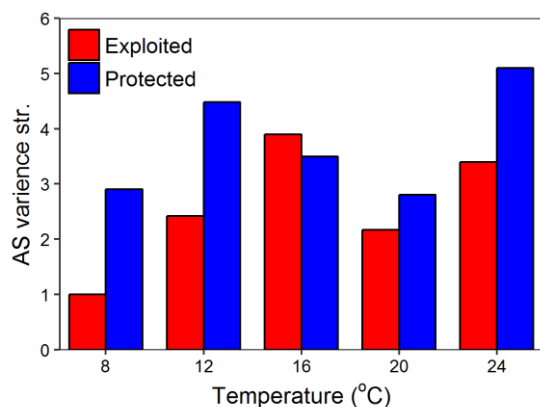


**Figure 3.9:** Variance structure of the absolute aerobic scope generalised least squares model (AS variance str) partitioned by temperature and population for exploited (red) and protected (blue) populations.

### 3.3.5 Cold shock

Standard metabolic rates scaled predictably with temperature except at 8 °C (Figure 3.10), where SMR were higher than the predicted linear relationship. A piecewise linear breakpoint analysis indicated that the point of departure from linearity for individuals from the exploited population occurred at 12.7 °C. The breakpoint could not be identified for individuals from the protected population as the breakpoint likely occurred between 12 and 8 °C, which meant there was insufficient data points to estimate a slope of the second linear model.

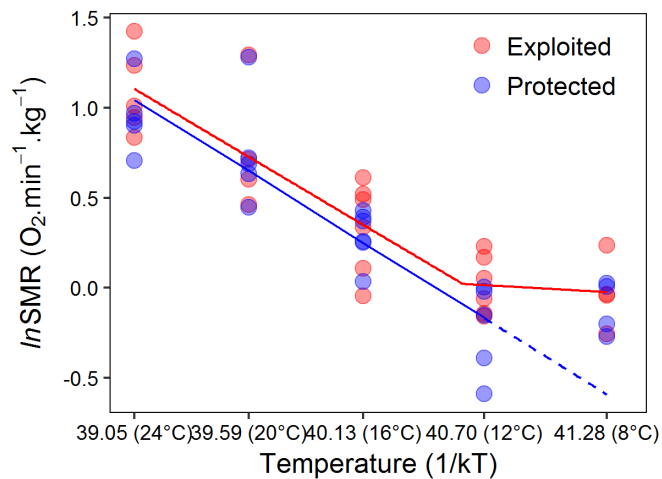


**Figure 3.10:** Linear temperature dependence of the natural logarithm of mass-corrected standard metabolic rate ( $\ln\text{SMR}$ ) and temperature ( $1/kT$ ), where temperature ( $T$ ) is measured in Kelvin and  $k$  is the Boltzmann constant, for exploited (red) and protected (blue) sampling populations. Corresponding test temperature in °Celsius is indicated in brackets. The regression line was derived using temperatures 39.05 to 40.70 (24 to 12 °C) and predicted towards 41.28 (8 °C) for the exploited population as no breakpoint relationship was measurable.

### 3.4 Discussion

Overall, this chapter finds that protected populations have more aerobic scope phenotypic diversity and more high performance aerobic scope phenotypes, indicating that fisheries exploitation can alter the diversity and distribution of physiological phenotypes among populations. The mechanism underpinning this finding may be the positive association between aerobic scope and passive-gear fishing vulnerability. Indeed, aggression and boldness are behavioural traits associated with a high vulnerability to capture in passive-gear fisheries (Wilson et al. 2015, Klefoth et al. 2017, Lennox et al. 2017). These behavioural traits are also associated with high aerobic scope phenotypes (Killen et al. 2014, Binder et al. 2016, Rupia et al. 2016). Furthermore, the findings are congruent with recent research on behavioural selection, where exploitation was shown to reduce behavioural diversity of largemouth bass (*Micropterus salmoides*) (Cooke et al. 2017), which can lead to populations with more timid individuals (Arlinghaus et al. 2017).

The OCLTT (Pörtner et al. 2017), suggests that high-performance aerobic scope phenotypes, which are characterised by an enhanced ability to raise metabolic rates above standard metabolic rate, will have a performance advantage (Clark et al. 2017). In this context, the lower aerobic scope phenotypes of exploited populations indicate that energetic processes can be more compromised, especially when temperatures are out of their optimal range and particularly at warmer temperatures. This may have important ramifications for energy budget partitioning during marine heatwaves which occur through *C. laticeps*' distribution and are predicted to increase in frequency and severity as climate change progresses with time (Schlegel et al. 2017, Frölicher et al. 2018, Oliver et al. 2018). High-performance aerobic scope phenotypes (greater difference between MMR and SMR) (Clark et al. 2017) however, can be characterised by higher standard metabolic rates that can be detrimental in sub-optimal conditions (Auer et al. 2015a). This was not the case in this study, as there were no significant differences in standard metabolic rates of individuals between populations across all thermal simulations. The OCLTT is, however, an active scientific debate and more evidence for or

against must be a priority physiological research area (Jutfelt et al. 2018, See General Discussion for further information).

In an increasingly variable and uncertain climatic future, maintaining the diversity of physiological phenotypes is important to maintain the adaptive potential of populations (Chown et al. 2010) and ensure population persistence across dynamic thermal contexts (Hofmann & Todgham 2010, Bernhardt & Leslie 2013, Norin et al. 2016, Sandblom et al. 2016). Furthermore, the ability of populations to acclimate to unprecedented rates of change in environmental variables can be achieved via behavioural plasticity as a first response (Wong & Candolin 2015, Beever et al. 2017). New research suggests that the capacity of an individual to exhibit behavioural plasticity is increased for individuals with high aerobic scope phenotypes (Biro et al. 2018). The reduced aerobic scope across all temperatures of exploited populations may therefore limit the potential for behavioural plasticity when coping with climate perturbations.

It is a concern that *C. laticeps* may already occur in regions where it is at its limit in terms of cold tolerance, as indicated by the reduced metabolic phenotype diversity and capacity, and the breakdown of standard metabolic rates scaling with temperature for both populations during extreme upwelling simulations (8 °C), likely due to cold shock. Cold shock results from a cascade of physiological and behavioural responses following the stress of an acute decline in temperature (Donaldson et al. 2008, Szekeres et al. 2016). The findings of cold shock are in accordance with a previous study on bonefish that described a reduced performance capacity at extreme cold event simulations (Szekeres et al. 2014). Furthermore, large fish mortalities have been reported following extreme temperature declines within the TNP MPA, with a number of dead *C. laticeps* documented following a cold event in 1981 (Hanekom et al. 1989). Despite the impact of extreme cold events on fish performance, such events have received relatively little attention in the climate change literature (Boucek et al. 2016).

The results highlight the potential negative impact of cold-related mortality in both exploited and protected populations which is particularly relevant for endemic linefish species in South

Africa, given that upwelling favourable winds have intensified in recent decades (Sydeman et al. 2014, García-Reyes et al. 2015). Greater frequencies and intensities of intermittent upwelling along the south coast have already been observed (Rouault et al. 2010) and cold events are more extreme on the south coast than those along the west and east coasts of South Africa (Schlegel et al. 2017). However, protected populations were able to maintain basal metabolic rates over greater acute declines in temperature than exploited populations, based on the piecewise breakpoint analysis (although no breakpoint could be identified for protected populations), which should enhance their ability to cope physiologically during extreme upwelling events.

While the findings of reduced high-performance aerobic scope phenotypes and aerobic phenotype diversity among exploited populations are interpreted as being attributable to fishing, other explanations were considered. For instance, different temperature signals, or the condition of fish between the two sampling populations could lead to different metabolic profiles of the two populations. However, similar long-term trends (Table 2.1, Figure 2.4 d) and similar magnitude and timing of acute thermal changes between study areas (Figure 2.6) were found in the previous chapter. There was also no significant difference in mass or condition between individuals collected from each of the populations (Table 3.1). If factors such as food availability were markedly different between the two areas, one would expect a difference in the standard metabolic rate between the two populations – which was not observed (Auer et al. 2016).

Because of the role that physiological phenotypes play in shaping the response of populations to the environment (Bernhardt & Leslie 2013), research into fisheries selection pressures on physiological phenotypes in the context of anthropogenic-induced climate change is emerging as an important area of conservation physiology research (Clark et al. 2017, Hollins et al. 2018). These phenotypes would need to be heritable, and certainly, growing evidence supports this contention (Philipp et al. 2009, Auer et al. 2018, Hollins et al. 2018). For example, Redpath et al. (2010) found populations of largemouth bass (*Micropterus salmoides*) that were

bred for high vulnerability to angling are associated with high aerobic scope phenotypes and Munday et al. (2017) bred multiple generations of reef damselfish (*Acanthochromis polyacanthus*) at elevated temperatures and found metabolic traits were heritable and contained a large component of adaptive genetic variation. The evidence of the potential for physiological-based fisheries-induced evolution and its likely effect on climate change resilience further highlights the need for an evolutionary enlightened management approach in capture fisheries (Jørgensen et al. 2007), which can be achieved through spatial protection.

At a community/ecosystem level, protection from fishing can facilitate temporal stability in the face of climate-related disturbances (Bates et al. 2014, Aller et al. 2017) or promote recovery following disturbance (Duffy et al. 2016) because of a higher functional trait complexity. At a population level, protection from fishing maintains larger populations that conserve age structures, life history parameters and maintain genetic diversity, which should enhance population stability by buffering the climate-recruitment relationship (Hsieh et al. 2006, Ottersen et al. 2006, Anderson et al. 2008) and maintain the raw material required for adaptation (Roberts et al. 2017). This study extends knowledge on how MPAs can be implemented as a climate management tool, by harbouring populations with greater physiological phenotype diversity and high-performance aerobic scope phenotypes. Given the spillover effect of MPAs (Kerwath et al. 2013a, Le Port et al. 2017), well-designed networks of MPAs have the potential to buffer the selective removal of high-performance metabolic phenotypes in commercial linefisheries, potentially leading to a greater level of physiological resilience of the population in a changing ocean.

## 4 Chapter 4

Upwelling intensity and post-spawning sea temperature drive the growth of *Chrysoblephus laticeps*



Two roman seabream swimming away from the camera on a cool-temperate rocky reef

(photo credit: Steven Benjamin)

## 4.1 Introduction

Ambient environmental variables, such as temperature, influence rates of reproduction, growth and survival, determine the demographic structure, and regulate the abundance of fish populations (Poloczanska et al. 2016). As such, anthropogenic-induced climate change can exert forces on demographic rates that may undermine the persistence of fish populations (Rijnsdorp et al. 2009, Planque et al. 2010). Population somatic growth rates are also key demographic parameters of productivity models which are used to set sustainable management strategies for commercial fish populations (Audzijonyte et al. 2013, Methot & Wetzel 2013, Lee et al. 2017). An understanding of which environmental variables drive growth is thus essential for predicting how fish population productivity and abundance will change in the future (Morrongiello et al. 2014, Doubleday et al. 2015).

Previous studies have identified a diverse set of environmental drivers on fish somatic growth at various times during their annual growth cycles and this highlights the need for quantifying species- and area-specific growth-environment relationships. For example, Black et al. (2011b) found that the strength of winter upwelling events influenced the growth patterns of the splitnose rockfish (*Sebastes diploproa*) and yelloweye rockfish (*S. ruberrimus*) off the coast of California. In contrast, Dzaugis et al. (2017) found that warm sea surface temperature anomalies, southeast wind stress and high sea level pressure in spring were associated with positive growth anomalies in red snapper (*Lutjanus campechanus*), grey snapper (*L. griseus*) and black drum (*Pogonia cromis*) in the Gulf of Mexico. Overall, the inter-annual variation in environmental variables that have been found to drive fish growth are often linked to large-scale global phenomena such as the ENSO or longer-term climate-system regime shifts that have themselves been found to modulate fish production (Mantua et al. 1997, Attrill & Power 2002, Stenseth et al. 2002).

These previous studies often develop environmental predictor variables with annual and seasonal temporal resolutions (e.g., Doubleday et al. 2015b) or, at most, monthly resolution (e.g., Black et al. 2008). Annual or monthly environmental predictors however, may not fully

capture any fine-scale, high-frequency environmental variability that can be important in explaining fish growth responses. Quantifying and incorporating this variability is likely to be particularly necessary for the South African coastal zone, where extreme environmental variability is a common occurrence (Chapter 2) and can exceed an organism's environmental niche (Chapter 3). Furthermore, this environmental variability is governed by global weather phenomena such as ENSO (Rouault et al. 2010) which is predicted to increase in frequency and severity with climate change (Cai et al. 2014, Wang et al. 2017).

To predict changes in the somatic growth rates of fish populations in response to climate change, the historical growth response to environmental variability is often first determined and extrapolated forward (Morrongiello et al. 2012). Long-term historical records of population demographic parameters such as growth rates are, however, rare in aquatic environments, making accurate climate change responses difficult to predict (Gillanders et al. 2012, Morrongiello et al. 2012). The unique properties of fish otoliths, such as the formation of annuli and the relationship between otolith size and fish size, allow the elucidation of individual annual growth throughout the life of a fish (Thresher et al. 2007, Gillanders et al. 2012). By supplementing contemporary otoliths with historical collections, long-term growth biochronologies of fish populations can be developed, permitting the influence of environmental variables on growth rates to be quantified (Morrongiello et al. 2012).

The width of an individual's otolith increment for a given year is potentially influenced by factors relating to the previous year, and by intrinsic (e.g., age-related decline in growth rate) and extrinsic (e.g., temperature) variables. A number of statistical approaches have been applied to remove this temporal autocorrelation, which allows the influence of extrinsic environmental variables on growth to be appropriately quantified (Morrongiello et al. 2012). Age-specific growth involves measuring otolith widths for a specific age, thus removing the repeated increment measurements among individuals and the age effect (e.g., Neuheimer et al. 2011; Thresher et al. 2007). The age-specific approach is, however, limited, as only a particular period of an individual's life history is examined and a staggered sampling protocol is required

to obtain sufficient temporal resolution (Morrongiello et al. 2012). Dendrochronological techniques (e.g., Black et al. 2008, 2011a, Rypel 2009) offer an alternative approach for removing the effect of age. Here the age effect is detrended and standardised for each individual and a master chronology developed by averaging individual standardised growth rates per year. The dendrochronological approach has limitations, including a lack of consideration for the ecological and physiological sources of variability within data and results in biochronologies with dimensionless indices that prohibit any elucidation of growth responses at an intra- and inter-population level (Lapointe-Garant et al. 2010, Morrongiello et al. 2012, Doubleday et al. 2015). By accounting for autocorrelated data through random effects structuring and incorporating intrinsic effects such as age in the modelling process, mixed effects models have overcome the limitations of age-specific and dendrochronological techniques for examining growth biochronologies (Weisberg et al. 2010, Morrongiello & Thresher 2015).

The overarching environmental driver of fish growth reported in studies is water temperature (e.g., Mazlouni et al. 2017; Rountrey et al. 2014; Stoessel et al. 2012). This is not surprising as fish are ectothermic, and ambient temperature determines the physiological rates that underpin growth (West et al. 2001). The effect of temperature on growth is, however, variable and can influence growth rates either positively or negatively, depending on where environmental temperatures lie in relation to species physiological optimum (Neuheimer et al. 2011). The growth-temperature response varies because excess energy can only be allocated to growth after meeting baseline energetic requirements, but is limited by maximum metabolic rates (Auer et al. 2015a). Because of the influence of physiology on growth rates, aquatic biochronology models should at the very least be interpreted in the context of physiological thresholds and optima (Morrongiello et al. 2012).

Selective exploitation can drive populations to altered physiological states (Chapter 3) and altered growth rates (Enberg et al. 2012) but the reasons why the growth of fishes in exploited populations tend to fluctuate more than those that are protected from exploitation remains less

established (Hsieh et al. 2006, Anderson et al. 2008). Whether exploitation has driven populations to more thermally sensitive and compromised physiological states that modulate the relationship between environmental variables and growth has not been resolved. The aim of this chapter was therefore to quantify environmental drivers on *C. laticeps*' growth and to compare the sensitivity of the growth response between exploited and protected populations in the context of the aerobic scope curves developed in Chapter 3. To do this, otolith-derived growth biochronologies of *C. laticeps* were developed from each sampling location and the influence of environmental variables on somatic growth explored using a mixed modelling framework (Weisberg et al. 2010, Morrongiello & Thresher 2015).

## **4.2 Methods**

### **4.2.1 Otolith collection and preparation**

Archived sagittal otolith collections from previous research on *C. laticeps* within the protected (TNP MPA) and the exploited area west of (PE) were obtained from the South African Institute for Aquatic Biodiversity (SAIAB). These otoliths were collected as part of a larger research programme examining the age and growth of Sparid fishes in the region (Buxton 1987). These historical collections were supplemented with contemporary otoliths collected during 2016. To examine the otoliths, the protocols of previous age and growth studies on *C. laticeps* (Buxton 1993, Götz et al. 2008) were followed. Each otolith was mounted in one-inch thick resin (Struers EpoFix) and cut transversely through the nucleus with a 400-micron diamond edge wafering blade on an Isomet slow-speed saw (Buehler). The exposed side was then hand ground on 15-micron silicon carbide, followed by three-micron aluminium oxide and mounted onto a glass slide with type 301 epoxy resin (Logitech). Mounted otoliths were sectioned to a thickness of between 0.35–0.45 mm with a PetroThin cutting and grinding trim saw (Buehler). Sectioned otoliths were then ground following the same protocol, before being polished for ten minutes with 0.3-micron aluminium oxide on a Petropol polisher (Buehler). Otoliths were viewed and photographed under a microscope, at a magnification of between 80–160 X, under

reflected light on a dark background, such that hyaline zones appeared black. If growth bands were distinct and the reader was able to accurately mark the beginning and end of each hyaline/opaque band, the otolith was photographed; otherwise it was discarded.

#### 4.2.2 Otolith increment measurements

*Chrysoblephus laticeps* deposits a single annulus a year with the hyaline zone (representing fast growth) occurring in autumn and winter (March to August) and the opaque zone (representing slow growth) in spring and summer (September to February) (Buxton 1987). Because the date of capture was known for each otolith sample, growth zones could be assigned a calendar growth year (CGY) working from the outermost growth zone inwards. The end of each hyaline zone (dark band) was marked along a measurement transect through the dorsal side of the sulcus acusticus (Figure 4.1) and measured to the nearest 0.0001 mm using the object J plugin for Image J (Schneider et al. 2017). A CGY therefore began in September (beginning of opaque band) and ended in August (end of hyaline band) the following year. Only years  $\geq 4$  were included to exclude immature fish and minimise error associated with false bands during early years.

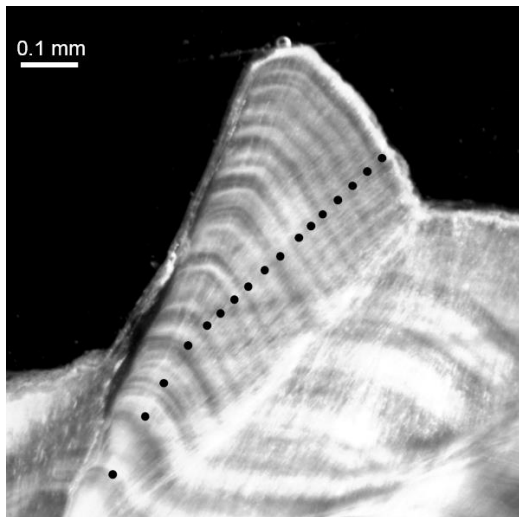


**Figure 4.1:** Sectioned *C. laticeps* otolith showing opaque (light) and translucent (dark) annual growth bands marked with dots between which increment widths were measured.

### 4.2.3 Environmental data

The TNP sea surface temperature (SST) data were obtained from South African National Parks (SANParks). These data consisted of mean monthly *in situ* sea temperatures from 1982 to 2014, measured at Storms River Mouth within the TNP by hand thermometer. Another *in situ* SST dataset from nearby Knysna, consisting of daily thermometer and UTR data from 1972–2009, was obtained from the DEA Oceans and Coasts. Missing data in the TNP dataset were filled in with corresponding Knysna data, as there were limited differences between the two measures when they overlapped, resulting in an *in situ* mean monthly SST time series from 1972 to 2013 for TNP. Unfortunately, no long-term environmental *in situ* data were available for the PE area. Based on the similarity of the SST regimes between TNP and PE (Chapter 2) and the close proximity (140 km) of the two areas, it was assumed that the TNP SST could be used to elucidate the long-term environmental growth drivers for the exploited population (PE) analysis.

Longer-term (monthly or annual) sea temperature data can provide sufficient temporal resolution to elucidate growth responses in stable environments; however, the south coast of South Africa is characterised by high-frequency thermal variability (Chapter 2), that may not be quantified adequately within mean monthly data. To quantify upwelling intensities, a daily SST dataset was constructed of daily UTR data from within the TNP MPA from 1991–2013, obtained from the DEA Oceans and Coasts, and combined with the daily Knysna SST data from 1972–1990, resulting in a daily SST dataset from 1972–2013. The intensity of upwelling events was estimated using the methods described by Tapia et al. (2009). Briefly, a 30-day moving average was fit through the daily SST time series data and the daily SST anomaly estimated as the difference between the moving average and observed SST. Only upwelling events that exceeded a  $-2\text{ }^{\circ}\text{C}$  anomaly threshold were considered as *C. laticeps* has a good ability to deal with minor acute temperature fluctuations (Chapter 3). Integrated cooling (IC) and integrated anomaly (IA) indices were estimated as the area under the anomaly curve of the cooling phase (highest SST anomaly at the onset of upwelling to the lowest SST anomaly

during an upwelling event, Figure 4.2 light grey shading) and the area between the anomaly curve and zero during the cold phase (area between the SST anomaly curve and zero line during an upwelling event, Figure 4.2 dark grey shading) respectively (Tapia et al. 2009). Monthly southern oscillation index (SOI) data were obtained from the National Oceanic and Atmospheric Administration (NOAA) National Climatic Data Centre for the years 1973–2015.

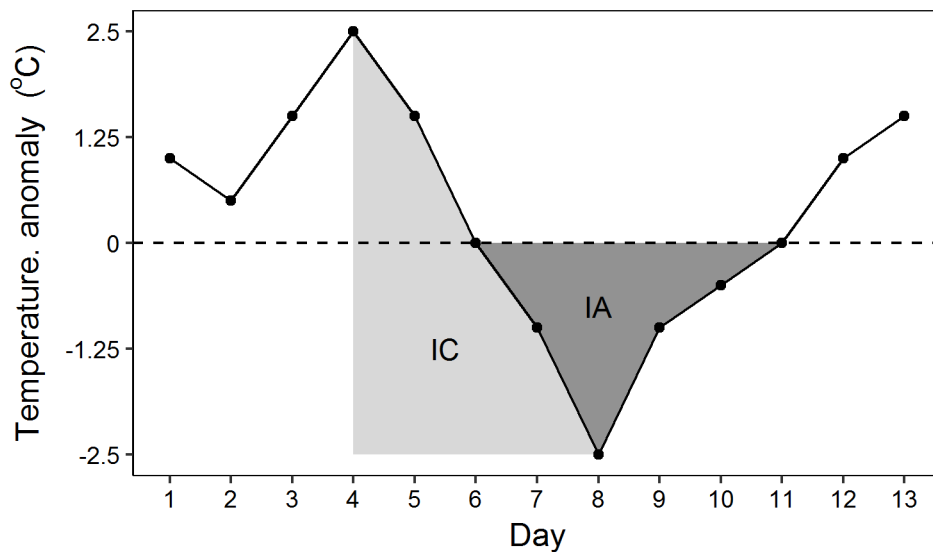


**Figure 4.2:** Example of how integrated cooling (IC, light grey shading) and integrated anomaly (IA, dark grey shading) were calculated (area of shaded regions) for extreme ( $> 2^{\circ}\text{C}$ ) upwelling anomalies following (Tapia et al. 2009). Points represent daily temperature anomalies calculated as departures from a 30-day moving average.

To assess whether SST was a good approximation for bottom temperature, thermistor string data (12, 19, 27 and 35 m depths) from the TNP MPA were obtained from DEA Oceans and Coasts, and the relationship between daily surface temperature and temperature at various depths explored with linear correlations.

## 4.2.4 Modelling approach

### 4.2.4.1 Fixed effects

Intrinsic effects on fish growth are internal biological processes that influence growth rates, such as the ontogenetic decline in somatic growth (West et al. 2001) or sexually dimorphic growth rates (Newman et al. 1996). To account for age-related trends in growth, the age of each individual at each CGY increment width (age) was included as an intrinsic effect (Table 4.1). The complicated life history of *C. laticeps*, including a change in sex from female to male between 275–350 mm FL (Buxton 1993), made it difficult to include sex explicitly as an intrinsic effect as old males and young males would have spent a different proportion of time growing as a male. The inclusion of age-at-capture (aac) as an intrinsic effect however, not only accounted for age selectivity, but also the relative proportion that an individual grew as either sex because sex change in *C. laticeps* is age/size-specific.

Extrinsic effects on fish growth are any environmental variable that directly influences growth rates, e.g., temperature, or food availability. The SST time series was used to develop a number of temperature indices that corresponded to each CGY (September–August) (Table 4.1). These included the mean CGY SST (September–August), the mean seasonal SST (summer = December–February, winter = June–August, autumn = March–May, spring = September–November) and the mean SST of fast (March–August) and slow (September–February) growth periods for each CGY. The sum of the IC and IA indices for each CGY was calculated as an indication of the cumulative upwelling intensity for that particular period (Table 4.1). Southern oscillation index data were used to develop mean CGY, fast growth months (March–August) and slow growth months (September–February) SOI per CGY (Table 4.1).

### 4.2.4.2 Random effects

To account for repeated growth increment measurements for each individual fish, a random intercept for each fish (1|id) was included as a parameter in all models (Morrongiello & Thresher 2015). A random year intercept (1|year) was tested as a crossed random effect with

fish ID, which induced a correlation among fish increment widths from the same year. The random year intercept created a temporarily resolved estimate of whether overall population growth was good or poor and accounted for some of the temporal autocorrelation among the data (Weisberg et al. 2010, Doubleday et al. 2015, Morrongiello & Thresher 2015). Because fish spawned in different environmental windows could be subject to specific conditions that subsequently affect growth throughout ontogeny (Whitten et al. 2013), such as varying levels of competition or contrasting environmental conditions as juveniles, a random intercept for a cohort (1|cohort) was also tested as a model parameter (Morrongiello & Thresher 2015, Izzo et al. 2016). A random age slope was tested for each random intercept, which would account for any individual variability in age-related responses (Table 4.1).

**Table 4.1:** Description of intrinsic, extrinsic and random effects used in the mixed modelling approach of *C. laticeps* growth biochronology.

Parameter	Description
Fixed intrinsic effects	
age	age at which CGY occurred
aac	age at which specimen was captured
Fixed extrinsic effects	
temperature	
year temp	average SST of CGY
fast temp	average SST fast growth months (March–August) in CGY
slow temp	average SST slow growth months (September–February) in CGY
summer temp	average SST during summer (December–February) in CGY
winter temp	average SST during winter (June–August) in CGY
autumn temp	average SST during autumn (March–May) in CGY
spring temp	average SST during spring (September–November) in CGY
Upwelling indices	
IC	Sum of integrated cooling (IC) per CGY
IA	Sum of integrated anomaly (IA) per CGY
SOI	
year SOI	average SOI of CGY
fast SOI	average SOI fast growth months (March–August) in CGY
Slow SOI	average SOI slow growth months (September–February) in CGY
Random effects	
1 year	random intercept for CGY
1 id	random intercept for each specimen
1 cohort	random intercept for cohort
age (year/id/cohort)	random age slope for each random intercept

#### 4.2.4.3 Modelling process

A mixed modelling approach (Morrongiello & Thresher 2015) was used to assess which of the selected environmental variables drive inter-annual variations in the growth of *C. laticeps*. Models were applied separately for the exploited and protected populations. All mixed modelling was done in R (R Core Team 2017), using the lme4 package (Bates et al. 2015) and the forward stepwise procedure described by Morrongiello & Thresher (2015). For all models, CGY width (mm) was log transformed to meet model assumptions and models were ranked according to Akaike's information criterion corrected for small sample sizes (AICc) (Burnham & Anderson 2004). All model predictor variables were centred around a mean of zero to minimise any effect of multicollinearity among predictor variables. The optimal random effects structure was first determined by fitting increasingly complex random effects structured models with all fixed intrinsic effects (age + aac) using restricted maximum likelihood estimation (REML). If multiple random effects models fell within two of the lowest AICc, the model with the lowest AICc was further built upon if it made biological sense. The optimum random effects structured model, based on AICc, was then refit with and without aac using maximum likelihood (ML) to determine the optimum random and fixed intrinsic effects structured base model. Building on from the base model, more complex models were fit and ranked with each fixed extrinsic effect separately using ML and ranked by AICc. The best models, with an AICc < 2 of the top model (Burnham & Anderson 2004) were refit with REML to obtain more accurate parameter estimates (Zuur et al. 2009) and considered further. Extrinsic effects were added to these best models to test for additive or synergistic effects but not presented if increased model complexity did not result in improvements of AICc > 2. More than two fixed extrinsic effects were not considered because AIC tends to favour overparametrized models (Harrison et al. 2018). For the best models, p-values were calculated using Wald tests and treated as a continuous measure approximating the relative support of including the fixed extrinsic effect in the model (Killen et al. 2018). The packages AICcmodavg (Mazerolle 2017), Effects (Fox 2003) and car (Fox & Weisberg 2011) were used

to generate AICc, prediction and confidence intervals and generate parameter p-values respectively.

### 4.3 Results

#### 4.3.1 Data preparation

Of the 189 historical and contemporary otoliths, 62 (representing 34 individual fish from the protected (TNP) and 28 from the exploited (PE) areas) were clear enough to make accurate CGY measurements and were included in the models. After excluding juvenile years (< 4 years), 522 CGY increments were measured from the protected and 272 from the exploited population that spanned the years 1965–2015 (excluding 1994–1996) and 1999–2015 for protected and exploited populations, respectively (Figure 4.3 a). The clear ontogenetic decline in growth rate is indicated in Figure 4.3 b.

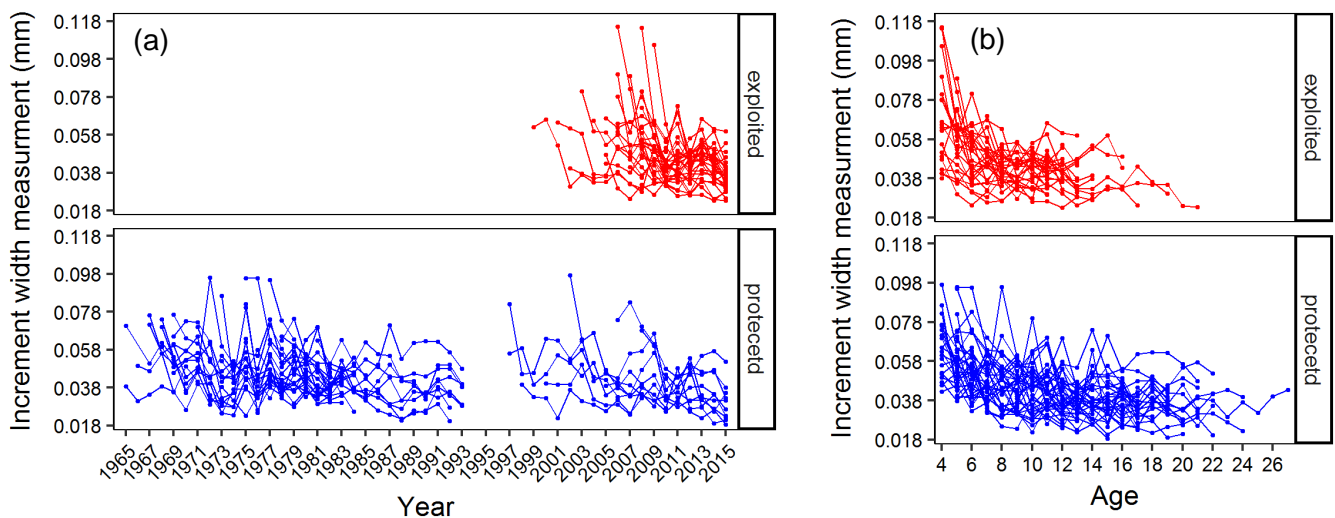


**Figure 4.3:** Raw otolith increment width measurement (mm) per exploited (red, PE) and protected (blue, TNP) sampling populations across all years (a) and ages (b). Each point represents a single width measurement and successive width measurements from the same individual are connected with a solid line.

There was a significant positive relationship ( $p$ -value < 0.001,  $R^2 = 0.44$ ) between the total width of all measured increments (age  $\geq 4$ ) and the fork length of each individual, indicating that otolith increment approximates somatic growth in *C. laticeps*, although there was variability around the linear relationship (Figure 4.4).

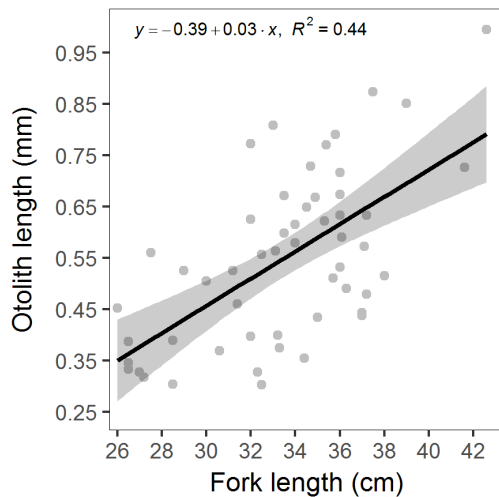


**Figure 4.4:** Relationship between otolith length (mm) along the measurement plane for 4+ year olds and fish fork length (cm) from the 62 *C. laticeps* otoliths used in this study.

There were significant linear correlations between surface *in situ* SST measurements and the temperature data from the thermistor string (Figure 4.5 a, b, c, d). The correlation was strongest at 12 m ( $R^2 = 0.87$ ), but became weaker with depth. Nevertheless, the correlation between surface temperature and temperature at depth patterns persisted even at 27 m and, to some extent, at 35 m (Figure 4.5 c, d and Figure 4.6). While the predictive power of these correlations decreased with depth, extreme high or low temperatures remained correlated with each other, even at 35 m despite decreases of  $R^2$  to 0.07. These correlations provide evidence that SST is at least a valid proxy for bottom temperature and allows one to explore the relationship between the SST variability and growth of *C. laticeps*.

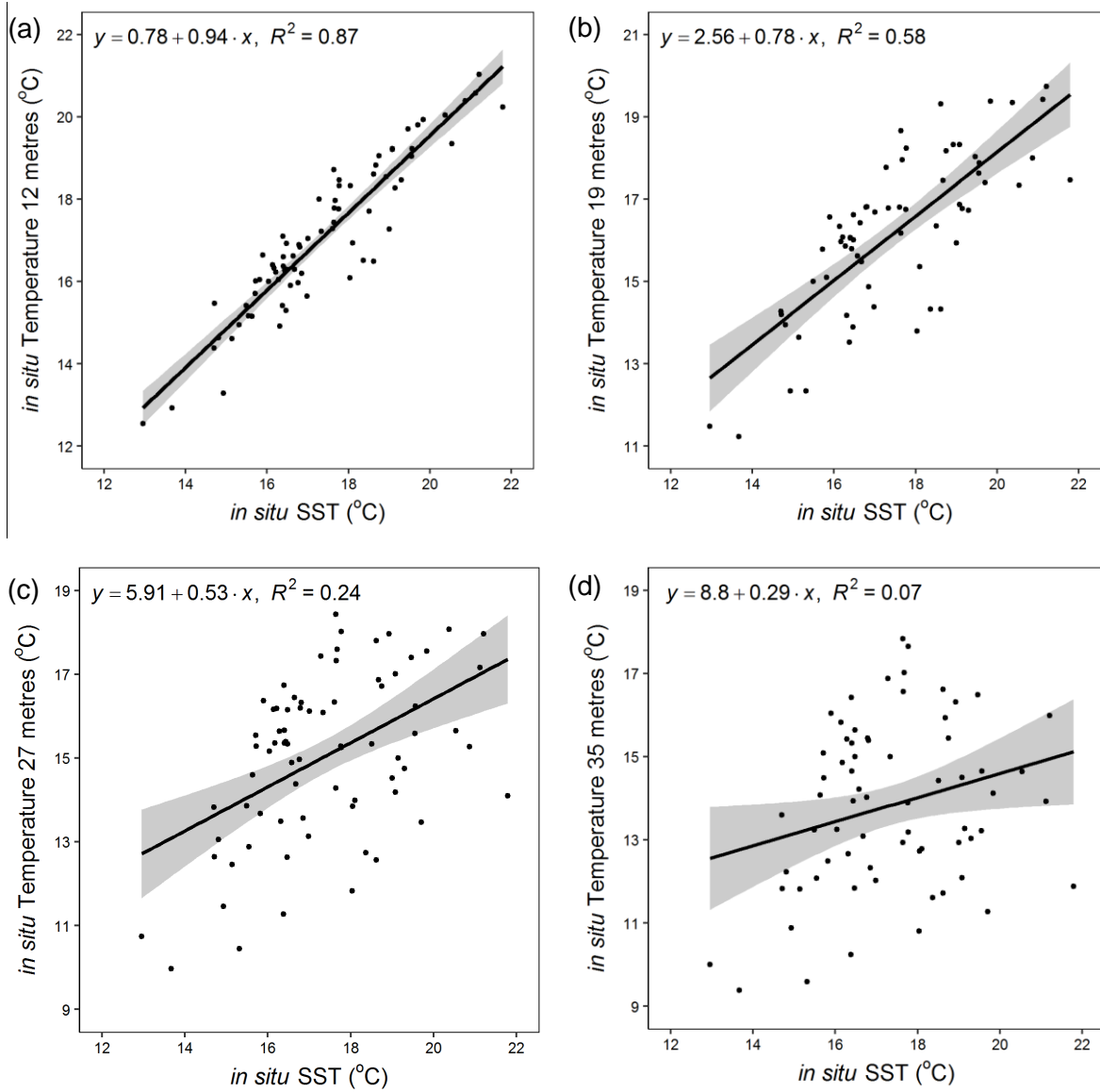


**Figure 4.5:** Linear relationship (black line) between monthly (black dot) *in situ* sea surface temperatures on the surface (SANParks data) and temperatures at 12 m (a), 19 m (b), 27 m (c) and 35 m (d) depths (thermistor string data) (1994–2004). The 95% confidence intervals shaded grey

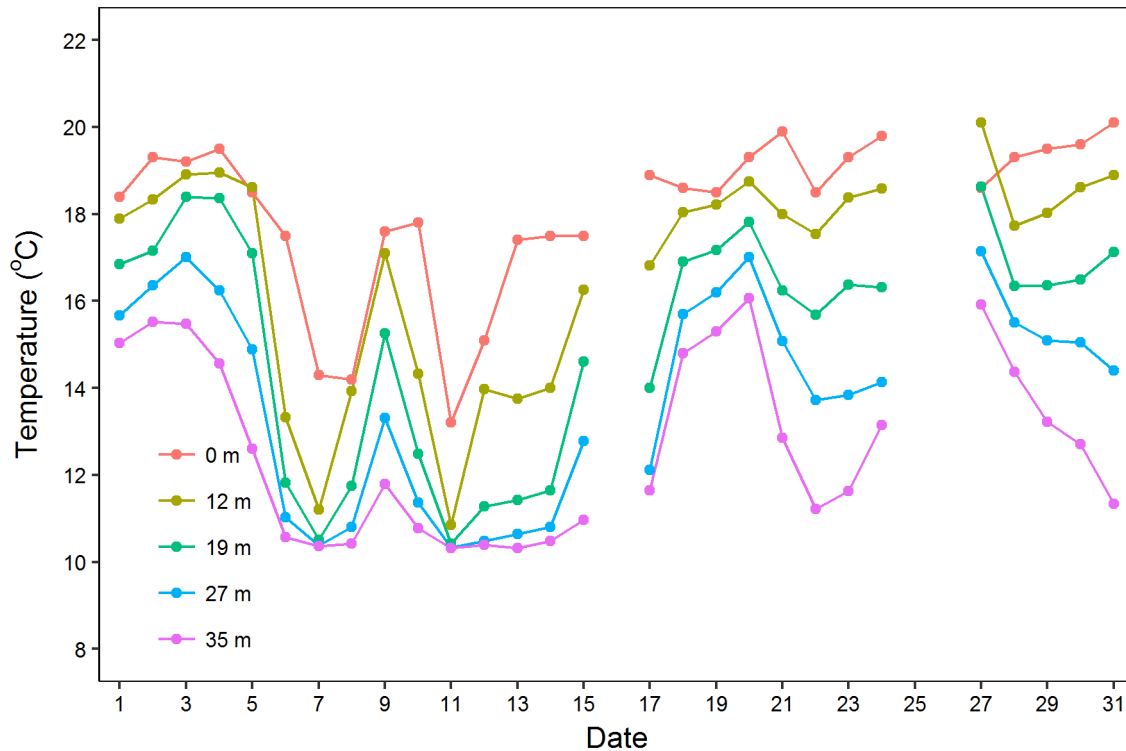


**Figure 4.6:** Time series of daily sea temperature measurements (dots) per depth from thermistor string data (12–37 m depths) and SANParks *in situ* data (0 m) from December 2002.

#### 4.3.2 Protected population (TNP) mixed modelling results

The best base model from which to explore extrinsic drivers on *C. laticeps* growth included a random age slope for both a random id intercept (age|id) and random year intercept (age|year), with age as the only fixed intrinsic effect (model t3a, Table 4.2). Building on this base model, the best extrinsic effects model for the protected population included IC (model t4k), mean autumn temperature (t4a) or mean year temperature (t4e) (Table 4.2).

The top three full intrinsic + extrinsic effects models refit with REML (Table 4.3) indicate that predicted growth decreases with CGY cumulative IC (Figure 4.8 a), increases with mean autumn temperature (Figure 4.8 b) and increases with CGY mean temperature (Figure 4.8 c).

The model with the strongest support was model t4k, which included IC as an extrinsic effect, as it had the lowest *p*-value and AICc scores (Table 4.3).

**Table 4.2:** Summary of considered models for optimal random effects (1a–2h), intrinsic effects (I. effects) (3a–b) and extrinsic effects (4a–l) models for fish growth in the protected (TNP) population. Each model (M) and its associated degrees of freedom (df), fixed intrinsic effects structure, fixed extrinsic effects structure, random effects structure, Akaike’s information criterion corrected for small sample size (AICc), change in AIC ( $\Delta$ AIC), AIC weight (AICwt) and restricted (models 1a–3b) or maximum (models 4a–l) log likelihood (LL) ranked based on lowest AIC at each modelling step with the most parsimonious model highlighted in bold.

M	df	I. effects	Extrinsic effects	Random effects	AICc	$\Delta$ AIC	AICwt	LL
<b>t1b</b>	<b>7</b>	<b>age, aac</b>		<b>age id</b>	<b>-52.32</b>	<b>0</b>	<b>1</b>	<b>33.27</b>
t1a	5	age, aac		1 id	-11.31	41.1	0	10.72
<b>t2c</b>	<b>10</b>	<b>age, aac</b>		<b>age id, age year</b>	<b>-81.86</b>	<b>0</b>	<b>0.46</b>	<b>51.15</b>
t2a	8	age, aac		age id, 1 year	-80.32	1.54	0.21	48.30
t2f	11	age, aac		age id, age year, 1 cohort	-79.87	1.99	0.17	51.20
t2e	9	age, aac		age id, 1 year, 1 cohort	-78.70	3.16	0.09	48.53
t2h	13	age, aac		age id, age year, age cohort	-77.11	4.75	0.04	51.92
t2g	11	age, aac		age id, 1 year, age cohort	-75.98	5.89	0.02	49.25
t1b	7	age, aac		age id	-53.32	29.55	0	33.27
t2b	8	age, aac		age id, 1 cohort	-50.44	31.42	0	33.36
t2d	10	age, aac		age id, age cohort	-47.52	34.35	0	33.98
<b>t3a</b>	<b>9</b>	<b>age</b>		<b>age id, age year</b>	<b>-105.8</b>	<b>0</b>	<b>0.73</b>	<b>62.08</b>
t3b	10	age, aac		age id, age year	-103.76	2.04	0.27	62.10
<b>t4k</b>	<b>10</b>	<b>age</b>	<b>IC</b>	<b>age id, age year</b>	<b>-110.59</b>	<b>0</b>	<b>0.26</b>	<b>65.56</b>
<b>t4a</b>	<b>10</b>	<b>age</b>	<b>autumn temp</b>	<b>age id, age year</b>	<b>-110.08</b>	<b>0.51</b>	<b>0.2</b>	<b>65.31</b>
<b>t4e</b>	<b>10</b>	<b>age</b>	<b>year temp</b>	<b>age id, age year</b>	<b>-109.51</b>	<b>1.08</b>	<b>0.15</b>	<b>65.02</b>
t4f	10	age	fast temp	age id, age year	-108.05	2.54	0.07	64.29
t4g	10	age	slow temp	age id, age year	-107.96	2.63	0.07	64.25
t4c	10	age	summer temp	age id, age year	-107.67	2.91	0.06	64.11
t4l	10	age	IA	age id, age year	-107.63	2.96	0.06	64.08
t4b	10	age	spring temp	age id, age year	-106.07	4.52	0.03	63.30
t3a	9	age	base	age id, age year	-105.80	4.79	0.02	62.08
t4j	10	age	year SOI	age id, age year	-105.54	5.05	0.02	63.03
t4h	10	age	fast SOI	age id, age year	-105.47	5.12	0.02	62.99
t4d	10	age	winter temp	age id, age year	-105.36	5.22	0.02	62.95
t4i	10	age	slow SOI	age id, age year	-105.03	5.55	0.02	62.77

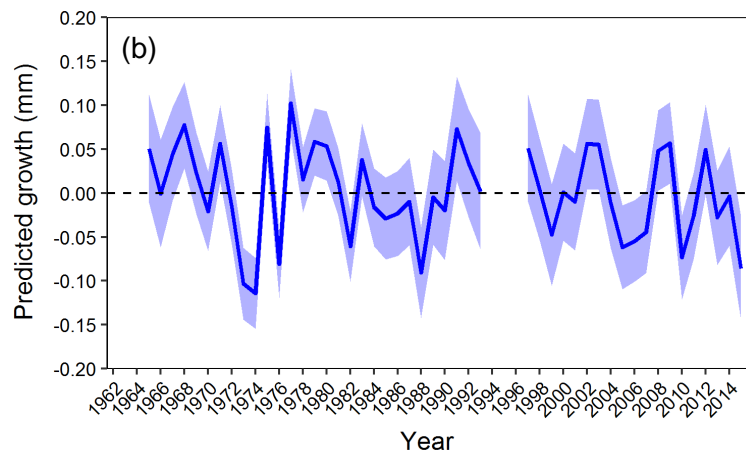
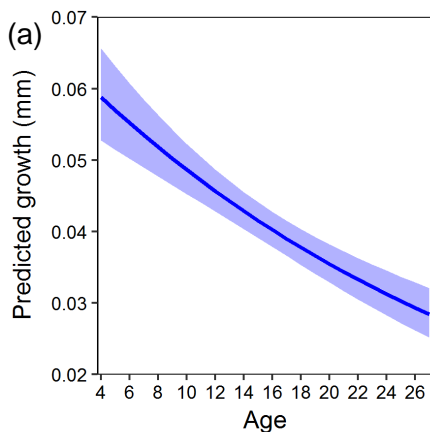


**Figure 4.7:** Predicted growth of the protected (TNP) population of *C. laticeps* otolith increment (mm) at each age (solid blue line) with 95% confidence intervals shaded in blue (a) and annual growth variation after accounting for intrinsic effects represented by the Year random-effect conditional modes (solid blue line) +/- SE (shaded blue) for *C. laticeps* from 1962–2015 (b).

**Table 4.3:** Summary of the most parsimonious mixed effects models (t4k, t4a and t4e) for growth of *C. laticeps* from the protected (TNP) population showing extrinsic fixed effects parameter estimates, standard errors (Std. Error), parameter upper and lower confidence intervals (CI), t statistic (*t*) and parameter p-values. IC is cumulative integrated cooling, autumn temp is mean autumn temperature and CGY temp is mean calendar growth year temperature.

Model	fixed effect	Parameter	Std. error	Lower 95% CI	Upper 95% CI	<i>t</i>	p-value
t4k	IC	-0.0012	0.0005	-0.0023	-0.0002	2.3200	0.0205
t4a	autumn temp	0.0250	0.0112	0.0027	0.0473	2.2300	0.0254
t4e	CGY temp	0.0439	0.0213	0.0019	0.0863	2.0600	0.0393

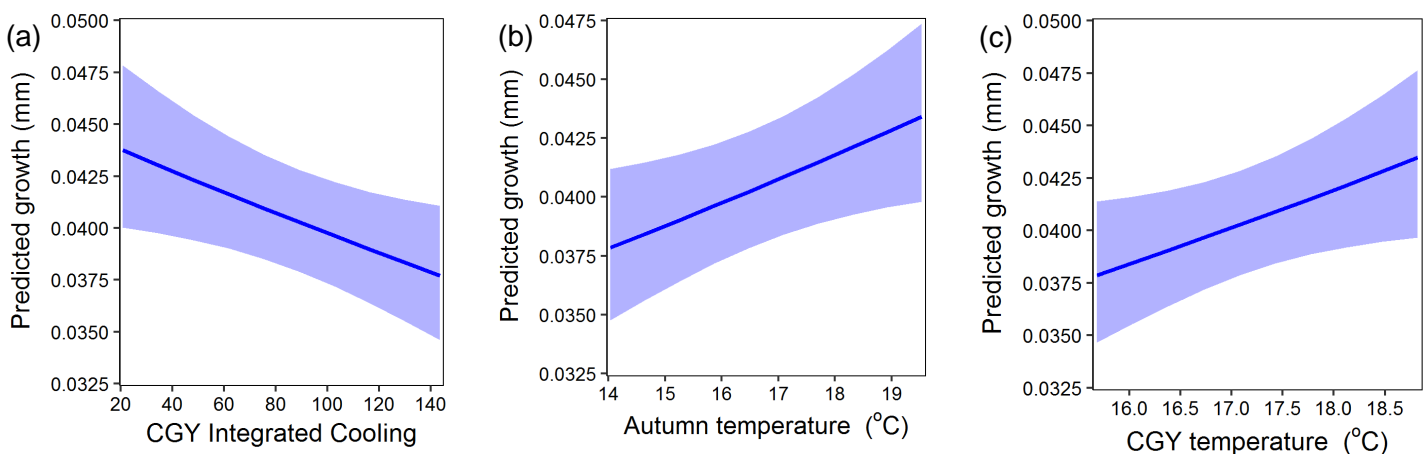


**Figure 4.8:** Predicted growth (solid blue line) and 95% confidence intervals (shaded blue) of *C. laticeps* from protected (TNP) population across the sum of integrated cooling index per calendar growth year (CGY) (a), autumn temperature (b) and mean calendar growth year (CGY) temperature(c).

#### 4.3.3 Exploited (PE) mixed modelling results

The best base model from which to explore extrinsic drivers on *C. laticeps* growth from the exploited population included a random age slope for a random id intercept (age|id) and a random year intercept (1|year), with age as the only fixed intrinsic effect (model p3a, Table 4.4). The inclusion of extrinsic fixed effects did not improve the base model based on AICc and the best base model refit with REML (Table 4.5) only explained the decrease in growth with age (Figure 4.9 a).

**Table 4.4:** Summary of considered models for optimal random effects (p1a–p2h), intrinsic effects (l. effects) (p3a–b) and extrinsic effects (4a–l) models for fish growth from the exploited, Port Elizabeth population. Each model (M) and its associated degrees of freedom (df), intrinsic effects structure, extrinsic effects structure, random effects structure, Akaike’s information criterion corrected for small sample size (AICc) change in AIC ( $\Delta$ AIC), AIC weight (AICwt) and restricted (models 1a–3b) or maximum (models 4a–l) log likelihood (LL) ranked based on lowest AIC at each modelling step with the optimum model highlighted in bold.

M	df	l. effects	Extrinsic effects	Random effects	AICc	$\Delta$ AIC	AICwt	LL
<b>p1b</b>	<b>7</b>	<b>age, aac</b>		<b>age id</b>	<b>-52.8</b>	<b>0</b>	<b>0.99</b>	<b>33.61</b>
p1a	5	age, aac		1 id	-43.5	9.3	0.01	26.86
<b>p2a</b>	<b>8</b>	<b>age, aac</b>		<b>age id, 1 year</b>	<b>-70.3</b>	<b>0</b>	<b>0.46</b>	<b>43.43</b>
p2c	10	age, aac		age id, age year	-68.99	1.32	0.24	44.92
p2e	9	age, aac		age id, 1 year, 1 cohort	-68.16	2.14	0.26	43.43
p2f	11	age, aac		age id, age year, 1 cohort	-66.82	3.49	0.08	44.92
p2g	11	age, aac		age id, 1 year, age cohort	-65.71	4.6	0.05	44.36
p2h	13	age, aac		age id, age year, age cohort	-63.58	6.72	0.02	45.5
p1b	7	age, aac		age id	-52.8	17.5	0	33.61
p2b	8	age, aac		age id, 1 cohort	-50.68	19.63	0	33.61
p2d	10	age, aac		age id, age cohort	-47.21	23.09	0	34.03
<b>p3a</b>	<b>7</b>	<b>age</b>		<b>age id, 1 year</b>	<b>-90.58</b>	<b>0</b>	<b>0.62</b>	<b>52.5</b>
p3b	8	age, aac		age id, 1 year	-89.6	0.97	0.38	53.08
<b>p3a</b>	<b>7</b>	<b>age</b>	<b>base</b>	<b>age id, 1 year</b>	<b>-90.58</b>	<b>0</b>	<b>0.48</b>	<b>52.5</b>
p4i	8	age	slow SOI	age id, 1 year	-88.65	1.93	0.18	52.60
p4j	8	age	year SOI	age id, 1 year	-88.49	2.09	0.17	52.52
p4h	8	age	fast SOI	age id, 1 year	-88.46	2.12	0.17	52.50
p4a	8	age	autumn temp	age id, 1 year	-53.36	37.21	0	36.12
p4b	8	age	spring temp	age id, 1 year	-49.54	41.04	0	33.11
p4f	8	age	fast temp	age id, 1 year	-46.49	44.09	0	31.59
p4d	8	age	winter temp	age id, 1 year	-46.35	44.23	0	31.52
p4c	8	age	summer temp	age id, 1 year	-44.68	44.68	0	31.29
P4k	8	age	IC	age id, 1 year	-45.83	44.75	0	31.26
p4e	8	age	year temp	age id, 1 year	-45.22	45.35	0	30.96
p4g	8	age	slow temp	age id, 1 year	-45.22	45.36	0	30.96
p4l	8	age	IA	age id, 1 year	-45.06	45.51	0	30.88

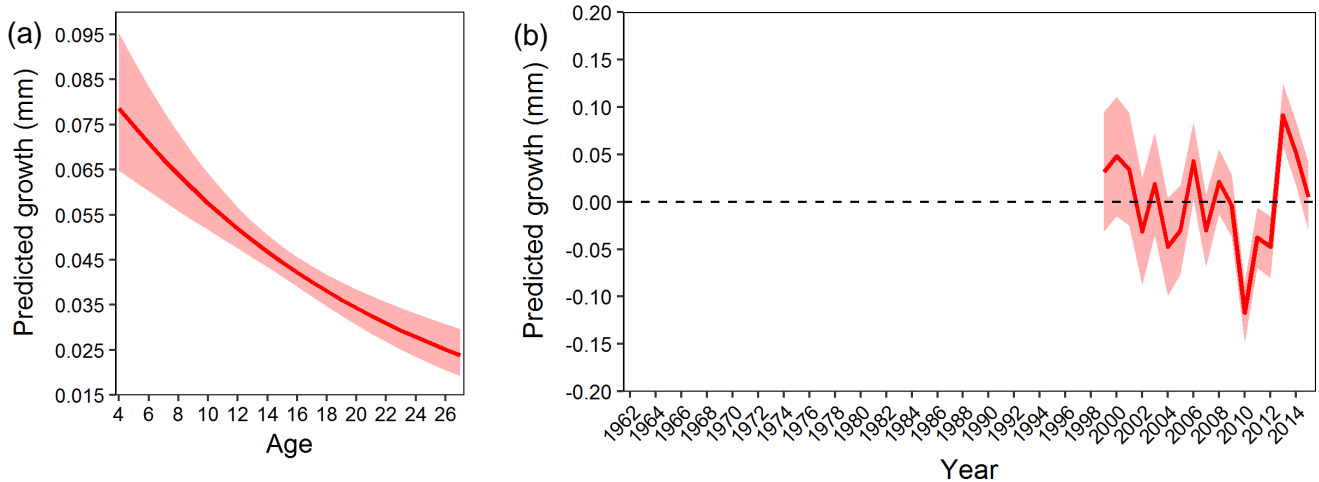


**Figure 4.9:** Predicted growth of the exploited (PE) population of *C. laticeps* otolith increment (mm) at each age (solid red line) with 95% confidence intervals shaded in red (a) and annual

growth variation after accounting for intrinsic effects represented by the Year random-effect conditional modes (solid red line) +/- SE (shaded red) for *C. laticeps* from 1999–2015 (b).

**Table 4.5:** Summary of the most parsimonious mixed effect model (p3a) for growth of *C. laticeps* from Port Elizabeth showing parameter estimates, standard errors (Std. Error) and t statistic (t-stat). Number of obs. Is total number of increments, ID is unique fish identifier, AICc is Akaike’s information criterion corrected for small sample sizes,  $R^2_{(m)}$  is marginal  $R^2$  and  $R^2_{(c)}$  is conditional  $R^2$ .

Parameter	Estimate	Std. Error	t-stat
Intercept	-3.138	0.037	-82.84
Age	-0.051	0.008	-6.24

#### 4.3.4 Base model comparisons

*Chrysoblephus laticeps*’ somatic growth was higher in younger fish from the exploited population compared to protected populations but, declined with age faster until growth rates of older fish were higher among protected populations (Figure 4.10 a). The inter-annual trend in growth variability from 1999 to 2015 was similar for exploited and protected populations but differed in 2006 and 2013, when growth rates spiked in the exploited population but remained constant in the protected population (Figure 4.10 b).

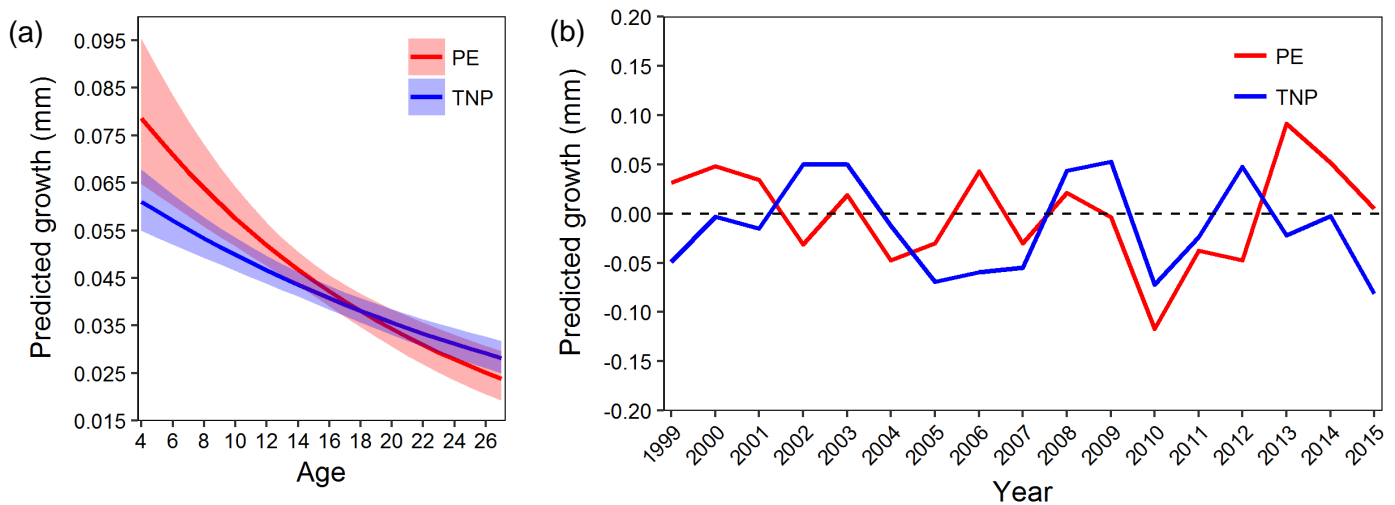


**Figure 4.10:** Comparison of the ontogenetic decline in growth with age of *Chrysoblephus laticeps* (a) and the inter-annual variability in growth response (b) between exploited (red, PE) and protected (blue, TNP) sampling populations. Data was extracted from the best base model with no extrinsic fixed effects.

### 4.3.5 Long-term trend in growth

For the protected population, adding year as a continuous predictor improved the best base model based on AICc (Table 4.6). The improved model indicated that growth had decreased over time (Table 4.7, Figure 4.11).

**Table 4.6:** Modelling results for testing the temporal trend in growth over time for the protected (TNP) population. Each model (M) and its associated degrees of freedom (df), fixed intrinsic effects structure, fixed extrinsic effects structure, random effects structure, Akaike's information criterion corrected for small sample size (AICc), change in AIC ( $\Delta$ AIC), AIC weight (AICwt) and maximum log likelihood (LL) ranked based on lowest AIC with the most parsimonious model highlighted in bold.

M	df	Intrinsic effects	Extrinsic effects	Random effects	AICc	$\Delta$ AIC	AICwt	LL
<b>t5a</b>	<b>10</b>	<b>age</b>	<b>Year (cont.)</b>	<b>age id, age year</b>	<b>-107.17</b>	<b>0</b>	<b>0.67</b>	<b>63.81</b>
t3a	9	age		age id, age year	-105.80	1.37	0.33	62.08

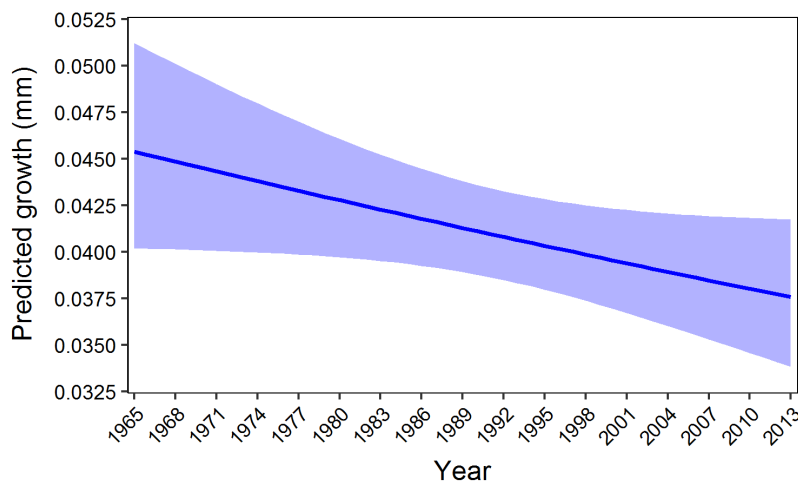


**Figure 4.11:** Predicted growth over time for *C. laticeps* otolith increment (mm) (solid blue line) with 95% confidence intervals shaded in blue for the protected (TNP) population.

**Table 4.7:** Summary of the mixed effects model (t5a) revealing the temporal trend of growth based on otolith increment (mm) for protected (TNP) population showing parameter estimates, standard errors (Std. Error) and t statistic (t-stat). Number of obs. Is total number of increments, ID is unique fish identifier, AICc is Akaike's information criterion corrected for small sample sizes,  $R^2_{(m)}$  is marginal  $R^2$ ,  $R^2_{(c)}$  is conditional  $R^2$  and Year is the continuous year predictor.

---

Number of obs: 508, groups: ID, 34; Year, 48  
 AIC: -107.17,  $R^2_{(m)} = 0.2436$ ,  $R^2_{(c)} = 0.67$

---

Parameter	Estimate	Std. Error	t-stat
Intercept	-3.191	0.029	-106.75
Age	-0.028	0.004	-6.08
Year	-0.004	0.002	-1.91

In contrast to the protected population, the addition of year as a continuous predictor did not improve the best base model for the exploited population (Table 4.8).

**Table 4.8:** Modelling results for testing the temporal trend in growth over time for PE. Each model (M) and its associated degrees of freedom (df), fixed intrinsic effects structure, fixed extrinsic effects structure, random effects structure, Akaike’s information criterion corrected for small sample size (AICc), change in AIC ( $\Delta$ AIC), AIC weight (AICwt) and maximum log likelihood (LL) ranked based on lowest AIC with the most parsimonious model highlighted in bold.

M	df	Intrinsic effects	Extrinsic effects	Random effects	AICc	$\Delta$ AIC	AICwt	LL
<b>p3a</b>	<b>10</b>	<b>age</b>		<b>age id, 1 year</b>	<b>-91.00</b>	<b>0</b>	<b>0.63</b>	<b>52.50</b>
p5a	9	age	Year (cont.)	age id, 1 year	-89.55	1.02	0.37	53.05

#### 4.4 Discussion

This chapter finds that variability in ocean temperature, and cold spells particularly, may influence the growth trajectory of *C. laticeps*, highlighted by the finding that CGYs with a high cumulative intensity of extreme upwelling events ( $> 2$  °C anomaly) (IC) correlates with poor growth years for the protected population. This result is in accordance with earlier physiological work (Chapter 3) where extreme upwelling simulations caused “cold shock” (Donaldson et al. 2008), resulting in reduced metabolic capacity above SMR. Physiological mechanisms for thermal compensation during extreme cold temperatures require increased allocation of energy that can translate to reduced available energy for other processes such as growth (Pörtner et al. 2001, Wang et al. 2014).

However, variability may also be positive for growth, suggesting context-dependency. For instance, previous studies have found a positive association between rockfish (*Sebastes* spp.) otolith-derived growth and upwelling in the Californian current ecosystem (Black et al. 2005, 2008, 2010, 2011b). In this case, increased productivity is associated with upwelling leading

to an increase in food availability and bottom-up enrichment of fish growth (von Biela et al. 2015). The species studied, however, generally occur at depths greater than 100 m (Boehlert & Kappenman 1980), well below the thermocline, where upwelling-induced temperature fluctuations are negligible (Bograd & Lynn 2003). The results of this chapter show that acute temperature fluctuations associated with intermittent upwelling may affect coastal fisheries species directly by reducing their growth, if these temperature fluctuations exceed a species' thermal niche.

This study has also highlighted the importance of autumn (March–May) sea temperature for the growth of *C. laticeps*. The autumn months (March–May) correspond to the formation of the hyaline zone, which represents the fast growth period, in the otoliths of *C. laticeps* (Buxton 1987). Previous studies also point to the importance of temperature in driving fish growth during their primary growing period. For example, Tao et al. (2015) and van der Sleen et al. (2018) found growth is associated with temperature, primarily during the growing season, for the Selincuo naked carp (*Gymnocypris selincuoensis*), and juvenile European plaice (*Pleuronectes platessa*) respectively.

The autumn period (March–May) in this study also occurs directly after the summer spawning window, between October and February, for *C. laticeps* (Buxton 1990). This may suggest that *C. laticeps* employs a compensatory growth strategy, defined as a period of increased growth when conditions (intrinsic or extrinsic) become favourable, following periods of growth depression (Ali et al. 2003). In the case of *C. laticeps*, the intra-specific competition and elaborate courtship behaviour during the breeding season period is most likely energetically expensive and may reduce foraging time. A shift in energy allocation from somatic to gonad growth during reproductive windows is well documented in fishes (Rijnsdorp 1990, Ali et al. 2003). Reductions in the energy available for growth, such as periods of food deprivation, or reproduction, may be followed by compensatory growth (Metcalf et al. 2002). In temperate environments with strong seasonality, the optimal strategy for organisms constrained by energy partitioning to somatic growth or reproductive investment is often an indeterminate

growth strategy where a period of somatic growth should precede a period of reproductive investment (Kozłowski 1996, Lester et al. 2004).

This chapter found a decrease in growth over time for the protected (TNP) population indicated by the negative coefficient of the continuous year predictor. The decrease in growth is likely a result of an increase in intermittent upwelling over time along the South African coastal zone (Roy et al. 2007, Rouault et al. 2010) and the negative relationship between cumulative IC and growth. The data of localised upwelling intensities (IC) calculated for this study over time support the notion that intermittent upwelling has increased over recent time along the South African south coast (Figure 4.12). Furthermore, the overriding influence of cumulative IC, rather than longer-term mean changes, on *C. laticeps* growth highlights the importance of high frequency and intensity of thermal variability on organism performance.

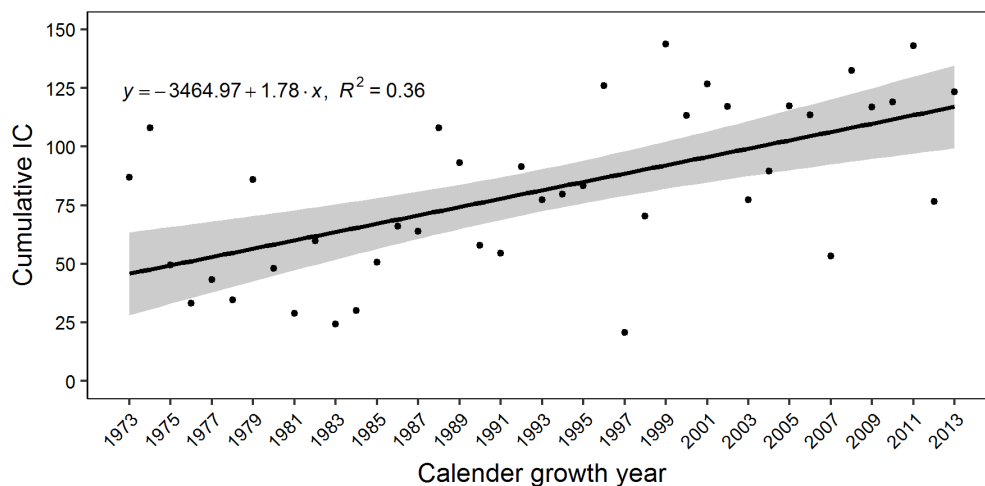


**Figure 4.12:** Cumulative integrated cooling (IC) per calendar growth year (black points) with best-fit linear equation (black line) and 95% confidence intervals (shaded grey) depicting an increase in IC over time.

The inability to identify an environmental driver on *C. laticeps*' growth from the exploited population, unlike the protected one, suggests that a multi-decadal biochronology length may be required to detect environmental growth drivers of species (Dzaugis et al. 2017), particularly in highly variable regions. When the data from the protected population were shortened to overlap with the exploited population data, the corresponding analyses were also

unable to quantify an extrinsic environmental growth driver; however, it is likely that the same extrinsic environmental drivers influence growth of both protected and exploited populations. While different environmental drivers of growth have been identified for some species over large (>1000 km) geographical scales (Ong et al. 2017), at more local scales, synchronous growth and similar drivers have been commonly identified (~ 500–1500 km) (Black et al. 2008, Helser et al. 2012). In addition, the drivers of growth among species with comparable life history traits and in the same geographical area are often similar (Black et al. 2010, Dzaugis et al. 2017).

The failure to detect an environmental driver of growth for fish from the exploited population is probably caused by the difficulty in interpreting the relationships between environmental variables and biochronology relationships when the length of the biochronology is short, or there is little environmental variability throughout the biochronology time period (Morrongiello et al. 2012, Dzaugis et al. 2017). Unfortunately, historical otolith samples from exploited populations were sparse and many of the otoliths did not yield sufficient clarity when sectioned to identify growth zones accurately. The resulting exploited population biochronology which overlapped the environmental variables was only 14 years as opposed to the protected population biochronology, which overlapped with 37 years of environmental predictor variables (Figure 4.13 a, b). Furthermore, if one assumes that the same environmental variables (mean autumn temperature or IC) are driving the growth patterns of fish in the exploited population, then it is likely that the observed variability of these variables during that period may not have been sufficiently large to identify these as important extrinsic drivers (Figure 4.13 a, b). Indeed, most mean autumn SSTs and IC CGY data that overlapped with the exploited population biochronology appeared to be close to, or above the long-term mean autumn SST or IC (Figure 4.13 a, b). In contrast, the protected population biochronology spanned a broad range of mean autumn sea temperatures and ICs, which could then be used to predict fish growth (Figure 4.13 a, b).

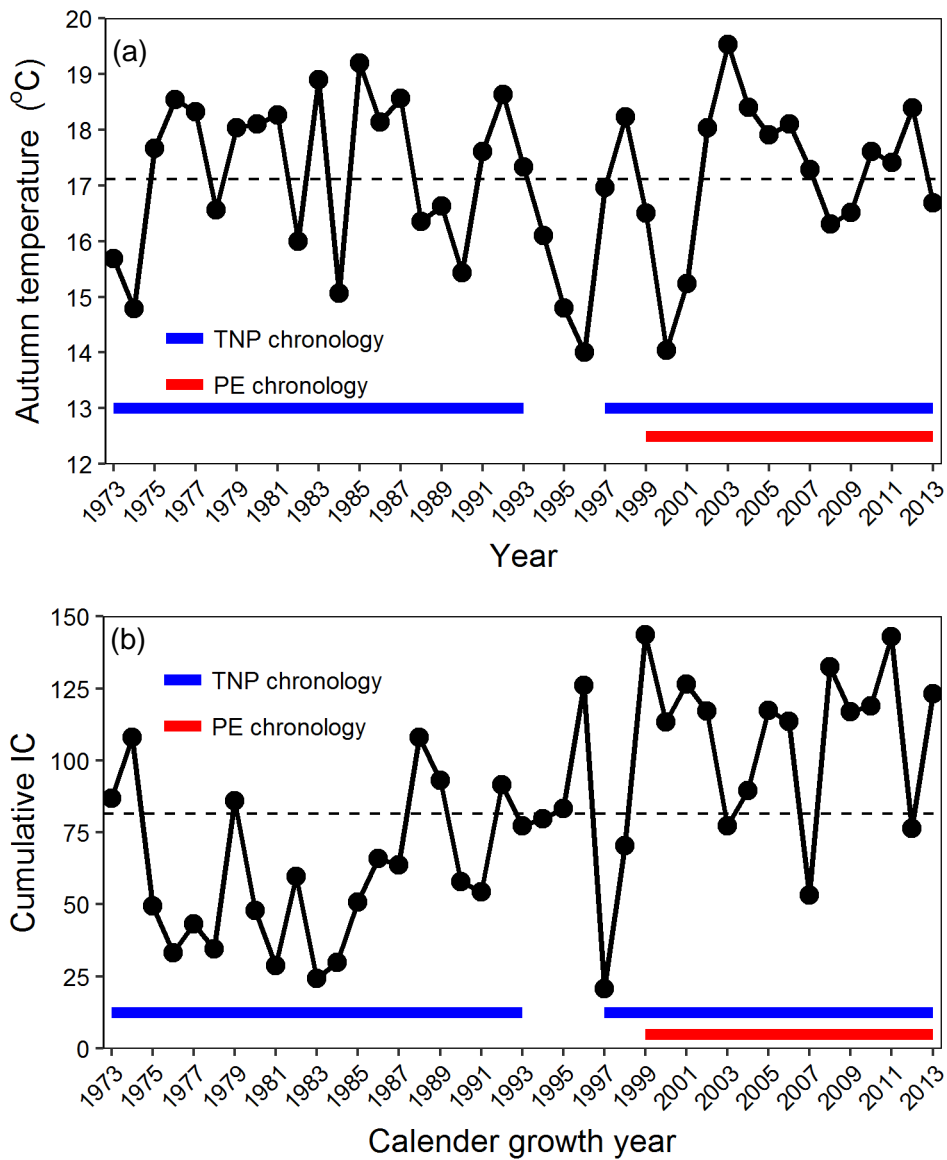


**Figure 4.13:** TNP annual mean autumn (Mar–May) *in situ* sea surface temperature time series (a) (black dots and solid line) and TNP cumulative integrated cooling (IC) time series (b) (black dots and solid line). Overall mean autumn sea temperature of 17.11 °C and cumulative IC of 81.4 (dashed lines) and years spanning protected (TNP, blue line) and exploited (PE, red line) biochronologies are indicated.

The second possible reason for the inability to identify an extrinsic driver on somatic growth for the exploited population is that individuals did not have the metabolic capacity, in terms of aerobic scope, to take advantage of warm autumn sea temperature periods. The mean annual

autumn sea temperatures, which drove positive growth rates for the protected population, all fell over the temperature range where aerobic scope was increasing before the optimum temperature of aerobic scope was reached (Figure 4.14 a, see Chapter 3). In contrast, if it is assumed that the extrinsic drivers for growth of the fish from the exploited population are the same, the observed mean autumn temperatures only overlapped the temperature range where aerobic scope was maximised and not increasing (Figure 4.14 b). Although greater aerobic scope should enhance the capacity for growth (e.g., Khan et al. 2014, Auer et al. 2015b), a number of studies report maximum growth rates in fishes at temperatures where aerobic scope is not maximal (Clark et al. 2013). For example, maximum aerobic scope of barramundi (*Lates calcarifer*) occurred at 38 °C (Norin et al. 2014), while growth studies indicate reduced growth at this temperature (Katersky & Carter 2007). Similarly, mismatches between the temperatures that maximise aerobic scope and temperatures where growth is maximised have been reported for Atlantic halibut (*Hippoglossus hippoglossus*) (Gräns et al. 2014) and the common killifish (*Fundulus heteroclitus*) (Healy & Schulte 2012). These mismatches may be caused by mitochondria becoming leaky and hence less efficient at producing ATP per molecule of oxygen at high temperatures which can result in superficially high MMR and AS (Iftikar & Hickey 2013). Alternatively, the optimum temperature for growth and metabolism can be context dependant based on food availability which can further obscure this relationship (Brett 1971).

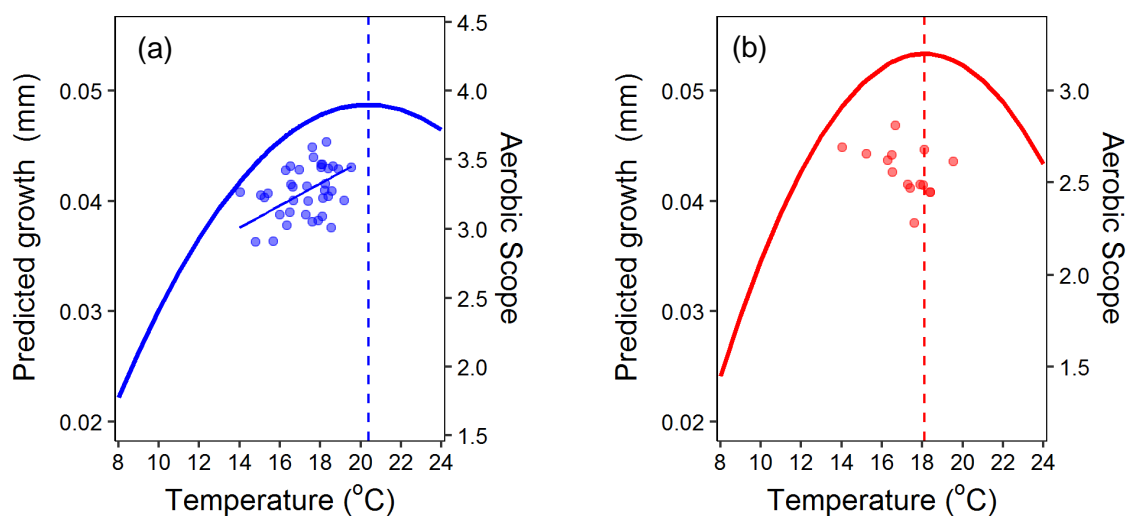


**Figure 4.14:** Predicted annual growth (solid dots) after accounting for intrinsic effects per mean autumn temperature of CGY for protected (a, blue) and exploited (b, red) populations. Curved lines represent aerobic scope from Chapter 3, dashed line is the temperature where aerobic scope is maximised, and the solid linear blue line is the fixed mean autumn temperature effect from model t4p. No extrinsic effect was identified for the exploited population.

A number of sources of error in the dependant and independent variables could also obscure the relationships between extrinsic factors and fish growth. Firstly, there is the difficulty of accurately interpreting growth rings in sectioned fish otoliths. In this study however, measurement error was minimised by including only the clearest (33%) of the otoliths. Furthermore, there may be interpretation error when accurately identifying the outermost growth zone, which is a common potential bias of all biochronology studies. To mitigate this, the outermost ring was excluded from measurement so that a fish caught in 2016 was measured from the more clearly defined 2015 annulus.

Certain intrinsic biological factors could also not be accounted for in the statistical analysis. For example, *C. laticeps* undergoes a protogynous sex change that is often associated with accelerated growth (Garratt et al. 1993, Walker & McCormick 2004). Because this sex change occurs over a relatively broad age/size range, identifying which years were spent as male or female was difficult. In this study, the age-at-capture (aac) term was incorporated in the modelling process to account for time spent as one sex over the other and juvenile years were excluded from the analysis. Nevertheless, further ontogenetic growth variation (growth acceleration following sex change) would add noise to the data. The error in the data would only obscure any true relationship between somatic growth and environmental variables, thus the relationship identified, between mean autumn temperature, cumulative upwelling intensity (IC), and somatic growth is probably accurate as it makes biological sense for *C. laticeps* and is supported by the physiology work in Chapter 3.

Comparing the base model of the two populations for the same time period revealed some distinct differences in growth rates. Firstly, growth rates were higher in exploited populations at young ages but this pattern reversed in older fish (Figure 4.10 a). Thus, overall, growth is rapid in younger fish in the exploited population and decreases markedly with age, while

growth rate is more consistent in the protected population. When populations are harvested, the release of competition and higher food availability can sometimes increase individual growth rates (Hilborn et al. 1995, Botsford et al. 1997) which may explain the higher growth rates at younger ages in the exploited population. Annual mismatches in growth between the two populations was most evident in 2006 and 2013 where the exploited population exhibited higher growth than the protected population. The mismatch in growth between the populations may be a result of internal biological processes and the uneven distribution of ages at a given year between the samples of both populations. For example, in 2006, 2/11 fish from the protected population and 9/16 fish from the exploited population were between the ages of four and five, which may correspond to a growth acceleration following maturity. In 2013, 13/31 fish from the exploited population were between the ages eight and ten, which may correspond to a growth acceleration following sex change (Garratt et al. 1993), while no fish from the protected population were in this age bracket.

Overall, this study has identified how thermal variability in South Africa's coastal zone can modulate the growth response of an endemic linefish. Understanding the sensitivity of fishes to environmental variability is important to assess the vulnerability of species and implement management plans (Izzo et al. 2016). To date, assessments of the sensitivity of species to climate change has largely considered shifts in distributions (Rountrey et al. 2014). Including the effect of variability in growth patterns, however, could more accurately describe the dynamics of fish populations (Lee et al. 2017) as even small changes in fish body size can have large effects on stock productivity in terms of mortality, biomass and catch (Audzijonyte et al. 2013). Understanding growth variability is particularly important for the multi-species South African linefishery, which is based on many endemic fishes (mainly Sparidae) with vulnerable life history characteristics and a fluctuating thermal environment. A first step would be updating age-growth relationships for these species, which were last done ~ 20–30 years ago, and incorporating historical and contemporary otoliths from these age-growth studies to assess climate-growth relationships.



## 5 Chapter 5

**High temperatures and low oxygen availability  
constrain the edges of *C. laticeps* distribution by  
limiting metabolic potential**



A roman seabream among kelp (Photo credit: Steven Benjamin)

## 5.1 Introduction

Species distribution ranges are naturally dynamic over time; however, climate change is accelerating and modulating the redistribution of species across the globe (Poloczanska et al. 2013, Pecl et al. 2017). Environmental envelopes, which represent the thresholds within which a species can persist, are shifting, which can trigger species distributions to follow suit in order to maintain their physiological rates and functions (Walther et al. 2002, Parmesan 2006, Cheung et al. 2009). The general warming trend of the ocean, has on a broad scale, already driven a shift in the distribution of fishes into higher latitudes (Perry et al. 2005) or deeper depths (Dulvy et al. 2008). Because marine species fill more of their potential latitudinal ranges than terrestrial species, they may be more affected by changes in environmental variables around their thermal limits (Sunday et al. 2012, 2015). Furthermore, characteristics such as high levels of endemism or the synergies between multiple climate drivers and exploitation can promote distribution shifts when environmental envelopes shift (Brook et al. 2008, Wernberg et al. 2011).

Theory suggests that the synergistic interaction between climate stressors and fishing results in greater climate-mediated distribution shifts of fisheries species (Lucey & Nye 2010). For example, changes in the distribution of North Sea cod (*Gadus morhua*) could not be solely attributed to either climate change or fishing pressure, but rather to the combination of both stressors (Engelhard et al. 2014). The exact mechanisms causing this interaction are, however, harder to discern. One mechanism could be changes in recruitment dynamics of species resulting from age-truncated populations. For example, Hsieh et al. (2008) show that exploited species off California exhibit greater distribution shifts than non-exploited species and hypothesise that this is because of fishery-induced geographic range constriction and age-truncated populations. Other proposed mechanisms include the closer affinity of exploited species with higher habitat suitability indices due to decreased biomass and competitive interactions (Planque et al. 2010). Up to now, no studies (other than this one – Chapter 3) have explored the effect of exploitation on changing physiological traits of populations, which

could render exploited populations more sensitive to climate-mediated distribution shifts. Predicting distribution shifts is particularly relevant for managing commercially exploited fishes, to ensure that the management structures are proactive and adaptive to anticipated distribution shifts of targeted species (Brander 2007, Link et al. 2011).

One approach to predict range shifts has revolved around the use of species distribution models (SDMs) which combine the quantification of a species' environmental envelope with predictive modelling of climate-mediated distribution changes (Zimmermann et al. 2010). Almost all SDMs involve a correlative approach between species occurrence data and spatial environmental data (Kearney et al. 2008). Unfortunately, these correlative models have limited ecological application if there is a weak match between distribution and physical environmental variables, as their underlying assumptions are that occurrence data accurately represent the ecological niche of a species and that the niche is solely determined by environment (Araújo & Guisan 2006, Araujo & Townsend Peterson 2012). A recent addition to the SDM approach has been an attempt to incorporate physiological rates and thresholds to develop more mechanistic-based interpretations of the range limits of species (Kearney & Porter 2009). Incorporating physiological processes into SDMs may be more informative than the purely correlative approaches (Kearney & Porter 2009, Teal et al. 2015), as it is physiological responses to environmental conditions that underpin the relationship between an organism and its environment. The incorporation of mechanistic processes or capacities of species into SDMs can therefore increase their accuracy and interpretability (Kearney & Porter 2009, Pacifici et al. 2015).

Combining mechanistic processes into SDMs comes with challenges. Study organisms are often not suitable for laboratory-based physiology research, have unknown ecological requirements (Evans et al. 2015, Teal et al. 2015), and there are difficulties with linking physiological processes to spatial environmental data (Kearney & Porter 2009, Sinclair et al. 2016). Furthermore, experimentally derived thresholds of the performance of organisms may not represent the actual performance in the wild. To overcome these limitations, a hybrid

approach, where environmental data is transformed into an index of physiological-based habitat suitability and combined with a correlative SDM may improve model interpretability and accuracy (Austin 2007, Kearney et al. 2008, Kearney & Porter 2009) and can incorporate the influence of physiology.

Physiological indicators, like aerobic scope, allow projections beyond the range of data and have recently been incorporated into predictive models for fisheries species (Peck et al. 2016; Teal et al. 2015). For example, Teal et al. (2015) used experimentally derived aerobic scopes of two fish species, the seabream (*Salpa salpa*) and the marbled spinefoot (*Siganus rivulatus*) in the Mediterranean to develop a spatial thermal habitat suitability index, which underpins projections of both species' future distributions. Cucco et al. (2012) developed an aerobic scope-based physiological model and combined it with temporally resolved oceanographic data to demonstrate that the migration of flathead mullet (*Mugil cephalus*) in the Mediterranean generally tracks the environmental conditions that optimised aerobic scope. Although these physiological-based mechanistic models overcome many of the limitations associated with correlative SDMs, they often assume that temperature is the only environmental variable which modulates how a fish population relates to its immediate environment (Sinclair et al. 2016).

Temperature, together with oxygen availability, however, are considered the primary controlling and limiting factors on fish physiology respectively (Claireaux & Chabot 2016). Temperature regulates the demand for oxygen by ectotherms (Vaquer-Sunyer & Duarte 2008, Rogers et al. 2016, Motyka et al. 2017, Townhill et al. 2017) and the solubility of oxygen in water diminishes in warm water (Stramma et al. 2010), while the amount of oxygen available limits the amount of oxygen that can be used by an organism. Temperature and oxygen availability thus have the potential to interact and influence fish in the context of climate change by influencing oxygen supply and demand (Rogers et al. 2016). Despite the importance of temperature and oxygen in governing the physiological rates of fishes, relatively few studies predicting the effects of climate change on fish have included both variables (Townhill et al.

2017), most probably because a mechanistic model that can evaluate how oxygen availability and temperature interact to limit the geographical distributions of aquatic organisms is required. Deutsch et al. (2015) have recently developed such a model, which may have greater ability to predict both abundance and distribution patterns, and thus make predictions that are relevant to fisheries.

Deutsch et al. (2015) propose a metabolic index ( $\phi$ ), which represents the ratio of O<sub>2</sub> supply to resting O<sub>2</sub> demand and incorporates the effect of temperature on oxygen partial pressure and temperature effects on standard metabolic rate and oxygen availability. Most fish species can maintain stable metabolic rates across a range of oxygen saturation levels (oxy-regulators) until a point where the levels limit the rate at which fish can use oxygen to create energy (oxy-conformers) (Cerezo & García García 2004). Each individual (and species) thus has a corresponding oxygen level below which standard metabolic rates cannot be maintained (Snyder et al. 2016). Since the parameters used for calculating  $\phi$  vary among species (Deutsch et al. 2015), the index needs to be calibrated with population-specific data before it can be applied. This is done by calculating a limiting oxygen level (LOL) curve, which is defined as the relationship between the level of oxygen saturation that becomes limiting at various metabolic rates (Neill et al. 1994, Claireaux & Chabot 2016) across a range of temperatures. The LOL at an organism's standard metabolic rate (SMR) is termed O<sub>2crit</sub> and is interpreted as the minimum level of oxygen required to sustain the metabolic demands required for maintenance beyond which anaerobic metabolism must compensate for energy shortfalls.

Because  $\phi$  incorporates both oxygen availability and temperature, it can be used 1) to explore how variability in these two important environmental variables controls the distribution of marine species and 2) to predict the impact of changes in these two parameters on the distribution of species. This is particularly important for South Africa's coastal zone, as temperature and oxygen saturation are highly variable in space and time (Roberts 2005). Along the west coast, the Benguela Current dominates oceanographic processes, with the southern Benguela characterised by a relatively consistent yet seasonally varying, upwelling

zone with a low oxygen level (Hutchings et al. 2009). The southern and eastern coasts of South Africa are influenced by the warm Agulhas current and wind-induced upwelling that can result in localised variability in oceanographic processes and their associated temperature and oxygen saturation (Schumann et al. 1995, Lutjeharms et al. 2000). These upwelling events are predicted to increase with climate change (Rouault et al. 2010), as are globally low oxygen zones (Stramma et al. 2010, 2012).

The aim of this chapter was therefore to discern if exploitation can alter the metabolic index ( $\phi$ ) of *C. laticeps* by calibrating it with data from exploited and protected populations and to develop predictions on the future distribution of *C. laticeps* based on  $\phi$ . To do this, novel SDMs that incorporate  $\phi$  and occurrence data for *C. laticeps* were developed using random forest classification trees.

## 5.2 Methods

### 5.2.1 Metabolic index

The metabolic index ( $\phi$ ) (Equation 5.1) represents the ratio of O<sub>2</sub> supply to O<sub>2</sub> demand, taking into account the oxygen partial pressure at depth and temperature effects on standard metabolic rate and oxygen availability (Deutsch et al. 2015), and is calculated as follows:

$$\phi = A_0 B^n \frac{PO_2}{\exp\left(-\frac{E_0}{k_B T}\right)} \quad (\text{Equation 5.1})$$

where the parameters of the metabolic index ( $A_0$  and  $-E_0$ ) are derived from the slope and intercept of the linear relationships between mass normalised  $pO_{2crit}$  and the inverse of  $k_B T$  (the product of temperature in kelvin and the Boltzmann constant).

The estimated  $\phi$  model parameters  $A_0$ ,  $-E_0$ , are taken from the intercept and slope, respectively, of the linear relationships between mass normalised critical oxygen partial pressures ( $pO_{2crit}$ ) and the inverse of  $k_B T$ . To explore whether exploitation may alter population level  $\phi$ , the model was first calibrated with laboratory-derived parameter estimates per exploited/protected population as described in the following sections.

### 5.2.2 Critical oxygen saturation

After metabolic rates were determined (detailed in Chapter 3), each individual was left in the respirometer and given time to recover to levels approximating SMR (~ four to five hours). Respirometers were then closed and the rate of decline in oxygen was measured in five-minute intervals until an individual showed distinct signs of stress or impaired performance. Each measurement period was converted to a mass-specific metabolic rate at a given  $O_2$  saturation. The calc  $O_{2crit}$  function, developed by Claireaux & Chabot (2016), was used to determine  $O_{2crit}$  (% air saturation).  $O_{2crit}$  was defined as the oxygen saturation level where SMR and the linear decline in oxygen below SMR intersected (Figure 5.1). The maximum number of points for the regression was set to 15 and the resulting plot inspected. If the plot indicated an overestimation of  $O_{2crit}$  because the experiment was terminated prematurely, the maximum number of points was limited to four points below the pivot point.

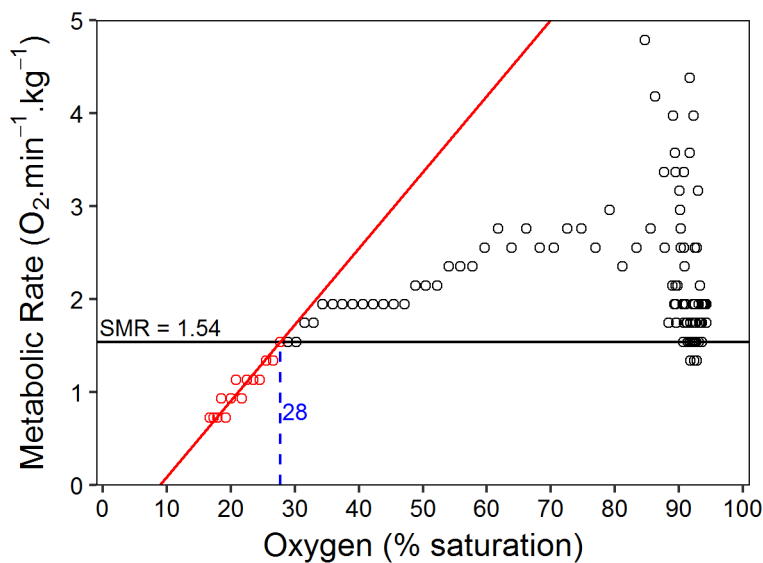


**Figure 5.1:** Dataset demonstrating the determination of  $O_{2crit}$  for an individual specimen at a set temperature. Each circle represents a metabolic rate at an  $O_2$  saturation. The solid black line is SMR calculated as the 0.2 percentile of metabolic rates in normoxia (>70%). The solid red line is the linear relationship between metabolic rate and  $O_2$  saturation for MR below SMR. The intersection of both solid lines is the critical oxygen saturation (dotted blue line).

### 5.2.3 Data standardisation

All critical oxygen thresholds (% saturation) were converted to corresponding critical oxygen partial pressures ( $pO_{2crit}$ , Torr) using the solubility of  $O_2$  in seawater at experimental test temperatures, salinity and atmospheric pressure. Because SMR is influenced by factors such as temperature and mass,  $pO_{2crit}$  is influenced by the same factors (Claireaux & Chabot 2016). Smaller animals and animals in warmer temperatures tend to exhibit higher mass-specific metabolic rates. To remove the effect of size on  $pO_{2crit}$ , all data were first temperature standardised by dividing by the Arrhenius function and finding the best-fit exponent of the mass- $pO_{2crit}$  power law relationship (Deutsch et al. 2015). To test for differences in  $pO_{2crit}$  between exploited and protected populations, the linear relationship between mass normalised  $pO_{2crit}$  and temperature was modelled including population (exploited/protected) as an interaction term for temperatures between 12 and 24 °C.

### 5.2.4 Environmental and occurrence data

Spatial environmental data were obtained from a high-resolution (0.25° horizontal resolution) coupled ocean-biogeochemistry model (Yool et al. 2015, Popova et al. 2016) for the periods between 2005–2009 (current) and projections towards 2095–2099 (future). The model framework is built on the physical Nucleus for European Modelling of the Ocean (NEMO) model (Madec 2008) coupled with a Model of Ecosystem Dynamics, nutrient utilisation, sequestration and acidification (MEDUSA 2.0) (Yool et al. 2013). The forward projection is based on the IPCC representative concentration pathway 8.5, which is the worst case, business-as-usual scenario of future greenhouse gas concentrations (IPCC 2014). Monthly current and future oxygen concentration ( $mmol.m^{-3}$ ), salinity (psu) and temperature (°C) were extracted from the layer of cells closest to the sea floor for depths between 0–100 m below sea level around the southern African coast (17 – 36°S and 15 – 36°E). Oxygen concentration was converted to partial pressure (Torr) based on grid cell salinity, temperature, oxygen concentration and pressure at the depth of each cell using the presens package (Birk 2016). The mean of surrounding cells was used to estimate values for cells with no data near the

coast. The resolution of environmental data was increased to 0.125° horizontal resolution (13.31–11.27 km) by locally resampling using bilinear interpolation with the raster package (Hijmans 2016).

Monthly  $\phi$  grid cells were generated by projecting the calibrated  $\phi$  equation across the spatial and temporal extent of temperature and oxygen partial pressure data from the ocean model. Predicted monthly mean, minimum and maximum  $\phi$  layers were developed for current (2005–2009) and future (2095–2099) scenarios together with depth as predictor variables. Gridded bathymetry data were obtained from the General Bathymetric Chart of the Oceans (GEBCO) website at a 30 arc second resolution and resampled to a 0.125° horizontal resolution (13.31–11.27 km) by taking the mean depth of every cell within the 0.125° grid (13.31–11.27 km).

Occurrence data for *C. laticeps* were obtained from a commercial and recreational database of geo-referenced catch data in the national marine linefish system (NMLS) from 2000–2010 made available from the DAFF. A total of 14 934 occurrence points were obtained and reduced to 206 points once duplicates were removed from the 0.125° grid cell resolution.

#### 5.2.5 Distribution modelling

A machine learning approach was implemented, using the random forest algorithm (Breiman 2001) to model the current distribution, quantify the  $\phi_{crit}$  and predict future distributions of *C. laticeps* up to 2099 using the randomForest package (Liaw & Weiner 2002). Random forests are an extension of traditional classification trees, where many trees are grown using bootstrapped samples of data, and a random selection of predictor variables at each tree node is used for classification (Cutler et al. 2007).

The guidelines of Barbet-Massin et al. (2012) were followed when using random forest to model the distribution of *C. laticeps*. A data set consisting of 206 known occurrence points was combined with 206 pseudo-absence data points. Background data points were generated by randomly selecting cells throughout the extent of the predictor variables but excluding cells adjacent to known occurrence points. The dataset (n = 412) was then randomly subdivided

into model training (80%) and model testing (20%) datasets. The predictive performance of each trained model was assessed based on the accuracy of correctly classifying the test data set. Variable importance for the predictors of each model was calculated from the out-of-bag classification accuracy before and after permuting each predictor variable using the caret package (Kuhn 2008).

To assess what temporally resolved value of  $\phi$  may limit the distribution of *C. laticeps* ( $\phi_{crit}$ ), ten full random forest models were trained and assessed with maximum, minimum and mean  $\phi$ , together with depth as predictor variables for the current period. Ten more reduced random forest models were then re-trained and tested using only the top two predictor variables. The predictive accuracy of the full versus the reduced models was then compared. The simplest model with the highest accuracy (measured as a proportion of correctly identified test data cells) was chosen as the best predictive model and used to model current and future distributions of *C. laticeps*. Current and future distributions of *C. laticeps* were estimated as the average of ten random forest models trained on unique combinations of presence-absence data (described above) and projected across the extent of predictor variables. To quantify the occurrence thresholds of predictor variables, the feature contribution of each training data point was extracted from the random forest model using the forestFloor package (Welling et al. 2016) for all ten current model runs, and combined. Depth data was fitted with a 2<sup>nd</sup> order polynomial and the x intercepts taken as depth thresholds. Metabolic index ( $\phi$ ) feature contribution data were converted into binary data by reclassifying negative feature class contributions to zero and positive contributions to one, fitting the data with a logistic regression and taking the threshold at the point of intersection of  $y = 0.5$ .

## 5.3 Results

### 5.3.1 Calibration of the metabolic index

There was a weak positive relationship between mass and  $pO_{2crit}$ , with the mass scaling exponent estimated at 0.155 (Figure 5.2). Mass normalised  $pO_{2crit}$  data revealed a positive

linear relationship with temperature (12–24 °C), which was not significantly different between exploited/unexploited populations ( $p$ -value > 0.05, Figure 5.3). Although there was a negative relationship between  $pO_{2crit}$  and temperature between 8–12 °C, the small sample size ( $n = 3$ ) at 8 °C prohibited further analysis of differences between exploited and unexploited populations for this temperature range. Consequently, all data were pooled to determine the  $\phi$  – distribution relationship for *C. laticeps*.

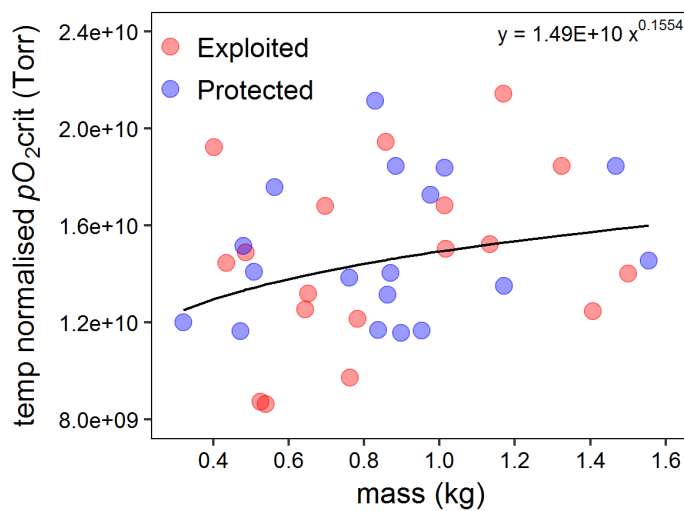


**Figure 5.2:** Power law relationship (black line) between mass (kg) and temperature normalised  $pO_{2crit}$  (Torr), indicating a mass scaling exponent of 0.155 for combined exploited (red points) and protected (blue points) populations.

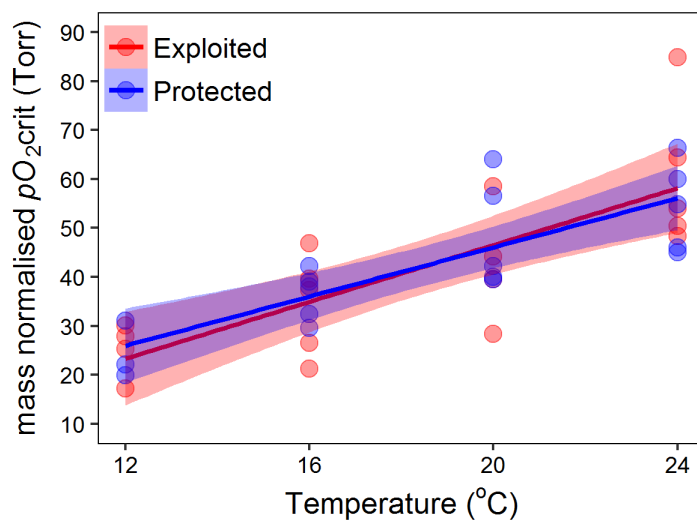


**Figure 5.3:** Temperature effect on mass normalised critical oxygen partial pressure ( $pO_{2crit}$ ) per exploited (red) and protected (blue) populations. Points represent individual data points fit with the linear relationship (solid line) and 95% confidence interval (shaded) for each sampling population.

The differing slopes of the  $pO_{2crit}$  – temperature relationship (8–12 °C and 12–24 °C) permitted fitting a piecewise relationship to estimate  $\phi$  parameters either side of 12 °C (Figure 5.4).

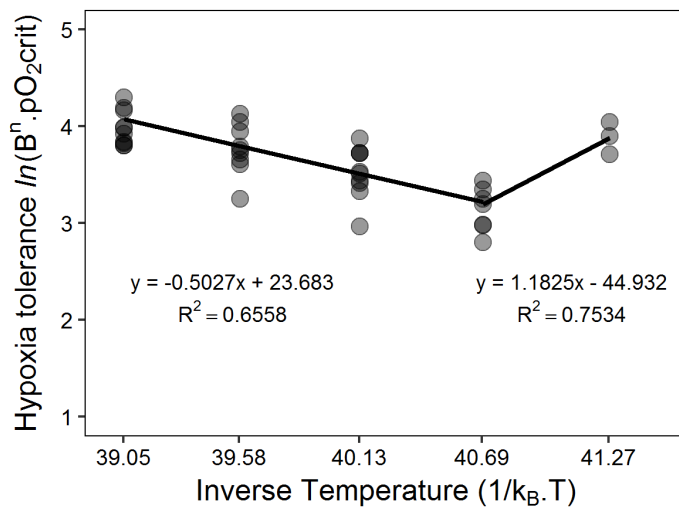


**Figure 5.4:** Piecewise (12 °C) relationship between the natural logarithm of standardised mass-specific hypoxia tolerance ( $\ln(B^n \cdot pO_{2crit})$ ) and the inverse product of temperature (T in kelvin) and the Boltzmann constant ( $k_B$  in ev) for combined exploited and protected data.

The estimated  $\phi$  model parameters  $A_o$ ,  $-E_o$ , taken from the intercept and slope respectively, could thus be estimated for each linear relationship and are presented in Table 5.1. A graphical representation of the calibrated piecewise  $\phi$  for *C. laticeps* is presented (Figure 5.5) across a matrix of temperatures (°C) and oxygen levels (% saturation) indicating how temperature or oxygen availability can limit  $\phi$ .

**Table 5.1:** Model parameters of calibrated piecewise metabolic index model.  $k_B$  is the Boltzmann constant,  $n$  is the mass scaling exponent,  $-E_o$  is the temperature dependence, and  $A_o$  is the ratio of oxygen supply and demand rate coefficients.

	$\geq 12$ °C	$< 12$ °C
$A_o$	5.18327E-11	3.2637E+19
$n$	-0.159	-0.159
$-E_o$	0.5027	-1.1825
$k_B$	8.61734E-05	8.61734E-05

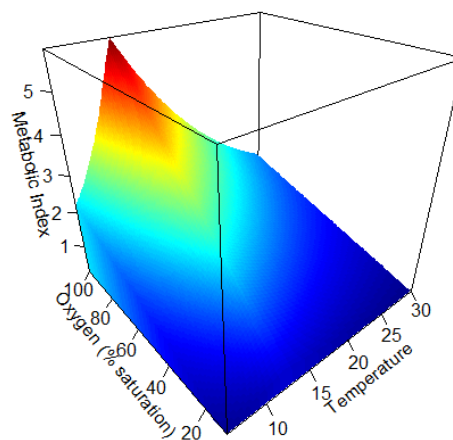


**Figure 5.5:** Graphical representation of the metabolic index for *C. laticeps* across a matrix of temperature and oxygen saturations.

### 5.3.2 Environmental and occurrence data

Occurrence points were distributed throughout the South African south coast, which was in accordance with the published distribution of *C. laticeps* (Figure 5.6 a). Mean current (2005–2010) spatial bottom temperature (Figure 5.6 b) and oxygen concentration (Figure 5.6 c) were variable throughout the extent of the modelling domain. Mean current bottom temperatures ranged from 13.1–27.3 °C and were coolest along South Africa’s south coast, and increasing east and west towards higher latitudes (Figure 5.6 b). Mean current oxygen concentration ranged from 171–220 mmolO<sub>2</sub>.m<sup>-3</sup>, with low oxygen zones occurring offshore of South Africa’s west and central south coasts (Figure 5.6 c). The spatial variability in temperature and oxygen resulted in a heterogeneous mean  $\phi$  for *C. laticeps* throughout the modelling domain (Figure 5.6 d). The mean  $\phi$  for the current period ranged from 2.17 to 4.78 and was greatest along the south coast as warm temperatures along the east coast and low oxygen availability along the west coast limited the  $\phi$ .

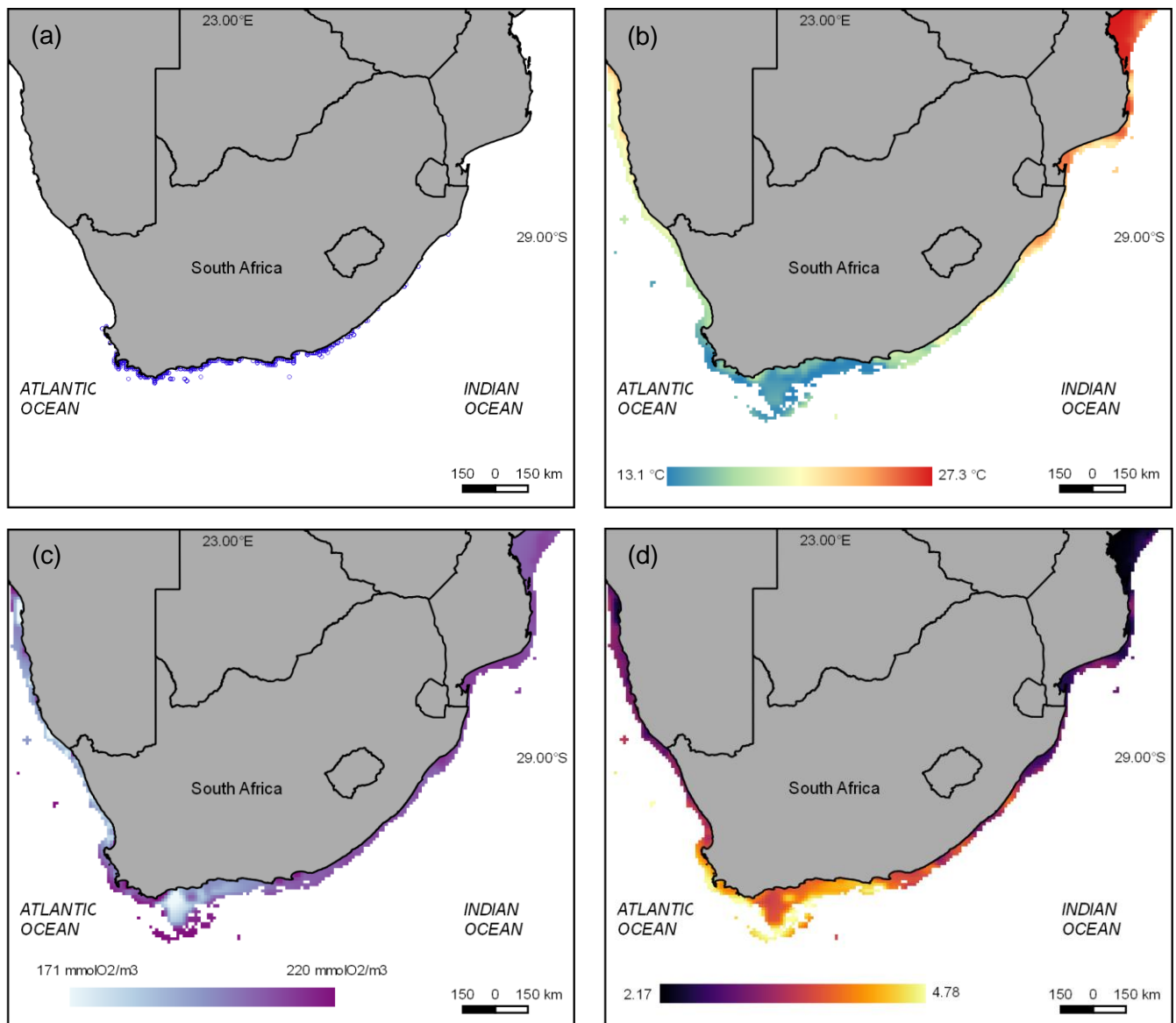


**Figure 5.6:** Spatial representation of *C. laticeps* occurrence data (blue dots) from 2000–2010 (a), mean bottom temperature (°C) between 2005–2010 (b), mean bottom oxygen concentration (mmol.m<sup>-3</sup>) between 2005–2010 (c) and the mean metabolic index ( $\phi$ ) for *C. laticeps* between 2005–2010 (d) at depths less than -100 m below seas level.

### 5.3.3 Species distribution modelling

The full random forest model based on all magnitudes (minimum, maximum and mean) of current  $\phi$  and depth had a mean predictive accuracy of 0.93 across all ten runs (Table 5.2). Depth and minimum  $\phi$  were the two most important predictor variables in all model runs. There was no significant difference in a mean model's predictive accuracy ( $p$ -value > 0.05) when running models with just depth and minimum  $\phi$  as predictor variables (Table 5.2).

**Table 5.2:** Mean model predictive accuracy based on ten runs for full  $\phi$  model (a) and reduced  $\phi$  model (b).

Model	Predictors	n	Mean accuracy
full	depth, mean $\phi$ , max $\phi$ , min $\phi$	10	0.93 ( $\pm$ 0.02)
reduced	depth, min $\phi$	10	0.92 ( $\pm$ 0.03)

Extracting contributions from parameters of the trained, reduced models indicated that suitable depths for *C. laticeps* occur between 15 and 72 m below sea level (Figure 5.7 a), and the threshold of minimum  $\phi$  ( $\phi_{crit}$ ) below which *C. laticeps* can no longer persist is 2.9 (Figure 5.7 b).

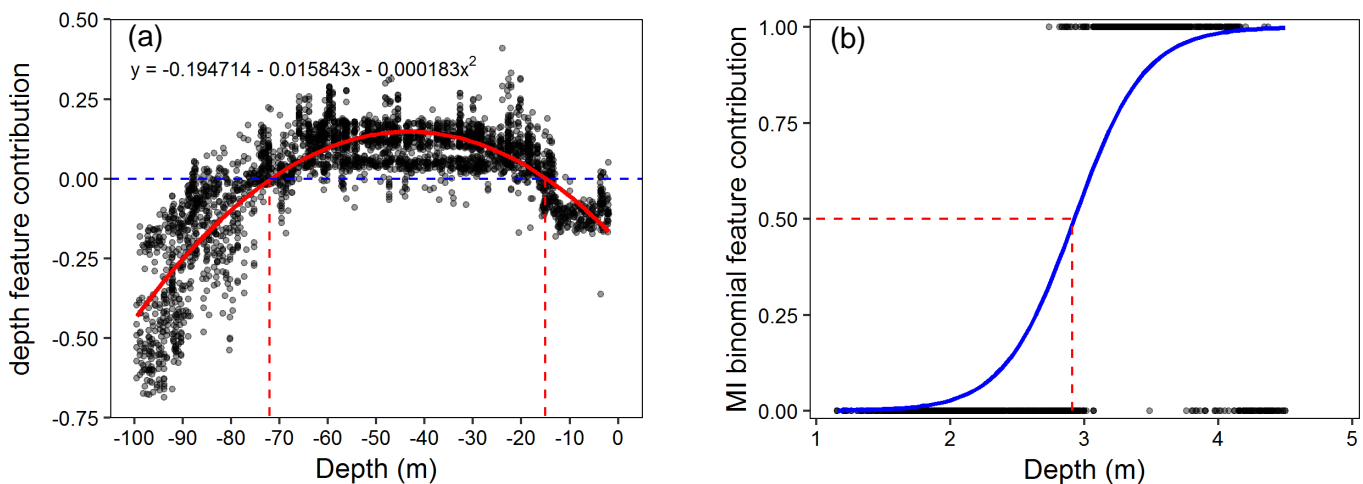


**Figure 5.7:** Feature contribution (black dots) of depth cells (a) and minimum  $\phi$  cells (b) for all ten random forest reduced models. Depth thresholds for occurrence were between -72 and -15 metres below sea level (red dashed lines in (a)) taken as the x intercepts for  $y = 0$  of the quadratic relationship (solid red line) and minimum metabolic  $\phi$  threshold of 2.9 (red dashed lines (b)) taken as the 0.5 threshold of the logistic regression (solid blue line).

The current modelled distribution indicated a core range for *C. laticeps* from the Cape Peninsula in the west towards Port St Johns in the east, with a break and a small patch of suitable habitat in the east (Figure 5.8 a). Projections indicate that this core distribution will persist up until 2100 but the western and eastern edges of the species distribution will contract slightly (Figure 5.8 b, c). There was high model agreement among current and projected distributions indicated by the dominant number of pixels = 1 indicating that all ten models agreed on the occurrence/absence of a cell (dark red, Figure 5.8 a, b).

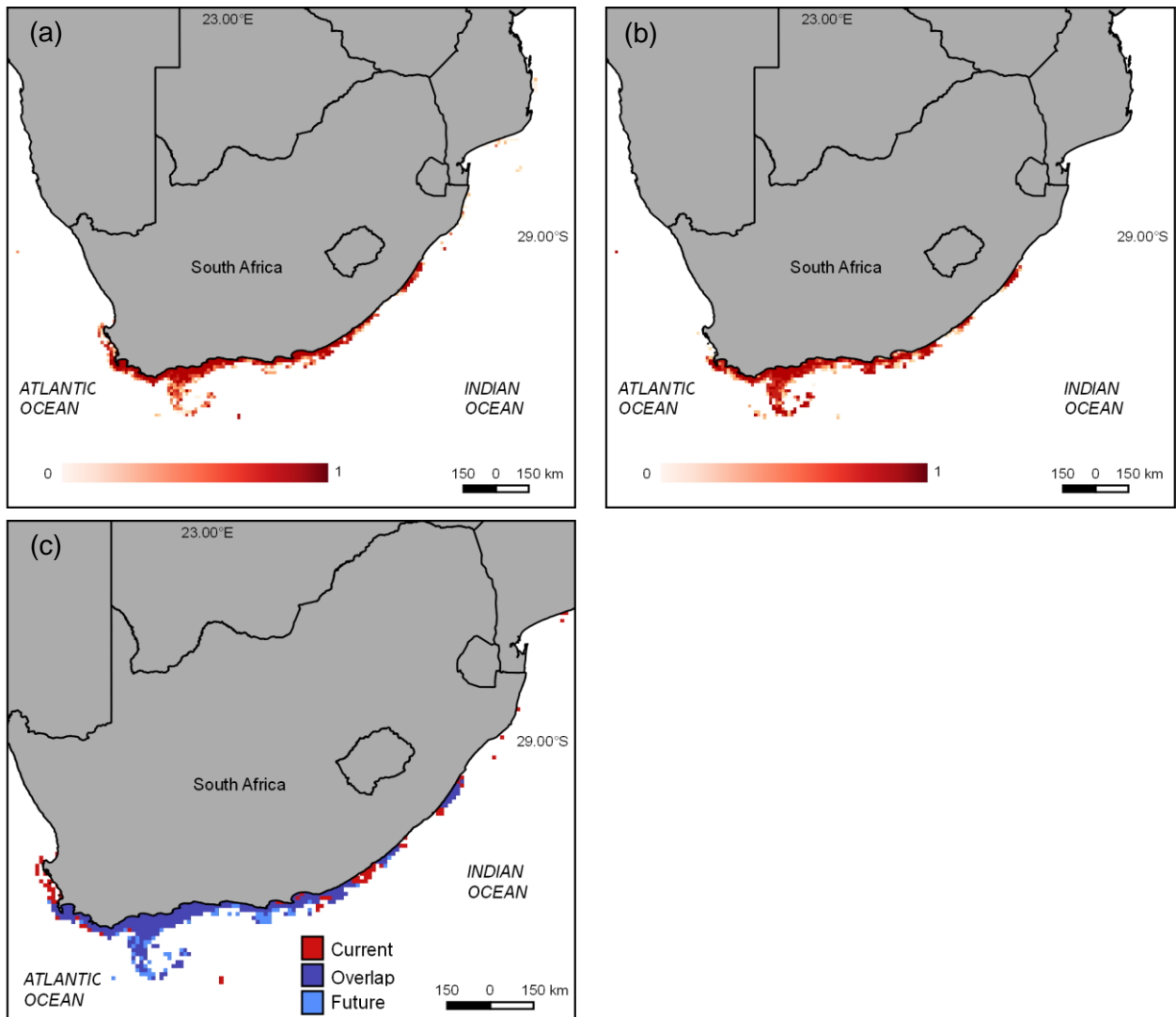


**Figure 5.8:** Modelled current (a) and future (b) distribution of *C. laticeps* based on the probability of occurrence among ten random forest projections on current and future changes in minimum metabolic index and predicted change in *C. laticeps* distribution (c) between current (2005–2010) and future (2095–2099) binary projections taken with 0.5 as the probability threshold of occurrence.

## 5.4 Discussion

This chapter finds that the geographic distribution of *C. laticeps* is constrained by a minimum  $\phi$  threshold of 2.9, which is limited in the west by low oxygen and in the east by high temperatures. Projections for the end of the century indicate that the western and eastern edges of *C. laticeps*' distribution will contract slightly owing to the general warming trend and subsequent reductions in oxygen levels, further constraining  $\phi$ . Overall, the core distribution

of *C. laticeps* is, however, predicted to persist up until at least 2100 as the ocean model projections over the core fishing areas indicate that  $\phi$  will remain above the 2.9 threshold.

Finding consistent patterns in physiological traits that limit the distribution of species across taxa is rare (Bozinovic et al. 2011, Evans et al. 2015). The  $\phi_{crit}$  values for *C. laticeps* (2.9) were similar to the summer  $\phi_{crit}$  (3.2) found for the closely related sharpsnout seabream (*Diplodus puntazzo*) in the north Atlantic (Deutsch et al. 2015). Deutsch et al. (2015) show consistent patterns between taxa regarding the equatorward limit of  $\phi$  with summer  $\phi_{crit}$  ranging from 2.2 for common eelpout (*Zoarces viviparus*) to 3.3 for Atlantic cod (*Gadus morhua*), probably due to the antagonistic effect of rising temperature on  $\phi$ . The piecewise relationship between hypoxia tolerance and temperature (Figure 5.4), developed here, shows how  $\phi$  can limit both warm and cool edges of a species distribution.

A piecewise relationship between  $\phi$  and temperature was possible because the acute temperature decrease to 8 °C resulted in cold shock and an elevated SMR, which broke the consistent scaling of SMR with temperature between 12 to 24 °C (Chapter 3). The elevated SMR at 8 °C caused SMR to intersect the LOL curve at a higher point, resulting in a higher  $O_{2crit}$  (Killen et al. 2012). While this finding is theoretically sound, the applicability of estimating  $O_{2crit}$  during metabolically stressful events in the lab needs consideration, as these events must be ecologically relevant. Strong upwelling events, however, are frequent throughout *C. laticeps* distribution, and very few grid cells had a minimum monthly temperature below 12 °C, suggesting results would be similar if the  $\phi$  parameters between 12–24 °C were extended to lower temperatures.

The predicted contraction of *C. laticeps*' distribution is consistent with climate-mediated distribution shifts of fish species already recorded off the temperate South African coastal zone (Whitfield et al. 2016). For example, the Cape anchovy (*Engraulis encrasicolus*) shifted its distribution from the southern Benguela to the Agulhas Bank during the mid-1990s which was attributed to an increase in upwelling off the Agulhas Bank (Roy et al. 2007). Along the east coast, warming has resulted in a southward extension in distribution and abundance of tropical

species (James et al. 2008, Lloyd et al. 2012), which is consistent with the general poleward shift observed for fish species globally (Last et al. 2011). The extension of cool temperate habitat and species in the west, and sub-tropical habitat and species in the east is suggested to put a “squeeze” on potential distribution shifts of warm/cool temperate species around South Africa (Potts et al 2015, Whitfield et al. 2016) which is corroborated by the findings from this chapter.

While a predicted distribution contraction is a concern for any species, the most productive fishing grounds for *C. laticeps* in terms of catch per unit effort, west of Port Alfred and east of the Cape Peninsula (Kerwath et al. 2013b), are predicted to persist up until 2100 (Figure 5.8 c). Catches of *C. laticeps* are rare west of the Cape Peninsula and other shore-based linefish stocks have already been reported as collapsed in that area (Attwood & Farquhar 1999). East of Port Alfred, where the distribution of *C. laticeps* is predicted to disappear, catches are again relatively low (Kerwath et al. 2013b) and the area cannot be considered a commercially important zone for this species. These results have shown how minimum monthly  $\phi$  limits the distribution of *C. laticeps*, but whether  $\phi$  affects the productivity, and hence catch returns, of *C. laticeps* remains unresolved, although exploring spatial trends in CPUE and  $\phi$  could clarify whether any relationships exist.

The predicted contraction of *C. laticeps*' distribution by the end of the century is in accordance with the few other correlative SDM studies on endemic fish species in southern Africa. Duncan (2013), Coppinger (2013) and Isemonger (2013) predict that the distribution of the endemic sub-tropical linefish species, slinger (*Chrysoblephus puniceus*), scotsman (*Polysteganus praeorbitalis*) and catface rockcod (*Epinephelus andersoni*) would contract in the future. The predicted contraction is attributed to a combination of a warming trend in the east and intensification of cold upwelling cells in the south that limits the poleward distribution shift in the south. Other lines of evidence also provide support for the validity of the SDM in this study. The current distribution model of *C. laticeps* indicates a core range between Cape Point in the west and the southern Transkei in the east which overlaps with its known distribution (Buxton

1987, Griffiths & Wilke 2002, Götz & Kerwath 2013). The optimal depth range (15–72 m below sea level) of the current model is also within the maximum depth (100 m) described for the species (Götz & Kerwath 2013). Furthermore, all ten current random forest models predicted a patch of isolated suitable habitat in the east despite few occurrence points from the area used in model training (Figure 5.9 a). This suitable habitat corresponds to the distribution of many historical occurrence points (1970–2000), which were not included in data used to build the projections of suitable habitat (Figure 5.9 c).

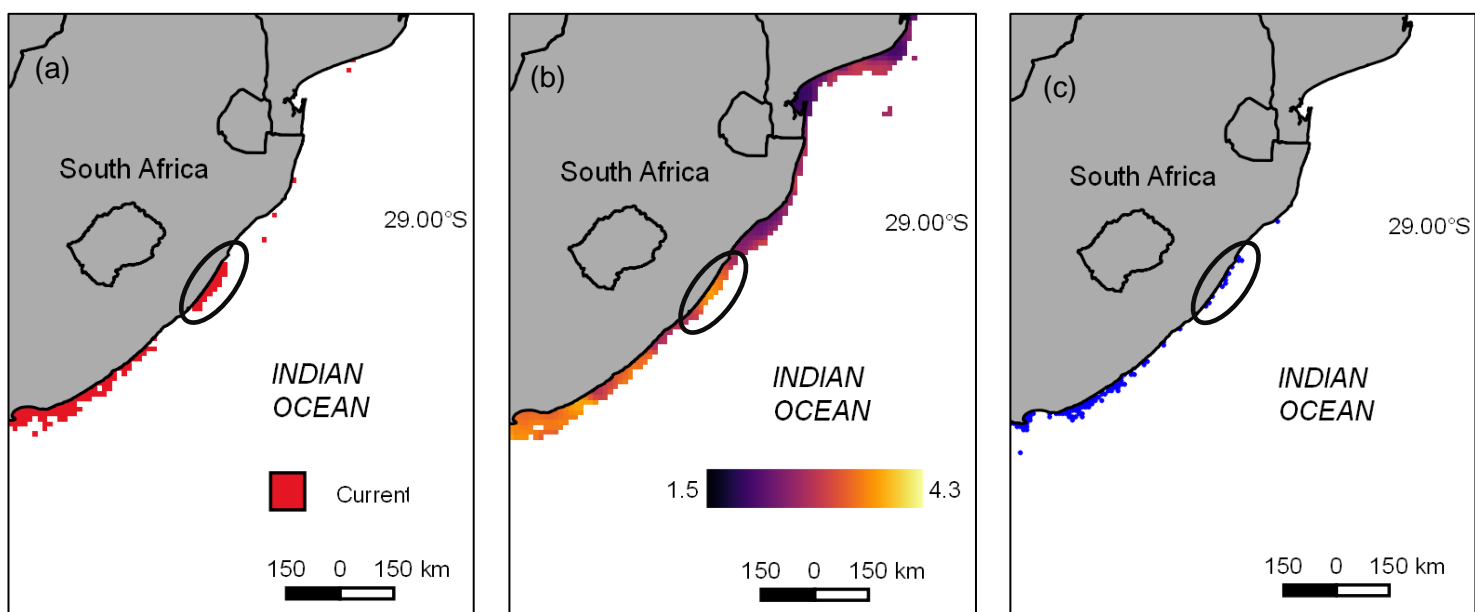


**Figure 5.9:** Current distribution from ten random forest models added together and occurrence threshold taken at 50% agreement between all ten models (a), minimum monthly  $\phi$  from ocean model 2005–2010 (b) and the historical and contemporary (1970–2016) occurrence data for *C. laticeps* from the NMLS of South Africa housed at DAFF (c).

Global studies employing correlative SDMs have predicted large distribution contractions and extinctions of species in the future under projected climate change. For example, Lasram et al. (2010) predict that by 2070–2099 a total of 45 of the 75 fishes that were assessed in the Mediterranean will qualify for the IUCN red list based on extensive range contractions and fragmentation, while 14 are predicted to become extinct. Again in the Mediterranean, Albouy et al. (2013) predict that 54 of 288 coastal fish species will completely lose their suitable habitat

by the end of the 21<sup>st</sup> century. In contrast, while the future projection of *C. laticeps* indicates a range contraction, the core range of *C. laticeps* is predicted to persist up until 2100.

The broad range of environmental fluctuations on a scale of hours along South Africa's coastal zone may provide some acclimation of *C. laticeps* to monthly changes in these environmental variables. For example, in the north-western Mediterranean, Garrabou et al. (2009) studied the effect of a heatwave and record temperatures on mass mortalities of invertebrates. To quantify the record temperatures, Garrabou et al. (2009) compared the maximum sea temperatures during the heatwave to historical means at multiple sites. At depths from below ten metres, the highest temperature anomaly from the mean was 3.1 °C. In contrast, for the TNP UTR daily sea temperature dataset (depth 12 m) the highest recorded temperature was 6.6 °C above the annual mean. The reported daily temperature anomalies again support the implementation of acute thermal stress events in laboratory experiments used to calibrate  $\phi$ .

A number of factors regarding the experimental procedure need to be considered when evaluating the output of the present study. Closed respirometry was used to determine an individual's  $O_{2crit}$ . As the rate of oxygen decline is influenced by an individual's metabolic rate, the rates of oxygen decline were not consistent between individual trials. In reality, a combination of the severity and duration of exposure determines an organism's hypoxia tolerance as an anaerobic metabolism and behavioural modifications can facilitate short-term persistence (Claireaux & Chabot 2016). Behaviour and physiological modifications such as increasing ventilation rates, cardiac rates or haemoglobin binding capacity (e.g., Mandic et al. 2009, Rogers et al. 2016) allow fish to maintain oxygen extraction when environmental conditions are sub-optimal (Killen et al. 2012). Furthermore, in closed respirometry, the build-up of nitrogenous waste can exert an additional stress on fish that can influence the determination of  $O_{2crit}$ , although carbon dioxide should accumulate well before nitrogen. In a study by Snyder et al. (2016) on shiner perch (*Cymatogaster aggregate*), closed respirometry resulted in a higher  $O_{2crit}$  compared to intermittent flow respirometry, which could have been caused by the higher rate of  $O_2$  decline or nitrogenous waste build-up when using the closed

respirometry. While the most appropriate method for calculating  $O_{2crit}$  is an active area of research, this study determined  $O_{2crit}$  in accordance with a study on sharpsnout sea bream (*Diplodus puntazzo*) (Cerezo & García García 2004) which Deutsch et al. (2015) used to calibrate the  $\phi$  for this species.

The limitations of correlative SDMs also needs consideration when using laboratory-derived data to project future distributions. A number of assumptions are included within a purely correlative predictive model and these may result in exaggerated distributional changes. A primary assumption is that physiological processes do not vary over space or time and are not influenced by previous exposure to a stressor (Evans et al. 2015). Furthermore, the assumption that physiological characteristics do not vary over ontogeny is problematic as larval stages may have a constrained physiological window that could determine abundance and eventually distribution ranges (Sinclair et al. 2016). While these concerns need to be considered when implementing SDMs, these models remain the most useful tool to predict species distributions (Araujo & Townsend Peterson 2012) and considering the ecological plausibility of model predictions can improve researcher confidence in model results (Austin 2002). The approach used here incorporates a physiological index of how the two most important environmental variables (temperature and oxygen) affect the metabolic capacity of *C. laticeps*, combined with a high-resolution ocean model, and assessed in terms of ecological plausibility and previously documented shifts in other marine fishes.

Despite the influence of fisheries exploitation in shaping the aerobic scope capacity and diversity of aerobic scope phenotypes (Chapter 3), exploitation did not influence the  $\phi$  parameters, and thus distribution responses between the protected and exploited populations could not be modelled.  $O_{2crit}$  is primarily determined by SMR (Killen et al. 2012, Rogers et al. 2016); however, earlier research (Chapter 3) did not find a difference in SMR between sampling populations which then corresponded to no difference in  $O_{2crit}$ . Few studies have incorporated the role of hypoxia tolerance and metabolic rates in modifying the behaviour of individuals during hypoxic events, which have the potential to alter capture probabilities. Killen

et al. (2012) found that European sea bass (*Dicentrarchus labrax*) risk-taking behaviour (emergence in the presence of a potential predator to obtain food) is positively associated with routine metabolic rate only during severe hypoxia treatments, suggesting that high metabolic phenotypes may be more sensitive to hypoxia. However Cook et al. (2011) artificially reduced physiological capacity through anaemia in snapper (*Pagrus auratus*) and found that, despite no difference in SMR, reduced aerobic scope correlated with a higher  $O_{2crit}$  than control fish. As hypoxic dead zones are predicted to increase in the future (Diaz & Rosenberg 2008), discerning how fisheries exploitation may select for traits that influence hypoxia tolerance must emerge as an important avenue of research.

## 6 Chapter 6

### General discussion: synthesising research for current climate policy frameworks



A small-scale commercial linefishing vessel that targets roman seabream, among other species (Photo credit: Henk Kruger/Cape Argus)

## 6.1 Overview

This thesis is the first thermal physiological research of an endemic linefish from South Africa's warm temperate, highly variable thermal environment. Findings demonstrate that *C. laticeps* (and probably other similar species) may be physiologically resilient to the impacts of climate change in terms of warming and hypoxia tolerance, but may be more susceptible to increases in extreme intermittent upwelling events. At a metabolic level, *C. laticeps* has a broad thermal range that should allow the species to maintain energetic processes throughout most of their highly variable thermal habitat. However, when the largest observed upwelling events were simulated in the laboratory, fish appeared to go into "cold shock", suggesting that rapid cooling events may be the primary metabolically limiting processes in a more thermally variable future ocean. The metabolically taxing "cold shock" influenced the growth response of *C. laticeps* where years with a high cumulative upwelling intensity were associated with slower growth. The minimum monthly  $\phi$  was the best predictor of the distribution of *C. laticeps* and its core range was predicted to persist up to 2100 with slight contractions around its distribution edges. In congruence with emerging theory, this thesis found the diversity and distribution of metabolic phenotypes between exploited and protected populations was different and suggested that this is likely due to the commercial linefishery selecting against high-performance aerobic scope phenotypes. The reduced diversity and lack of high-performance aerobic scope phenotypes may have an impact on population level responses to future environmental variability (Bernhardt & Leslie 2013). Interestingly, despite the impact of exploitation on metabolic phenotypes, this did not appear to impact the growth response or predicted distribution of *C. laticeps* by 2100, although the otolith growth time series length from the exploited population was possibly not long enough to elucidate patterns.

There is growing awareness, particularly in the temperate region, of the importance of acute environmental variability rather than long-term changes in mean values, for shaping the response of populations to climate change (Thornton et al. 2014, Dillon et al. 2016, Bates et al. 2018). The results from all three research chapters again highlight the importance of

thermal variability, rather than long-term increases in mean temperature, as a more important predictor of *C. laticeps*' performance. As easterly winds intensify, the frequency and magnitude of upwelling events intensify, and they may have the biggest effect on organism performance in South Africa and other intermittent upwelling regions around the world. Incorporating future frequency and intensity of environmental anomalous events is thus emerging as an important component of models predicting the resilience of species to climate change (Wernberg et al. 2012, Vasseur et al. 2018).

To minimise global biodiversity losses, conservation practitioners need to identify those species that are most vulnerable to the impacts of climate change (Pacifiçi et al. 2015). In the absence of robust stock and ecosystem projections, a risk-based approach to identifying species climate vulnerability is suggested as the most logical approach (Pecl et al. 2014). Following the methodology developed by Pecl et al. (2014), the climate sensitivity of South African commercial linefishery resources was estimated by Ortega-Cisneros et al. (2018). Of the 40 species assessed, *C. laticeps* was one of fourteen classified as having a medium to high climate sensitivity and was ranked as the most sensitive small-scale, boat-based linefishery resource (Ortega-Cisneros et al. 2018). Since the approach used was based on broad scale information, the latitudinal coverage of adults is taken as a proxy for population physiological tolerance to climate change impacts (Pecl et al. 2014), rather than species-specific responses to localised environmental variability. The findings of this research, however, have revealed that *C. laticeps* may be more robust to the impacts of climate change where a core range is predicted to persist, despite some range contraction. This not only has major implications for climate management, but also highlights that, although valuable as a quick screening process, broad scale reviews may lack the scientific rigour required for accurate prediction. Ultimately, mechanistic-based approaches have the potential to improve accuracy in predicting future patterns and thus contribute knowledge on the processes driving the response of fishes to climate change, which can inform climate change management approaches.

A major challenge in the field of conservation physiology is how rigorous experimental procedures can translate into applied management and policy frameworks (Cooke & Connor 2010, McKenzie et al. 2016). Because individual physiological responses link the environment to organism fitness or persistence and transcend to the population level (Metcalf et al. 2012, Ward et al. 2016), physiological information should contribute towards assessing not only problems, but also solutions for marine fisheries in the Anthropocene (McKenzie et al. 2016). However, up to now, there have been few examples where the results from conservation physiology research have been incorporated into management frameworks or policy (Cooke & Connor 2010, Cooke et al. 2012, McKenzie et al. 2016).

One good example of how conservation physiology research can be incorporated into climate change management and policy framework is that of the Fraser River sockeye salmon (*Oncorhynchus nerka*) (Farrell et al. 2008, Patterson et al. 2016). Physiological research on the relationship between temperature, cardiac output, and aerobic scope (Farrell et al. 2008, Eliason et al. 2011) was used to predict temperature-induced mortality during river migrations, which was then used to determine and adjust harvest strategies for the fishery (Cooke et al. 2012). This physiological based management approach was driven by public outcry following failed river migrations of sockeye salmon. The consequent political support provided funding for the physiological research and the results were incorporated into management following consultation with multiple stakeholders (McKenzie et al. 2016). However, in most scenarios, the socio-political support for science-based management is not there; thus the responsibility for the translation of research findings into management lies with the researcher making recommendations accessible and aligning them with government climate policy. Researchers who ensure that their findings are applicable and communicated in such a way that policy makers can incorporate them into management frameworks will have the greatest real-world impact (Patterson et al. 2016).

For fisheries management to be successful in the Anthropocene, it needs to consider more than climate change impacts and mitigation measures; it must also prioritise areas where

these measures are likely to be most successful (Stein et al. 2014, Jones et al. 2016). Maynard et al. (2010) and Levy & Ban (2013) propose that future conservation areas should be those where populations are least likely to be affected by climate change. This can be done by incorporating these areas into a marine plan (MSP), where the spatial distribution of ocean activities are demarcated to ensure efficient ocean management (Foley et al. 2010). The incorporation of climate change adaptation into marine spatial planning is however, rare.

While no specific methodology has been developed to identify areas least likely to be affected by climate change, it is possible to use *C. laticeps* as a model to show how this may be achieved in the socio-political context of South Africa. Here, the findings from Chapters 3, 4 and 5 are combined with a high-resolution forecasting ocean model up to 2100 (Yool et al. 2015, Popova et al. 2016) to predict where the species is least likely to be affected by climate change. This information is discussed and evaluated in the context of current South African climate policy, including examining the efficacy of the existing and proposed MPAs for the species by the year 2100.

## **6.2 Incorporating physiological research to improve fisheries management in the Anthropocene**

### **6.2.1 Background of marine climate policy in South Africa**

For conservation physiology research to be incorporated into policy, the first step is to understand the current state of national/international policy developments. The second step is to present research findings in such a way that they can be easily incorporated by policy makers (Patterson et al. 2016).

In 2000, a state of emergency was declared in the South African linefishery, with reductions in fishing effort implemented to promote stock rebuilding (Branch & Clark 2006). Although some stocks have begun to show evidence of recovery as a result of these measures (Attwood et al. 2013, Parker et al. 2016), the southern coast of South Africa has subsequently been characterised as a climate change “hotspot”, where the rate of change of some environmental

parameters, such as temperature, are higher than the global average (Hobday & Pecl 2014). In response to the looming threat of climate change on environmental resources, the South African government developed a policy framework that aims to reduce greenhouse gas emissions and includes adaptation measures that promote resource resilience (The Government of the Republic of South Africa 2012). Following the promulgation of this legislation, the DAFF developed the climate change sector plan to address institutional arrangements, vulnerability assessments, mitigation and adaptation (DAFF 2013). As part of this mandate, DAFF is in the process of finalising the climate change adaptation and mitigation plan (CCAMP) where strategies for improved and adaptive management to sustain the economic benefit of linefish resources will be developed (DAFF 2016).

In the draft CCAMP, small-scale linefisheries were identified as the most vulnerable to climate change, primarily because of the large number of people that they support and their poor capacity to adapt to climate-mediated resource changes (DAFF 2016, Hampton et al. 2017). Resource sensitivity to anticipated climate change, based on expert knowledge, contributed towards the assessment, and linefish were again considered highly vulnerable (Hampton et al. 2017). Because of the anticipated vulnerability of South Africa's endemic linefish species (Ortega-Cisneros et al. 2018) and the lack of adaptive capacity of linefish resource-users, the CCAMP has proposed a number of management measures to alleviate the potential impact of climate change (DAFF 2016). Proposed adaptation measures include increasing fishing efficiency, shifting to larger vessels that can travel further to track shifting distributions, and the implementation of spatial protection (Hampton et al. 2017).

In order to achieve the objectives of the National Development Plan (National Planning Commission 2011), the South African government implemented Operation Phakisa, where unlocking the ocean economy was a principle objective (van Wyk 2015). One of the key focal areas of Operation Phakisa is sustainability and this is recognised as being inextricably linked to good ocean governance and marine protection services (Sink 2016). As part of Operation Phakisa, 21 new MPAs are proposed in South Africa's exclusive economic zone (Harris et al.

2014) and a draft gazette has been circulated (Department of Environmental Affairs 2016). Key to the successful implementation of Operation Phakisa and the CCAMP is knowledge of where linefish resources are least likely to be affected by predicted climate change. Thus, the aim of this final chapter is to combine the results from the physiology, growth, and distribution chapters to predict the optimal (least likely to be affected by climate change) areas for *C. laticeps* by 2100. This information can be used for both spatial planning and the adaptive management of this (and other) important linefish species.

## 6.2.2 Spatial plan of *C. laticeps*' vulnerability to predicted climate change

### 6.2.2.1 Metabolism and temperature

To maintain energetic processes, future temperatures must not exceed thresholds where the aerobic scope of individual begins to be compromised (Pörtner & Knust 2007, Bozinovic & Pörtner 2015). For eurythermal fish, determining the temperature ( $T_{pejus}$ ) where the percentage decrease in aerobic scope from optimum becomes limiting at ecologically relevant scales is difficult (Farrell 2016). For example, sockeye salmon (*Oncorhynchus nerka*) are estimated to use up to 80% of their maximum aerobic scope during spawning migrations (Farrell et al. 2008, Eliason et al. 2013b, Farrell 2016) indicating that setting a  $T_{pejus}$  threshold to 10% of optimum aerobic scope (e.g., Ferreira et al. 2014) may be too strict. Best practice may be to assign different percentages of aerobic scope to each ecologically relevant situation (Farrell 2016). For the purposes of this model, minimum and maximum monthly temperature thresholds were set at 20% of the optimum aerobic scope temperature and a mean temperature threshold was set to be within 10% of optimum aerobic scope temperature (Equations 6.1, 6.2 and 6.3 and Figure 6.1 a,b,c and d). These temperature thresholds may seem strict considering the enormous energetic expenditure of migrating salmon but ensured that potential climate resilience was not overestimated especially as variability around mean thermal changes was not additionally considered. To exclude geographic areas that may be metabolically limiting, binary thresholds were set related to the optimum aerobic scope temperature thresholds (Equations 6.1, 6.2 and 6.3) for exploited population aerobic scope curves (Chapter 3).

$$t_{min}(a) = \begin{cases} 0, & a < 12 \\ 1, & a \geq 12 \end{cases} \quad (\text{Equation 6.1})$$

where  $a$  = future minimum monthly sea temperature

$$t_{max}(b) = \begin{cases} 1, & b < 24.2 \\ 0, & b \geq 24.2 \end{cases} \quad (\text{Equation 6.2})$$

where  $b$  = future maximum monthly sea temperature

$$t_{mean}(c) = \begin{cases} 1, & 13.75 < c < 22.25 \\ 0, & \text{else} \end{cases} \quad (\text{Equation 6.3})$$

where  $c$  = future mean sea temperature

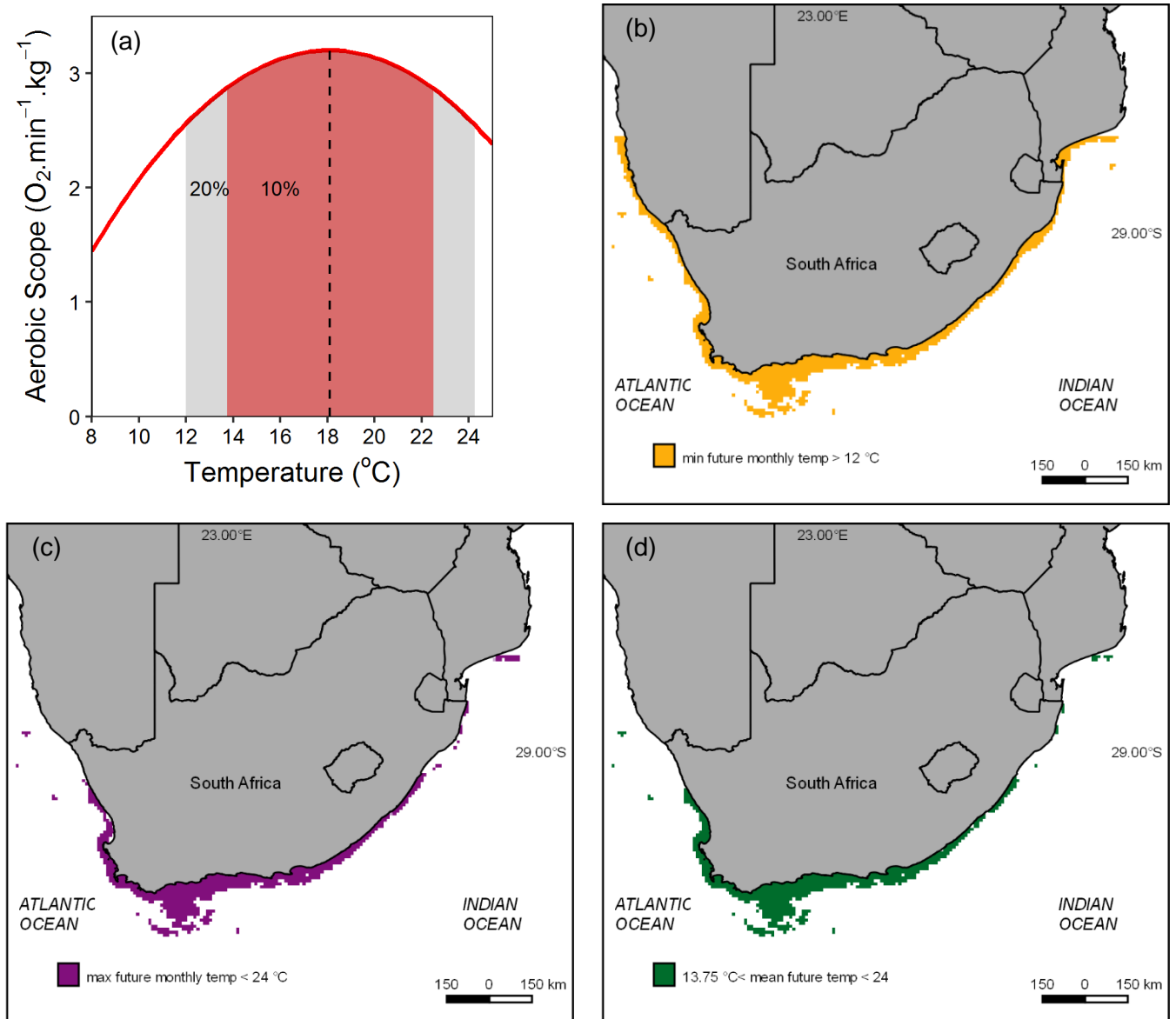


**Figure 6.1:** Temperature range where 20% (grey shaded) and 10% (red shaded) of maximum (black dotted line) aerobic scope (red line) is maintained (a), and spatial representation of these metabolic thresholds applied to temperature data up to 2100 for minimum (b), maximum (c) and mean (d).

### 6.2.2.2 Growth and temperature

With time, increases in intermittent upwelling have been reported for the south coast of South Africa (Roy et al. 2007, Rouault et al. 2010) and quantified in this study (Figure 4.12). The increased upwelling over time and the negative relationship between upwelling intensity and *C. laticeps* growth (Chapter 4) suggest that somatic growth will decrease in the future, based on this environmental relationship alone. However, because of the positive relationship between the growth of *C. laticeps* and mean autumn temperature (Chapter 4), areas where the mean autumn temperature is predicted to increase could minimise the negative effect of upwelling intensity on growth. By subtracting the mean future (2095–2100) autumn temperatures from the mean current (2005–2010) autumn temperatures (Equation 6.4), a continuous spatial dataset was created and was weighted by the predicted increase in autumn temperature (Figure 6.2).

$$t_{aut}(x) = \frac{1}{n} \sum_{i=1}^n x_f - \frac{1}{n} \sum_{i=1}^n x_c \quad (\text{Equation 6.4})$$

where  $x_f$  = future mean autumn months and  $x_c$  = current mean autumn months

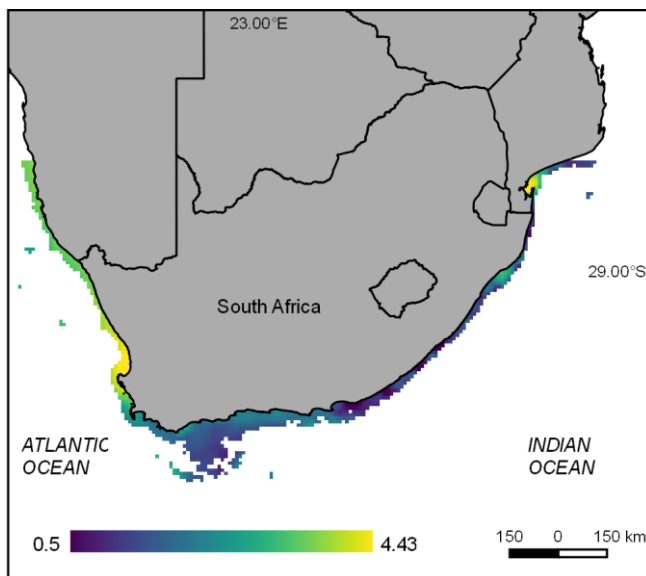


**Figure 6.2:** Spatial representation of mean change in autumn temperature (March–May) from 2005–2010 to 2095–2100, indicating that autumn temperatures will increase by a minimum of 0.5 °C up to 4.43 °C around the coast of southern Africa.

### 6.2.2.3 Distribution

The output of the final distribution model (Chapter 5) provided an estimate of the distribution response of *C. laticeps* by the year 2100. To convert the distribution model to a binary output, a threshold of 0.5 probability of occurrence was incorporated (Equation 6.5), which allowed the creation of a binary spatial data set of where *C. laticeps* was likely to persist up until 2100 (Figure 6.3).

$$d(y) = \begin{cases} 0, & y < 5 \\ 1, & y \geq 5 \end{cases} \quad (\text{Equation 6.5})$$

where  $y$  = sum of ten random forest presence/absence distribution models.

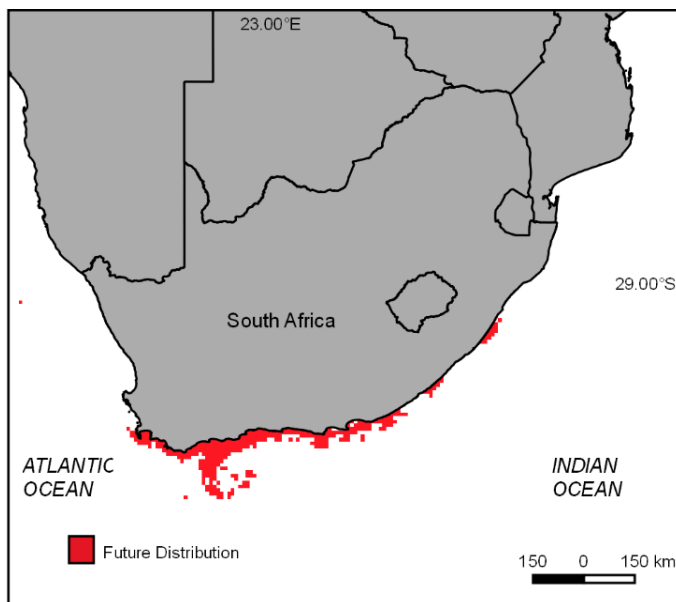


**Figure 6.3:** Predicted distribution of *C. laticeps* for 2100 based on a 0.5 threshold of occurrence from the future ten random forest model runs (see Chapter 5).

### 6.2.2.4 Production

It was difficult to quantify how  $\phi$  could influence fisheries production because no high-resolution spatial habitat type dataset could be obtained for the South African coastline. For example, the calibrated  $\phi$  for *C. laticeps* may have been highest over an unsuitable (e.g., sandy) habitat. In theory, a high  $\phi$  should translate to increased fisheries production, if other

resources like food are not limiting, as an energetically demanding process that contributes towards production (e.g., growth or gonadal development) should be supported in these areas. There is data support for a marked overlap between  $\phi$  and fisheries catch, with areas with the highest contemporary catches (> 10 000 kg per year) characterised by mean  $\phi$  values > 3.5 (Figure 6.4 a). Thus, for this model, a spatial binary dataset for mean  $\phi$  was developed by setting a threshold of 3.5 (Figure 6.4 b) based on Equation 6.6

$$Mi(z) = \begin{cases} 0, & z < 3.5 \\ 1, & z \geq 3.5 \end{cases} \quad (\text{Equation 6.6})$$

where  $z$  =future mean  $\phi$  up to 2100.

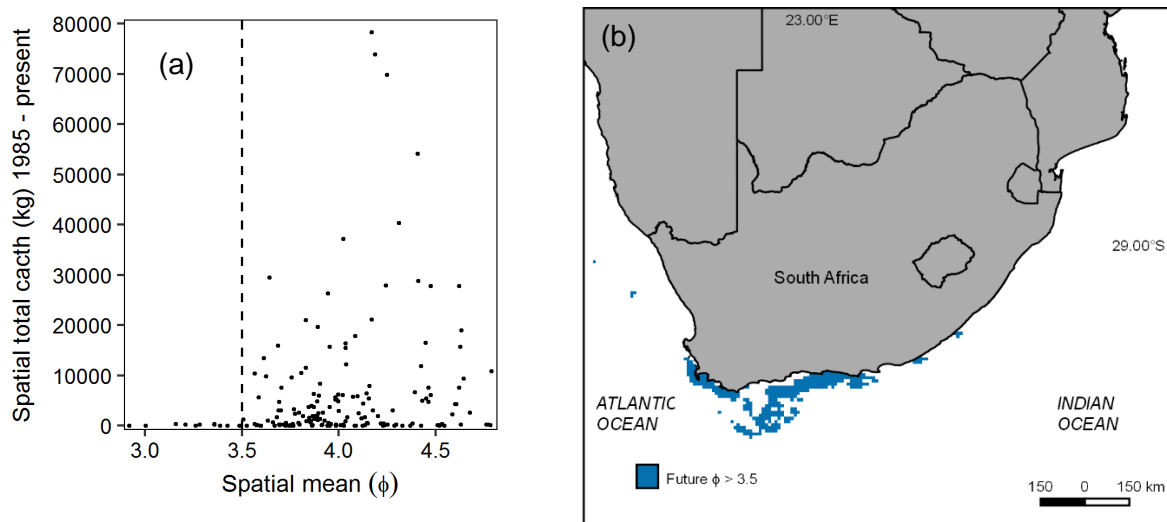


**Figure 6.4:** Total historical spatial commercial catch of *C. laticeps* against corresponding spatial mean current metabolic index ( $\phi$ ) calibrated for *C. laticeps* (a). Each point represents a grid location. Areas where the spatial mean of  $\phi$  is greater than the 3.5 threshold for 2095–2100 are indicated in blue (b).

#### 6.2.2.5 Combined model

Weighting different ecological resilience parameters in a single overall model is difficult as there is often no information on the relative importance of each parameter (Maynard et al. 2010). As all data, except autumn temperature change ( $t_{aut}$ ), has been converted to binary data, based on experimentally derived thresholds, the simple approach of multiplying each

parameter together produces a final spatial data set which can be referred to as the Growth, Distribution, Metabolism and Production index (*GDMP*) (Equation 6.7 and Figure 6.5). The final *GDMP* output thus predicts spatial areas where filled cells indicate areas where minimum, maximum and mean future bottom temperatures are not predicted to exceed the defined aerobic scope thresholds, the distribution of *C. laticeps* is predicted to persist, mean annual  $\phi$  is predicted to stay above the threshold for high fisheries production, and each cell is weighted by how much mean autumn temperatures are predicted to increase (Figure 6.6).

$$GDMP = t_{min}(a) \times t_{max}(b) \times t_{mean}(c) \times t_{aut}(x) \times d(y) \times Mi(z) \quad (\text{Equation 6.7})$$

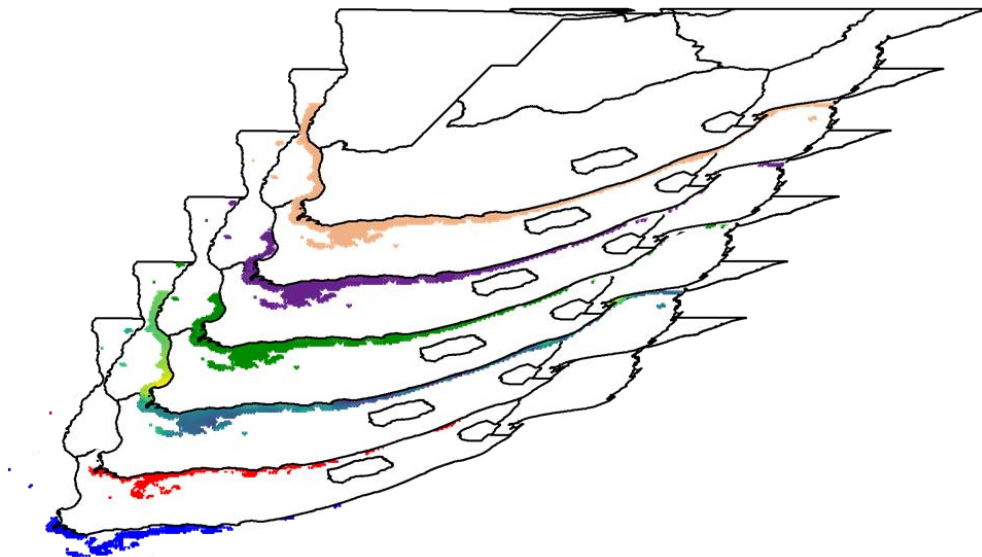


**Figure 6.5:** Conceptual diagram of the *GDMP* index showing the future (2100) spatial layers multiplied together to produce a final value. From top to bottom, binary transformed minimum monthly temperature (orange), binary transformed maximum monthly temperature (purple), binary transformed mean monthly temperature (green), change in mean autumn temperature (viridis colour scale), binary transformed predicted distribution (red) and binary transformed metabolic index production threshold (blue).

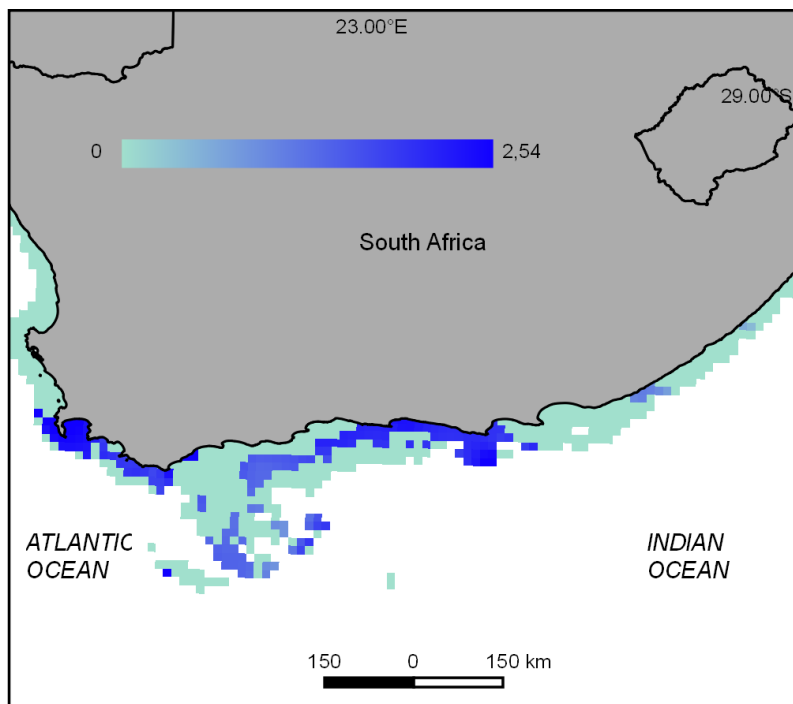


**Figure 6.6:** Predicted areas for optimum *C. laticeps* resilience up to 2100 based on growth, distribution, and metabolic responses (*GDMP*).

The *GDMP* model revealed that *C. laticeps* production (based on growth, distribution, and metabolism data) will be least affected by temperature and oxygen change, up to 2100, in areas from False Bay to Arniston and from Knysna through to St Francis Bay (Figure 6.6, dark blue shading). The *GDMP* model indicates that areas between Arniston and Knysna, and east of St Francis may be negatively affected by predicted climate change, especially because of temperature and oxygen changes reducing  $\phi$  below the 3.5 threshold by 2100 (Figure 6.6, light blue shading).

This spatial representation of *C. laticeps*' resilience to projected climate change in the form of the *GDMP* model can be refined and implemented for many species globally as ocean climate models increase in accuracy and availability to researchers (Meehl et al. 2007). The field of conservation physiology also has a well-established and ever-increasing toolbox which can be implemented in numerous ways to answer new questions and improve the accuracy of current predictions (Madliger et al. 2018). Furthermore, national policies for the sustainable use of the marine environment are now centred around the development of marine spatial

plans (Douvere 2008), making the uptake of conservation physiology into policy possible if presented in such a way.

### 6.2.3 Summary in management context

#### 6.2.3.1 The CCAMP

The most productive fishing grounds for *C. laticeps* lie on the south-west coast of South Africa, between the Cape Peninsula and Arniston, where most catches of more than 10 000 kg from 1985–present have been reported by the commercial linefishery (Figure 6.7 a) (Griffiths 2000, Kerwath et al. 2013b). This area corresponds to areas with high scores on the *GDMP* index indicating climate resilience (Figure 6.7 b). The area between Arniston and Knysna (central south coast), however, may be more vulnerable to predicted climate change, particularly due to temperature and oxygen change and the associated effect on  $\phi$  (Figure 6.7 b). This localised vulnerability to climate change suggests that this area should be prioritised in the CCAMP for climate adaptation management for linefishers that rely on *C. laticeps* and probably other similar reef-associated Sparid species. In the CCAMP, proposed adaptation measures such as moving to larger vessels to increase fishing range, adjusting fishing effort per zone according to resource availability, or switching effort to under-exploited resources, which may be climate “winners”, should be prioritised in areas with low *GDMP* scores.

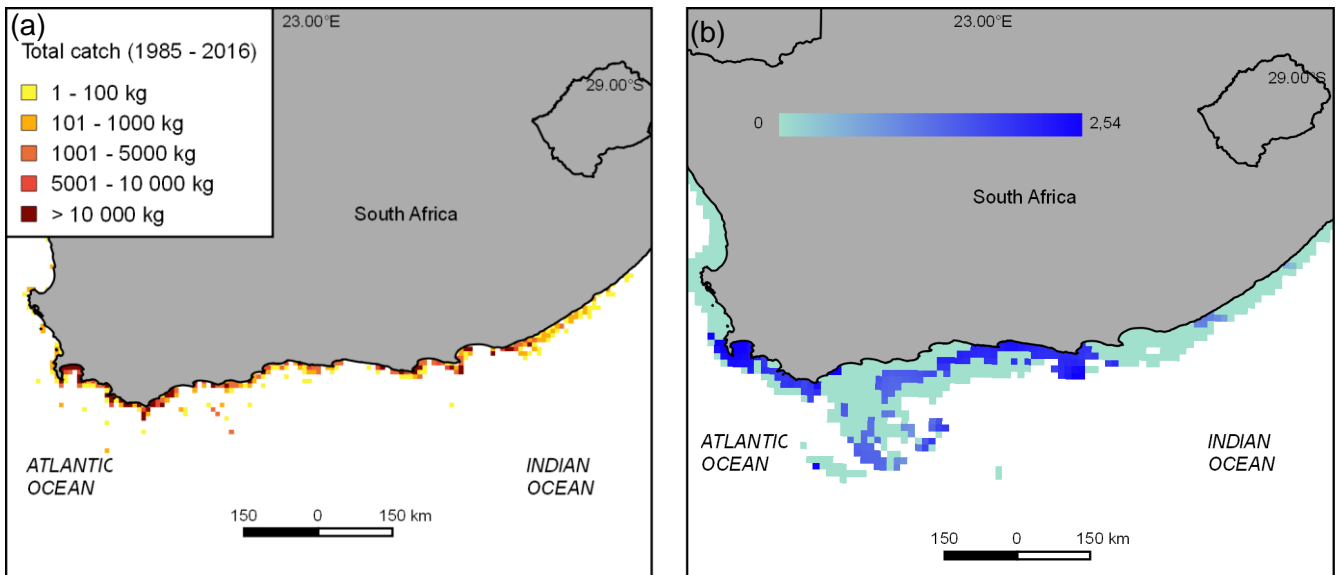


**Figure 6.7:** Total commercial catch of *C. laticeps* from 1985–present in kg (a) and areas where *C. laticeps* is least likely to be affected by predicted climate change (dark blue) based on this research (b).

### 6.2.3.2 Operation Phakisa

Marine protected areas, by eliminating fisheries exploitation as one of the drivers of fish population persistence, have been championed as an appropriate tool for improving the resilience of species to climate stressors (Green et al. 2014, Roberts et al. 2017). Our understanding of how MPAs can enhance climate change resilience for fish populations, however, remains largely theoretical, with few empirical examples observed in nature (Micheli et al. 2012). This thesis extends the role that MPAs can play in mitigating climate change impacts on biodiversity through conserving physiological trait capacity and diversity (Chapter 3), which can influence the variety of responses to thermal variability and increase the likelihood of persistence (Chown et al. 2010, Hofmann & Todgham 2010, Bernhardt & Leslie 2013).

Marine Protected Areas can achieve multiple objectives of fisheries management, including maintaining life history trait characteristics, genetic diversity, density, biomass and reproductive potential (Green et al. 2014, Roberts et al. 2017). However, the design of reserves is important to achieve the objectives of fisheries, biodiversity, or climate change, but

they are seldom designed with multiple objectives in mind (Green et al. 2014). Considerations for climate change mitigation include protecting areas where species are predicted to be most resilient to anticipated climate change (refugia) (Keller et al. 2009, Green et al. 2014). This can be achieved by conserving areas where individuals have withstood historical environmental stress (extinction filter) (Côté & Darling 2010), or areas where environmental change is least likely to negatively influence individuals (McLeod et al. 2009). The best technique for MPAs to transfer climate resilience is however, an active scientific debate (Côté & Darling 2010).

The current network of MPAs through *C. laticeps* distribution appears to be adequate (risk spreading) for *C. laticeps* in a sense that there are areas protected where environmental change is predicted to affect *C. laticeps* the least (refugia), and areas protected towards the edges of its distribution where rates of change are predicted to negatively influence *C. laticeps* (extinction filter) (Figure 6.8). Two major MPAs, the Tsitsikamma National Park and Table Mountain National Park, together with smaller MPAs like Robberg, Goukamma and Betty's Bay (Figure 6.8) are located in areas where the spatial model predicts *C. laticeps* to be least vulnerable to predicted climate change (refugia). By contrast, MPAs, including Dwesa-Cebe, Amathole and Bird Island, are in areas where *C. laticeps* may be vulnerable to anticipated climate change (extinction filter), particularly around its warm temperate/sub-tropical boundary in the east of its distribution.

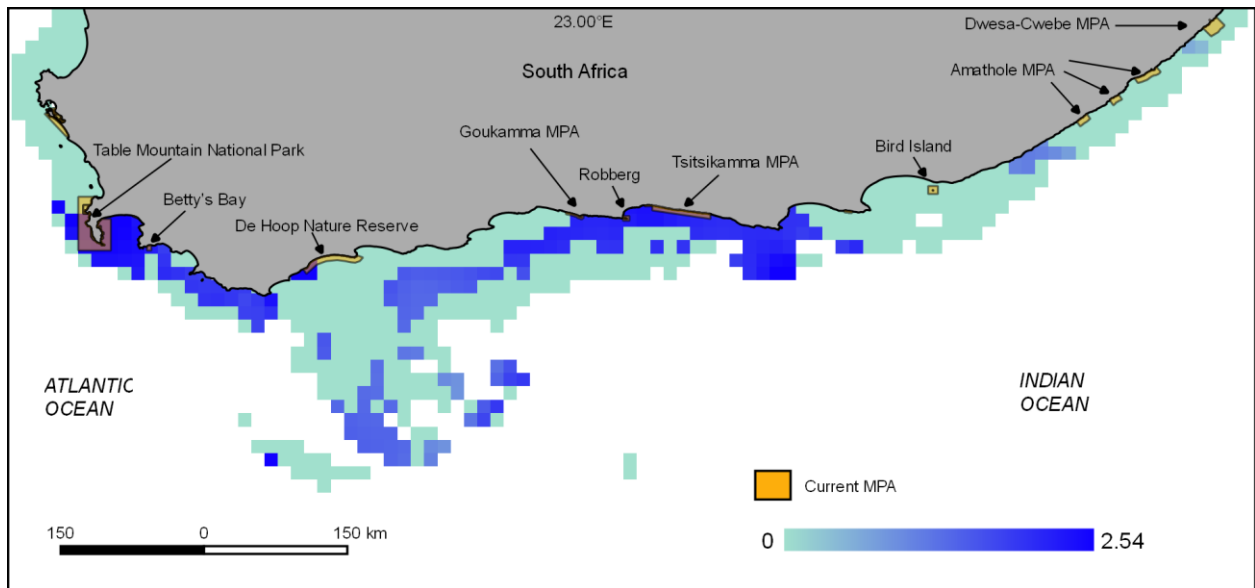


**Figure 6.8:** Location of major Marine Protected Areas (shaded orange) in relation to areas where *C. laticeps* is predicted to be resilient to climate change (blue scale). MPAs not indicated through *C. laticeps*' distribution are Helderberg, Stilbaai and Sardinia Bay, which are small and/or unenforced.

Two proposed new MPA initiatives, the Robben Island MPA and Amathole expansion (Harris et al. 2014), are located at the western and eastern edge of *C. laticeps*' core distribution. Together with recently draft-gazetted Addo MPA (near Bird Island) (Department of Environmental Affairs 2016), should provide increased spatial protection for *C. laticeps* in vulnerable areas and may act as further extinction filters. Furthermore, South Africa's National Protected Area Expansion Strategy targets protecting 20% of South Africa's coastal zone over the next 20 years (Government of South Africa 2010). By assessing key indicator species, like *C. laticeps*, conservation physiological research can aid in the design and location of these future MPAs.

### 6.3 Caveats of this study

#### 6.3.1 OCLTT critique

The idea that aerobic scope sets a limit on energetically demanding processes of organisms largely stems from the OCLTT theory (Pörtner & Knust 2007, Pörtner et al. 2017). While it is

an elegant solution to defining the thermal niche of an organism and inferring climate change effects (Farrell 2016), a growing body of empirical literature has failed to support the OCLTT theory for many species (e.g., Gräns et al. 2014, Norin et al. 2014, Clark & Mark 2017), and the generality of the theory has become a contentious subject among physiologists (Jutfelt et al. 2018). For example, in a meta-analysis of empirical research on fishes employing OCLTT theory, Lefevre (2016) found no consensus among the shape of aerobic scope curves or the effect of additional stressors on its magnitude. The main contention is whether the optimum temperature for organism performance ( $T_{opt}$ ) directly corresponds to the temperature where aerobic scope is maximised ( $T_{optAS}$ ), as there is often a mismatch between laboratory results and observed distributions of fish in the wild (Clark et al. 2013). In reality, multiple energy allocation budgets for various processes, combined with interacting biotic and abiotic factors, can determine organism performance (Schulte 2015). However, a recent analysis by Payne et al. (2016), linking laboratory optimal temperatures to wild optimum temperatures of several fish species, found congruency between estimates suggesting that aerobic scope thermal performance curves can be an appropriate metric for an individual's realised thermal niche. As more evidence for and against OCLTT is required, this study refrained, where possible, from using  $T_{optAS}$  to infer the optimal temperature for *C. laticeps* and rather used the framework to assess the variability in metabolic phenotypic traits, how that influences the overall height of AS curves, and to determine stressful temperature limits.

### 6.3.2 Plasticity and adaptability

It is uncertain whether laboratory-based studies can accurately predict the impacts of climate change on organisms as they do not take into account phenotypic plasticity or adaptation to projected climate change (Munday 2014). Impacts of climate change can be avoided if organisms move to more favourable habitats, compensate for climate change via phenotypic plasticity, or undergo evolutionary adaptation (Hoffmann & Sgró 2011). The ability of organisms to alter physiological rates when exposed to novel environmental regimes – physiological plasticity – can therefore promote climate change resilience (Hofmann &

Todgham 2010, Seebacher et al. 2015). For example, Donelson et al. (2011) found that complete aerobic scope capacity is restored through transgenerational plasticity to predicted warming temperatures for the tropical damselfish (*Acanthochromis polyacanthus*). Transgenerational plasticity is, however, not well understood and has been found to be maladaptive and limited to certain phenotypic traits or life history stages (Munday 2014). An under-appreciation of the potential for physiological plasticity can result in over-estimates of an organism's sensitivity to climate change (Gunderson & Stillman 2015, Seebacher et al. 2015).

Most work on fishes has involved attributing phenotypic change to plasticity; however, the interaction of phenotypic plasticity and evolutionary selection on phenotypic traits will also determine organism persistence (Handelsman et al. 2013, Munoz et al. 2015). Novel environments can exert directional selection on phenotypic traits but also change the distribution of phenotypic traits exposed to directional selection through phenotypic plasticity (Handelsman et al. 2013). Physiological phenotypic plasticity, if heritable and under selection, can therefore result in adaptive resilience to climate change. For example, (Munoz et al. 2015) found that for Pacific chinook salmon (*Oncorhynchus tshawytscha*) the Arrhenius breakpoint temperature of maximum heart rate was plastic through developmental acclimatisation, and heritable, which could facilitate evolutionary persistence in warming waters. The rate of climate change, generation time of organisms, type of phenotypic plasticity and the amount of adaptive genetic variation are among the factors that can influence population persistence in the face of climate change (Reed et al. 2011).

### 6.3.3 Pseudoreplication

Pseudoreplication is testing for treatment effects with an inappropriate error term for the hypothesis and can result in a mismatch with inference testing when treatment effects are non-replicated (Hulbert 1984). Much of this research, which aimed to elucidate the effect of exploitation on physiology, suffers from limited interspersions – all samples are taken from two segregated areas, which can promote type-I errors (Hulbert 1984). A trade-off, however,

sometimes needs to be made between the practical problems of experimental design and the pursuit of new empirical knowledge when dealing with large-scale, non-replicable systems (Oksanen 2001). When pseudoreplication is unavoidable, it must be acknowledged, results assessed in an ecologically meaningful context, and major covariates between areas accounted for (McGill 2014). This study accounted for the major covariate effect of thermal history on metabolic profile, and ecologically sensitive measurements like SMR were identical between areas. Furthermore, individuals were sampled from multiple different reefs within the protected and exploited areas. In an ideal situation, multiple MPAs and exploited areas would have been sampled. This was not feasible, as very few MPAs are old enough and considered in sufficiently pristine condition to offer a pre-exploitation baseline. The inclusion of multiple MPAs could also have introduced a number of undefined covariates and complicated the findings.

## **6.4 Future research**

### **6.4.1 Recruitment**

One aspect of climate change resilience not considered as part of this study was that of recruitment variability. Indeed, larvae of marine fish may be the most important life stage in determining continued persistence and productivity, given environmental variability and climate change (Rijnsdorp et al. 2009, Pankhurst & Munday 2011). The physiology of early life stages and spawning periods of Sparid species in particular, is linked closely to temperature patterns (Sheaves 2006). Furthermore, the associated increase in primary production with greater upwelling intensities is positively associated with fisheries production (Ware & Thomson 1991). Moreover, climate change can alter recruitment success not only through direct effects on larvae survival, but also through altering the phenology of spawning windows (Pankhurst & Munday 2011, Potts et al. 2014). For *C. laticeps*, Davis (1996) found that ovaries of fish caught during periods of upwelling had regressed, while Tilney & Buxton (1994) and Tilney et al. (1996) report lower abundance of Sparid ichthyoplankton during

upwelling events and suggest that ichthyoplankton were either transported offshore via Ekman transport or killed by thermal stress. This variability in *C. laticeps*' ichthyoplankton and stage of ovary development indicates that upwelling (and associated sea temperature variability) is either a cue for spawning or a prohibitor of spawning and should be studied further, particularly considering the increase in frequency and severity of upwelling events along the south coast (Figure 4.10). A physiological study quantifying the optimum environmental window for the development of *C. laticeps* larvae and incorporating this information in a time-series analysis of catch per unit effort (CPUE) and environmental variables, can quantify which environmental variables modulate recruitment into the fishery, and would contribute towards understanding recruitment-environment dynamics.

#### 6.4.2 Multiple stressors

Response to multiple stressors is complex and can be synergistic and negative, presenting a whole new perspective on organism climate change resilience (Hofmann & Todgham 2010). For example, Munday et al. (2009) find that for the fourline cardinalfish (*Ostorhinchus doederleini*) and yellowstriped cardinalfish (*O. cyanosoma*), increasing temperatures reduce aerobic scope, but this reduction is increased in acidified water, ultimately resulting in increased mortality of *O. doederleini*. Physiological research that involves carefully controlled environments to elucidate the effect of a single environmental stressor on organisms may lead to underestimating climate change responses in the natural environment (Todgham & Stillman 2013). However, in a review of synergistic stressors on organisms, Darling & Côté (2008) find no consensus among literature for synergistic, additive or antagonistic responses. Thus, in the context of climate change, ecological surprises may be more prevalent than previously thought. The inconsistencies among studies investigating interacting effects of multiple stressors highlight the need for species-specific studies.

## **6.5 Conclusion**

This study should serve as a starting point for future, mechanistic-based, research on South African linefish in the context of climate change. This is particularly timely as climate adaptation management plans are currently being developed for South Africa's fishery sectors. The study has further highlighted that understanding the role of environmental variability on organism performance may be more important than responses to long-term mean changes which is emerging as an important avenue of research globally (Dillon et al. 2016, Bates et al. 2018, Morash et al. 2018, Vasseur et al. 2018). Given the dynamic nature of South Africa's coastal marine environment and the link between this variability and global weather patterns, elucidating how this variability modulates the persistence of other endemic fishery species is therefore vital for more accurate climate resilience assessments.

## 7 Reference List

- ALBOUY, C., LEPRIEUR, F., LASRAM, F. B. R., SOMOT, S., AZNAR, R. & VELEZ, L. 2013. Projected climate change and the changing biogeography of coastal Mediterranean fishes. *Journal of Biogeography* 40:534–547.
- ALI, M., NICIEZA, A. & WOOTTON, R. J. 2003. Compensatory growth in fishes : a response to growth depression. *Fish and Fisheries* 4:147–190.
- ALLENDORF, F. W. & HARD, J. J. 2009. Human-induced evolution caused by unnatural selection through harvest of wild animals. *Proceedings of the National Academy of Sciences* 106:9987–9994.
- ALLER, E. A., JIDDAWI, N. S. & EKLO, J. S. 2017. Marine protected areas increase temporal stability of community structure , but not density or diversity , of tropical seagrass fish communities. *PLoS ONE* 12:e0183999.
- ANDERSON, C. N. K., HSIEH, C., SANDIN, S. A., HEWITT, R., HOLLOWED, A., BEDDINGTON, J., MAY, R. M. & SUGIHARA, G. 2008. Why fishing magnifies fluctuations in fish abundance. *Nature* 452:835–839.
- ARAÚJO, M. B. & GUISAN, A. 2006. Five (or so) challenges for species distribution modelling. *Journal of Biogeography* 33:1677–1688.
- ARAUJO, M. B. & TOWNSEND PETERSON, A. 2012. Uses and misuses of bioclimatic envelope modeling. *Ecology* 93:1527–1539.
- ARLINGHAUS, R., LASKOWSKI, K. L., ALÓS, J., KLEFOTH, T., MONK, C. T., NAKAYAMA, S. & SCHRÖDER, A. 2017. Passive gear-induced timidity syndrome in wild fish populations and its potential ecological and managerial implications. *Fish and Fisheries* 18:360–373.
- ATTRILL, M. J. & POWER, A. J. 2002. Climatic influences on a marine fish assemblage.

*Nature* 214:275–278.

ATTWOOD, C., BOOTH, T., KERWATH, S., MANN, B., MARR, S., BONTHUYS, J., DUNCAN, J. & POTTS, W. 2013. A decade after the emergency: The proceedings of the 4th linefish symposium. P. 288 *WWF South Africa Report Series - 2013/Marine/001*.

ATTWOOD, C. G. & FARQUHAR, M. 1999. Collapse of linefish stocks between Cape Hangklip and Walker Bay, South Africa. *South African Journal of Marine Science* 21:415–432.

AUDZIJONYTE, A., FULTON, E., HADDON, M., HELIDONIOTIS, F., HOBDAJ, A. J., KUPARINEN, A., MORRONGIELLO, J., SMITH, A. D. M., UPSTON, J. & WAPLES, R. S. 2016. Trends and management implications of human-influenced life-history changes in marine ectotherms. *Fish and Fisheries* 17:1005–1028.

AUDZIJONYTE, A., KUPARINEN, A., GORTON, R. & FULTON, E. A. 2013. Ecological consequences of body size decline in harvested fish species : positive feedback loops in trophic interactions amplify human impact. *Biology Letters* 9:doi: 10.1098/rsbl.2012.1103.

AUER, S. K., DICK, C. A., METCALFE, N. B. & REZNICK, D. N. 2018. Metabolic rate evolves rapidly and in parallel with the pace of life history. *Nature Communications* 9:doi: 10.1038/s41467-017-02514-z.

AUER, S. K., SALIN, K., ANDERSON, G. J. & METCALFE, N. B. 2015a. Aerobic scope explains individual variation in feeding capacity. *Biology Letters* 11:20150793.

AUER, S. K., SALIN, K., RUDOLF, A. M., ANDERSON, G. J. & METCALFE, N. B. 2015b. The optimal combination of standard metabolic rate and aerobic scope for somatic growth depends on food availability. *Functional Ecology* 29:479–486.

AUER, S. K., SALIN, K., RUDOLF, A. M., ANDERSON, G. J. & METCALFE, N. B. 2016. Differential effects of food availability on minimum and maximum rates of metabolism. *Biology letters* 12:20160586.

- AUSTIN, M. 2002. Spatial prediction of species distribution: an interface between ecological theory and statistical modelling. *Ecological Modelling* 157:101–118.
- AUSTIN, M. 2007. Species distribution models and ecological theory: A critical assessment and some possible new approaches. *Ecological Modelling* 200:1–19.
- BAITH, K., LINDSAY, R., FU, G. & MCCLAIN, C. R. 2001. Data analysis system developed for ocean color satellite sensors. *Eos, Transactions American Geophysical Union* 82:202.
- BARBET-MASSIN, M., JIGUET, F., ALBERT, C. H. & THUILLER, W. 2012. Selecting pseudo-absences for species distribution models: how, where and how many? *Methods in Ecology and Evolution* 3:327–338.
- BATES, A. E., BARRETT, N. S., STUART-SMITH, R. D., HOLBROOK, N. J., THOMPSON, P. A. & EDGAR, G. J. 2014. Resilience and signatures of tropicalization in protected reef fish communities. *Nature Climate Change* 4:62–67.
- BATES, A. E., HELMUTH, B., BURROWS, M. T., DUNCAN, M. I., GARRABOU, J., GUY-HAIM, T., LIMA, F., QUEIROS, A. M., SEABRA, R., MARSH, R., BELMAKER, J., BENSOUSSAN, N., DONG, Y., MAZARIS, A. D., SMALE, D., WAHL, M. & RILOV, G. 2018. Biologists ignore ocean weather at their peril. *Nature* 560:299–301.
- BATES, D., MÄCHLER, M., BOLKER, B. M. & WALKER, S. C. 2015. Fitting linear mixed-effects models using lme4. *Journal of Statistical Software* 67:doi: 10.18637/jss.v067.i01.
- BAUMANN, H., TALMAGE, S. C. & GOBLER, C. J. 2012. Reduced early life growth and survival in a fish in direct response to increased carbon dioxide. *Nature Climate Change* 2:38–41.
- BEAUGRAND, G., BRANDER, K. M., LINDLEY, J. A., SOUISSI, S. & REID, P. C. 2003. Plankton effect on cod recruitment in the North Sea. *Nature* 426:661–664.
- BECKLEY, L. E. 1983. Sea-surface temperature variability around Cape Recife, South Africa. *South African Journal of Science* 79:436–438.

- BEEVER, E. A., HALL, L. E., VARNER, J., LOOSEN, A. E., DUNHAM, J. B., GAHL, M. K., SMITH, F. A. & LAWLER, J. J. 2017. Behavioral flexibility as a mechanism for coping with climate change. *Frontiers in Ecology and the Environment* 15:299–308.
- BERNHARDT, J. R. & LESLIE, H. M. 2013. Resilience to climate change in coastal marine ecosystems. *Annual Review of Marine Science* 5:371–392.
- VON BIELA, V. R., KRUSE, G. H., MUETER, F. J., BLACK, B. A., DOUGLAS, D. C., HELSER, T. E. & ZIMMERMAN, C. E. 2015. Evidence of bottom-up limitations in nearshore marine systems based on otolith proxies of fish growth. *Marine Biology* 162:1019–1031.
- BINDER, T. R., WILSON, A. D. M., WILSON, S. M., SUSKI, C. D., GODIN, J. G. J. & COOKE, S. J. 2016. Is there a pace-of-life syndrome linking boldness and metabolic capacity for locomotion in bluegill sunfish? *Animal Behaviour* 121:175–183.
- BIRK, M. A. 2016. presens: Interface for PreSens fiber optic data. *R package*.
- BIRO, P. A., GARLAND, T., BECKMANN, C., UJVARI, B., THOMAS, F. & POST, J. R. 2018. Metabolic scope as a proximate constraint on individual behavioral variation: effects on personality, plasticity, and predictability. *American Naturalist* 192:142–154.
- BIRO, P. A. & POST, J. R. 2008. Rapid depletion of genotypes with fast growth and bold personality traits from harvested fish populations. *Proceedings of the National Academy of Sciences* 105:2919–2922.
- BLACK, B. A., ALLMAN, R. J., SCHROEDER, I. D. & SCHIRRIPA, M. J. 2011a. Multidecadal otolith growth histories for red and gray snapper (*Lutjanus* spp.) in the northern Gulf of Mexico, USA. *Fisheries Oceanography* 20:347–356.
- BLACK, B. A., BOEHLERT, G. W. & YOKLAVICH, M. M. 2005. Using tree-ring crossdating techniques to validate annual growth increments in long-lived fishes. *Canadian Journal of Fisheries and Aquatic Sciences* 62:2277–2284.
- BLACK, B. A., BOEHLERT, G. W. & YOKLAVICH, M. M. 2008. Establishing climate-growth

- relationships for yelloweye rockfish (*Sebastes ruberrimus*) in the northeast Pacific using a dendrochronological approach. *Fisheries Oceanography* 17:368–379.
- BLACK, B. A., SCHROEDER, I. D., SYDEMAN, W. J., BOGRAD, S. J. & LAWSON, P. W. 2010. Wintertime ocean conditions synchronize rockfish growth and seabird reproduction in the central California Current ecosystem. *Canadian Journal of Fisheries and Aquatic Sciences* 67:1149–1158.
- BLACK, B. A., SCHROEDER, I. D., SYDEMAN, W. J., BOGRAD, S. J., WELLS, B. K. & SCHWING, F. B. 2011b. Winter and summer upwelling modes and their biological importance in the California Current Ecosystem. *Global Change Biology* 17:2536–2545.
- BOEHLERT, G. W. & KAPPENMAN, R. F. 1980. Variation of growth with latitude in two species of rockfish (*Sebastes pinniger* and *S. diplorea*) from the northeast Pacific ocean. *Marine Ecology Progress Series* 3:1–10.
- BOGRAD, S. J. & LYNN, R. J. 2003. Long-term variability in the Southern California Current System. *Deep-Sea Research Part II* 50:2355–2370.
- BOTSFORD, L., CASTILLA, J. C. & PETERSON, C. H. 1997. The management of fisheries and marine ecosystems. *Science* 277:509–515.
- BOUCEK, R. E., GAISER, E. E., LIU, H. & REHAGE, J. S. 2016. A review of subtropical community resistance and resilience to extreme cold spells. *Ecosphere* 7:doi:10.1002/ecs2.1455.
- BOZINOVIC, F., CALOSI, P. & SPICER, J. I. 2011. Physiological correlates of geographic range in animals. *Annual Review of Ecology, Evolution, and Systematics* 42:155–179.
- BOZINOVIC, F. & PÖRTNER, H. O. 2015. Physiological ecology meets climate change. *Ecology and Evolution* 5:1025–1030.
- BRANCH, G. M. & CLARK, B. M. 2006. Fish stocks and their management: The changing face of fisheries in South Africa. *Marine Policy* 30:3–17.

- BRANDER, K. 2010. Impacts of climate change on fisheries. *Journal of Marine Systems* 79:389–402.
- BRANDER, K. M. 2007. Global fish production and climate change. *Proceedings of the National Academy of Sciences* 104:19709–19714.
- BREEGGEMANN, J. J., KAEMINGK, M. A., DEBATES, T. J., PAUKERT, C. P., KRAUSE, J. R., LETVIN, A. P., STEVENS, T. M., WILLIS, D. W. & CHIPPS, S. R. 2016. Potential direct and indirect effects of climate change on a shallow natural lake fish assemblage. *Ecology of Freshwater Fish* 25:487–499.
- BREIMAN, L. 2001. Random forests. *Machine Learning* 45:5–32.
- BRETT, J. R. 1971. Energetic responses of salmon to temperature. A study of some thermal relations in the physiology and freshwater ecology of sockeye salmon (*Oncorhynchus nerka*). *American Zoologist* 11:99-113.
- BROOK, B. W., SODHI, N. S. & BRADSHAW, C. J. A. 2008. Synergies among extinction drivers under global change. *Trends in Ecology and Evolution* 23:453–460.
- BROUWER, S. L. & BUXTON, C. D. 2002. Catch and effort of the shore and skiboat linefisheries along the South African Eastern Cape coast. *South African Journal of Marine Science* 24:341–354.
- BROWN, J. H., GILLOOLY, J. F., ALLEN, A. P., SAVAGE, V. M. & WEST, G. B. 2004. Toward a metabolic theory of ecology. *Ecology* 85:1771–1789.
- BROWNSCOMBE, J. W., GUTOWSKY, L. F. G., DANYLCHUK, A. J. & COOKE, S. J. 2014. Foraging behaviour and activity of a marine benthivorous fish estimated using tri-axial accelerometer biologgers. *Marine Ecology Progress Series* 505:241–251.
- BURNHAM, K. P. & ANDERSON, D. R. 2004. Multimodel inference understanding AIC and BIC in model selection. *Sociological Methods & Research* 33:261–304.

- BUXTON, C. D. 1987. Life history changes of two reef fish species in exploited and unexploited marine environment in South Africa. Rhodes University, PhD thesis. 229 pp.
- BUXTON, C. D. 1990. The reproductive biology of *Chrysoblephus laticeps* and *C. cristiceps* (Teleostei: Sparidae). *Journal of zoology* 220:497–511.
- BUXTON, C. D. 1993. Life-history changes in exploited reef fishes on the east coast of South Africa. *Environmental Biology of Fishes* 36:47–63.
- BUXTON, C. D. & SMALE, M. J. 1989. Abundance and distribution patterns of three temperate Marine reef fish (Teleostei: Sparidae) in exploited and unexploited areas off the southern cape coast. *Journal of Applied Ecology* 26:441–451.
- CAI, W., BORLACE, S., LENGAIGNE, M., RENSCH, P. VAN, COLLINS, M., VECCHI, G., TIMMERMANN, A., SANTOSO, A., MCPHADEN, M. J., WU, L., ENGLAND, M., GUILYARDI, E. & JIN, F. F. 2014. Increasing frequency of extreme El Niño events due to greenhouse warming. *Nature Climate Change* 4:111–116.
- CAI, W., SANTOSO, A., WANG, G., YEH, S. W., AN, S. IL, COBB, K. M., COLLINS, M., GUILYARDI, E., JIN, F. F., KUG, J. S., LENGAIGNE, M., MCPHADEN, M. J., TAKAHASHI, K., TIMMERMANN, A., VECCHI, G., WATANABE, M. & WU, L. 2015. ENSO and greenhouse warming. *Nature Climate Change* 5:849–859.
- CEREZO, J. & GARCÍA GARCÍA, B. 2004. The effects of oxygen levels on oxygen consumption, survival and ventilatory frequency of sharpsnout sea bream (*Diplodus puntazzo* Gmelin, 1789) at different conditions of temperature and fish weight. *Journal of Applied Ichthyology* 20:488–492.
- CHABOT, D., STEFFENSEN, J. F. & FARRELL, A. P. 2016. The determination of standard metabolic rate in fishes. *Journal of Fish Biology* 88:81–121.
- CHEUNG, W. W. L., LAM, V. W. Y., SARMIENTO, J. L., KEARNEY, K., WATSON, R. & PAULY, D. 2009. Projecting global marine biodiversity impacts under climate change

- scenarios. *Fish and Fisheries* 10:235–251.
- CHEUNG, W. W. L., LAM, V. W. Y., SARMIENTO, J. L., KEARNY, K., WATSON, R., ZELLER, D. & PAULY, D. 2010. Large-scale redistribution of maximum fisheries catch potential in the global ocean under climate change. *Global Change Biology* 16:24–35.
- CHOWN, S. L., HOFFMANN, A. A., KRISTENSEN, T. N., ANGILLETTA, M. J., STENSETH, N. C. & PERTOLDI, C. 2010. Adapting to climate change: A perspective from evolutionary physiology. *Climate Research* 43:3–15.
- CHRISTENSEN, J. H., KUMAR, K. K., ALDRIA, E., AN, S. I., CAVALCANTI, I. F. A., CASTRO, M. DE, DONG, W., GOSWAMI, P., HALL, A., KANYANGA, J. K., KITO, A., KOSSIN, J., LAU, N.-C., RENWICK, J., STEPHENSON, D. B., XIE, S. P. & ZHOU, T. 2013. Climate Phenomena and their Relevance for Future Regional Climate Change. P. 62 in Stocker, T. F., Qin, D., Plattner, G.-K., Tignor, M., Allen, S. K., Boschung, J., Nauels, A., Xia, Y., Bex, V. & Midgley, P. M. (eds.). *Climate Change 2013: The Physical Science Basis. Contribution of Working Group I to the Fifth Assessment Report of the Intergovernmental Panel on Climate Change*. Cambridge University Press, Cambridge, United Kingdom and New York, USA.
- CLAIREAUX, G. & CHABOT, D. 2016. Responses by fishes to environmental hypoxia: Integration through Fry's concept of aerobic metabolic scope. *Journal of Fish Biology* 88:232–251.
- CLARK, T. D., JEFFRIES, K. M., HINCH, S. G. & FARRELL, A. P. 2011. Exceptional aerobic scope and cardiovascular performance of pink salmon (*Oncorhynchus gorbuscha*) may underlie resilience in a warming climate. *The Journal of Experimental Biology* 214:3074–3081.
- CLARK, T. D. & MARK, F. C. 2017. An introduction to the Special Issue: "OCLTT: a universal concept?" *Journal of Thermal Biology* 68:147–148.

- CLARK, T. D., MESSMER, V., TOBIN, A. J., HOEY, A. S. & PRATCHETT, M. S. 2017. Rising temperatures may drive fishing-induced selection of low-performance phenotypes. *Nature Scientific Reports* 7:doi: 10.1038/srep40571.
- CLARK, T. D., SANDBLOM, E., HINCH, S. G., PATTERSON, D. A., FRAPPELL, P. B. & FARRELL, A. P. 2010. Simultaneous biologging of heart rate and acceleration , and their relationships with energy expenditure in free-swimming sockeye salmon (*Oncorhynchus nerka*). *Journal of Comparative Physiology B* 180:673–684.
- CLARK, T. D., SANDBLOM, E. & JUTFELT, F. 2013. Aerobic scope measurements of fishes in an era of climate change: respirometry, relevance and recommendations. *The Journal of Experimental Biology* 216:2771–82.
- COOK, D. G., WELLS, R. M. G. & HERBERT, N. A. 2011. Anaemia adjusts the aerobic physiology of snapper (*Pagrus auratus*) and modulates hypoxia avoidance behaviour during oxygen choice presentations. *Journal of Experimental Biology* 214:2927–2934.
- COOKE, E. L. L., WILSON, A. D. M., ELVIDGE, C. K. & COOKE, S. J. 2017. Does capture method or the presence of aquatic protected areas influence the selective harvest of behavioural types in largemouth bass? *Canadian Journal of Fisheries and Aquatic Sciences* 74:1151–1157.
- COOKE, S. J. & CONNOR, C. M. O. 2010. Making conservation physiology relevant to policy makers and conservation practitioners. *Conservation Letters* 3:159–166.
- COOKE, S. J., HINCH, S. G., DONALDSON, M. R., CLARK, T. D., ELIASON, E. J., CROSSIN, G. T., RABY, G. D., JEFFRIES, K. M., LAPOINTE, M., MILLER, K., PATTERSON, D. A. & FARRELL, A.P. 2012. Conservation physiology in practice : how physiological knowledge has improved our ability to sustainably manage Pacific salmon during up-river migration. *Philosophical Transactions of the Royal Society B* 367:1757–1769.
- COOKE, S. J., SACK, L., FRANKLIN, C. E., FARRELL, A. P., BEARDALL, J., WIKELSKI, M.

- & CHOWN, S. L. 2013. What is conservation physiology? Perspectives on an increasingly integrated and essential science. *Conservation Physiology* 1.
- COPPINGER, C. R. 2013. Assessing the genetic diversity of catfac rockcod, *Epinephelus andersoni* in the subtropical western indian ocean and modelling the effects of climate change on their distribution. Rhodes University, MSc thesis. 152 pp.
- CÔTÉ, I. M. & DARLING, E. S. 2010. Rethinking ecosystem resilience in the face of climate change. *PLoS Biology* 8:doi: 10.1371/journal.pbio.1000438.
- CROZIER, L. G., HENDRY, A. P., LAWSON, P. W., QUINN, T. P., MANTUA, N. J., BATTIN, J., SHAW, R. G. & HUEY, R. B. 2008. Potential responses to climate change in organisms with complex life histories: evolution and plasticity in Pacific salmon. *Evolutionary Applications* 1:252–270.
- CUCCO, A., SINERCHIA, M., LEFRANÇOIS, C., MAGNI, P., GHEZZO, M., UMGIESSER, G., PERILLI, A. & DOMENICI, P. 2012. A metabolic scope based model of fish response to environmental changes. *Ecological Modelling* 237–238:132–141.
- CUTLER, D. R., EDWARDS, T. C., BEARD, K. H., CUTLER, A., HESS, K. T., GIBSON, J. & LAWLER, J. J. 2007. Random forests for classification in ecology. *Ecology* 88:2783–2792.
- DAFF. 2013. Climate change sector plan for agriculture, forestry and fisheries. 91 pp.
- DAFF. 2014. Status of the South African marine fishery resources 2014. Cape Town. 84 pp.
- DAFF. 2016. Draft climate change adaptation and mitigation plan for South African agriculture, forestry, and fisheries sectors:82 pp.
- DARLING, E. S. & CÔTÉ, I. M. 2008. Quantifying the evidence for ecological synergies. *Ecology Letters* 11:1278–1286.
- DAVIS, J. A. 1996. Investigations into the larval rearing of two South African sparid species.

Rhodes University, MSc thesis. 147 pp.

DEPARTMENT OF ENVIRONMENTAL AFFAIRS. 2016. NATIONAL ENVIRONMENTAL MANAGEMENT: PROTECTED AREAS ACT, 2003 (ACT NO. 57 OF 2003).

DEUTSCH, C., FERREL, A., SEIBEL, B., PORTNER, H. O. & HUEY, R. B. 2015. Climate change tightens a metabolic constraint on marine habitats. *Science* 348:1132–1136.

DIAZ, R. J. & ROSENBERG, R. 2008. Spreading dead zones and consequences for marine ecosystems. *Science* 321:926–929.

DILLON, M. E., WOODS, H. A., WANG, G., FEY, S. B., VASSEUR, D. A., TELEMECO, R. S., MARSHALL, K. & PINCEBOURDE, S. 2016. Life in the frequency domain: The biological impacts of changes in climate variability at multiple time scales. *Integrative and Comparative Biology* 56:14–30.

DONALDSON, M. R., COOKE, S. J., PATTERSON, D. A. & MACDONALD, J. S. 2008. Cold shock and fish. *Journal of Fish Biology* 73:1491–1530.

DONELSON, J. M., MUNDAY, P. L., MCCORMICK, M. I. & PITCHER, C. R. 2011. Rapid transgenerational acclimation of a tropical reef fish to climate change. *Nature Climate Change* 2:30–32.

DOUBLEDAY, Z. A., IZZO, C., HADDY, J. A., LYLE, J. M., YE, Q. & GILLANDERS, B. M. 2015. Long-term patterns in estuarine fish growth across two climatically divergent regions. *Oecologia* 179:1079–1090.

DOUVERE, F. 2008. The importance of marine spatial planning in advancing ecosystem-based sea use management. *Marine Policy* 32:762–771.

DUFFY, J. E., LEFCHECK, J. S., STUART-SMITH, R. D., NAVARRETE, S. A. & EDGAR, G. J. 2016. Biodiversity enhances reef fish biomass and resistance to climate change. *Proceedings of the National Academy of Sciences* 113:6230–6235.

- DUFOIS, F. & ROUAULT, M. 2012. Sea surface temperature in False Bay (South Africa): Towards a better understanding of its seasonal and inter-annual variability. *Continental Shelf Research* 43:24–35.
- DULVY, N. K., ROGERS, S. I., JENNINGS, S., STELZENMÜLLER, V., DYE, S. R. & SKJOLDAL, H. R. 2008. Climate change and deepening of the North Sea fish assemblage: A biotic indicator of warming seas. *Journal of Applied Ecology* 45:1029–1039.
- DUNCAN, M. 2013. the Genetic Stock Structure and Distribution of *Chrysoblephus puniceus*, a commercially important transboundary linefish species, endemic to the South West Indian Ocean. Rhodes University, MSc thesis. 125 pp.
- DZAUGIS, M., ALLMAN, R. & BLACK, B. 2017. Importance of the spring transition in the northern Gulf of Mexico as inferred from marine fish biochronologies. *Marine Ecology Progress Series* 565:149–162.
- EDWORTHY, C. 2017. The metabolic physiology of early stage *Argyrosomus japonicus* with insight into the potential effects of pCO<sub>2</sub> induced ocean acidification by. Rhodes University, MSc thesis. 74 pp.
- ELIASON, E. J., CLARK, T. D., HAGUE, M. J., HANSON, L. M., GALLAGHER, Z. S., JEFFRIES, K. M., GALE, M. K., PATTERSON, D. A., HINCH, S. G. & FARRELL, A. P. 2011. Differences in thermal tolerance among sockeye salmon populations. *Science* 332:109–112.
- ELIASON, E. J., CLARK, T. D., HINCH, S. G. & FARRELL, A. P. 2013a. Cardiorespiratory performance and blood chemistry during swimming and recovery in three populations of elite swimmers : Adult sockeye salmon. *Comparative Biochemistry and Physiology, Part A* 166:385–397.
- ELIASON, E. J., WILSON, S. M., FARRELL, A. P., COOKE, S. J. & HINCH, S. G. 2013b. Low

- cardiac and aerobic scope in a coastal population of sockeye salmon *Oncorhynchus nerka* with a short upriver. *Journal of Fish Biology* 82:2104–2112.
- ENBERG, K., JØRGENSEN, C., DUNLOP, E. S., VARPE, Ø., BOUKAL, D. S., BAULIER, L., ELIASSEN, S. & HEINO, M. 2012. Fishing-induced evolution of growth: Concepts, mechanisms and the empirical evidence. *Marine Ecology* 33:1–25.
- ENGELHARD, G. H., RIGHTON, D. A. & PINNEGAR, J. K. 2014. Climate change and fishing : a century of shifting distribution in North Sea cod. *Global Change Biology* 20:2473–2483.
- ERASMUS, B. 2017. Effects of CO<sub>2</sub>-induced ocean acidification on the early development, growth, survival and skeletogenesis of the estuarine-dependant sciaenid *Argyrosomus japonicus*. Rhodes University, MSc thesis. 84 pp.
- EVANS, T. G., DIAMOND, S. E. & KELLY, M. W. 2015. Mechanistic species distribution modelling as a link between physiology and conservation. *Conservation Physiology* 3:doi: 10.1093/conphys/cov056.
- FARRELL, A. P. 2016. Pragmatic perspective on aerobic scope: Peaking, plummeting, pejus and apportioning. *Journal of Fish Biology* 88:322–343.
- FARRELL, A. P., HINCH, S. G., COOKE, S. J., PATTERSON, D. A., CROSSIN, G. T., LAPOINTE, M. & MATHES, M. T. 2008. Pacific salmon in hot water: applying aerobic scope models and biotelemetry to predict the success of spawning migrations. *Physiological and Biochemical Zoology* 81:697–708.
- FERREIRA, E. O., ANTTILA, K. & FARRELL, A. P. 2014. Thermal optima and tolerance in the eurythermic goldfish (*Carassius auratus*): relationships between whole-animal aerobic capacity and maximum heart rate. *Physiological and Biochemical Zoology* 87:599–611.
- FITZGIBBON, Q. P., JEFFS, A. G. & BATTAGLENE, S. C. 2014. The Achilles heel for spiny lobsters: The energetics of the non-feeding post-larval stage. *Fish and Fisheries* 15:312–326.

- FOLEY, M. M., HALPERN, B. S., MICHELI, F., ARMSBY, M. H., CALDWELL, M. R., CRAIN, C. M., PRAHLER, E., ROHR, N., SIVAS, D., BECK, M. W., CARR, M. H., CROWDER, L. B., DUFFY, J. E., HACKER, S. D., MCLEOD, K. L., PALUMBI, S. R., PETERSON, C. H., REGAN, H. M., RUCKELSHAUS, M. H., SANDIFER, P. A. & STENECK, R. S. 2010. Guiding ecological principles for marine spatial planning. *Marine Policy* 34:955–966.
- FOX, J. 2003. Effect displays in R for generalised linear models. *Journal of Statistical Software* 8:1–12.
- FOX, J. & WEISBERG, S. 2011. *An R companion to applied regression* (2nd edition). Sage, Thousand Oaks CA. 472 pp.
- FREITAS, C., OLSEN, E. M., MOLAND, E., CIANNELLI, L. & KNUTSEN, H. 2015. Behavioral responses of Atlantic cod to sea temperature changes. *Ecology and Evolution* 5:2070–2083.
- FRÖLICHER, T. L., FISCHER, E. M. & GRUBER, N. 2018. Marine heatwaves under global warming. *Nature* 560:360–364.
- FRY, F. E. J. 1947. Effects of the environment on animal activity. *Publications of the Ontario Fisheries Research Laboratory* 55:1–62. Academic Press, New York.
- FRY, F. E. J. 1971. The effect of environmental factors on the physiology of fish. Pp. 1–98 in Hoar, W. S. & Randall, D. J. (eds.). *Fish physiology, vol VI. Environmental relations and behavior* (Volume VI). Academic Press, New York.
- FULTON, E. A. 2011. Interesting times : winners, losers, and system shifts under climate change around Australia. *ICES Journal of Marine Science* 68:1329–1342.
- GARCÍA-REYES, M., SYDEMAN, W. J., SCHOEMAN, D. S., RYKACZEWSKI, R. R., BLACK, B. A., SMIT, A. J. & BOGRAD, S. J. 2015. Under pressure: Climate change, upwelling, and eastern boundary upwelling ecosystems. *Frontiers in Marine Science* 2:doi:10.3389/fmars.2015.00109.

- GARRABOU, J., COMA, R., BENSOUSSAN, N., BALLY, M., CHEVALDONNÉ, P., CIGLIANO, M., DIAZ, D., HARMELIN, J. G., GAMBI, M. C., KERSTING, D. K., LEDOUX, J. B., LEJEUSNE, C., LINARES, C., MARSCHAL, C., PÉREZ, T., RIBES, M., ROMANO, J. C., SERRANO, E., TEIXIDO, N., TORRENTS, O., ZABALA, M., ZUBERER, F. & CERRANO, C. 2009. Mass mortality in Northwestern Mediterranean rocky benthic communities: Effects of the 2003 heat wave. *Global Change Biology* 15:1090–1103.
- GARRATT, P. A., GOVENDER, A. & PUNT, A. E. 1993. Growth acceleration at sex change in the protogynous hermaphrodite *Chrysoblephus puniceus* (Pisces: Sparidae). *South African Journal of Marine Science* 13:187–193.
- GELL, F. R. & ROBERTS, C. M. 2003. Benefits beyond boundaries: The fishery effects of marine reserves. *Trends in Ecology and Evolution* 18:448–455.
- GILLANDERS, B. M., BLACK, B. A., MEEKAN, M. G. & MORRISON, M. A. 2012. Climatic effects on the growth of a temperate reef fish from the southern hemisphere: A biochronological approach. *Marine Biology* 159:1327–1333.
- GILLOOLY, J. F., BROWN, J. H., WEST, G. B., SAVAGE, V. M. & CHARNOV, E. L. 2001. Effects of size and temperature on metabolic rate. *Science* 293:2248–2251.
- GOELA, P. C., CORDEIRO, C., DANCHENKO, S., ICELY, J., CRISTINA, S. & NEWTON, A. 2016. Time series analysis of data for sea surface temperature and upwelling components from the southwest coast of Portugal. *Journal of Marine Systems* 163:12–22.
- GOSCHEN, W. S. & SCHUMANN, E. H. 1995. Upwelling and the occurrence of cold water around Cape Recife, Algoa Bay, South Africa. *South African Journal of Marine Science* 16:57–67.
- GOSCHEN, W. S. & SCHUMANN, E. H. 2011. The physical oceanographic processes of Algoa Bay, with emphasis on the western coastal region. *South African Environmental*

- Observation Network (SAEON), Internal Report.* South Africa. 85 pp.
- GÖTZ, A. & KERWATH, S. 2013. Roman (*Chrysoblephus laticeps*). P. 357 in Mann, B. Q. (ed.). *Southern African Marine Linefish Species Profiles* (Special publication). Oceanographic Research Institute, Durban.
- GÖTZ, A., KERWATH, S. E., ATTWOOD, C. G. & SAUER, W. H. H. 2008. Effects of fishing on population structure and life history of roman *Chrysoblephus laticeps* (Sparidae). *Marine Ecology Progress Series* 362:245–259.
- GOUHIER, T. C. & GUICHARD, F. 2014. Synchrony: Quantifying variability in space and time. *Methods in Ecology and Evolution* 5:524–533.
- GOVERNMENT OF SOUTH AFRICA. 2010. National protected area expansion strategy for South Africa 2008. Pretoria. 51 pp.
- GRÄNS, A., JUTFELT, F., SANDBLOM, E., JÖNSSON, E., WIKLANDER, K., SETH, H., OLSSON, C., DUPONT, S., ORTEGA-MARTINEZ, O., EINARSDOTTIR, I., BJÖRNSSON, B. T., SUNDELL, K. & AXELSSON, M. 2014. Aerobic scope fails to explain the detrimental effects on growth resulting from warming and elevated CO<sub>2</sub> in Atlantic halibut. *The Journal of Experimental Biology* 217:711–717.
- GREEN, A. L., FERNANDES, L., ALMANY, G., ABESAMIS, R., MCLEOD, E., ALIÑO, P. M., WHITE, A. T., SALM, R., TANZER, J. & PRESSEY, R. L. 2014. Designing marine reserves for fisheries management, biodiversity conservation, and climate change adaptation. *Coastal Management* 42:143–159.
- GRIFFITHS, M. H. 2000. Long-term trends in catch and effort of commercial linefish off South Africa's Cape Province: snapshots of the 20th century. *South African Journal of Marine Science* 22:81–110.
- GRIFFITHS, M. H. & WILKE, C. G. 2002. Long-term movement patterns of five temperate-reef fishes (Pisces: Sparidae): Implications for marine reserves. *Marine and Freshwater*

*Research* 53:233–244.

GRUBER, N. 2011. Warming up, turning sour, losing breath: Ocean biogeochemistry under global change. *Philosophical Transactions of the Royal Society A* 369:1980–1996.

GUNDERSON, A. R. & STILLMAN, J. H. 2015. Plasticity in thermal tolerance has limited potential to buffer ectotherms from global warming. *Proceedings of the Royal Society B* 282:doi: 10.1098/rspb.2015.0401.

HAIGH, R., IANSON, D., HOLT, C. A. & NEATE, H. E. 2015. Effects of ocean acidification on temperate coastal marine ecosystems and fisheries in the Northeast Pacific. *PLoS ONE* 10:doi: 10.1371/journal.pone.0117533.

HAMPTON, I., LAMBERTH, S. J., PITCHER, G. C. & PRETORIUS, M. 2017. Report on the DAFF Workshop on fisheries vulnerability to climate change, 2-3 September 2015, Foretrust House, Cape Town. Cape Town. 39 pp.

HANDELSMAN, C. A., BRODER, E. D., DALTON, C. M., RUELL, E. W., MYRICK, C. A., REZNICK, D. N. & GHALAMBOR, C. K. 2013. Predator-induced phenotypic plasticity in metabolism and rate of growth: Rapid adaptation to a novel environment. *Integrative and Comparative Biology* 53:975–988.

HANEKOM, N., HUTCHINGS, L., JOUBERT, P. A. & VAN DER BYL, P. C. N. 1989. Sea temperature variations in the tsitsikamma coastal national park, South Africa, with notes on the effect of cold conditions on some fish populations. *South African Journal of Marine Science* 8:145–153.

HARRIS, J. M., LIVINGSTONE, T., PHADIMA, J., KERRY, S., FASHEUN, T., BOYD, A. & MFEKA, X. 2014. Phakisa Initiative : fast-tracking establishment of an effective and representative network of Marine Protected Areas. P. 36 *Symposium of Contemporary Conservation Practice*.

HARRISON, X. A., DONALDSON, L., CORREA-CANO, M. E., EVANS, J., FISHER, D. N.,

- GOODWIN, C. E. D., ROBINSON, B. S., HODGSON, D. J. & INGER, R. 2018. A brief introduction to mixed effects modelling and multi-model inference in ecology. *Peer J* 6:doi: 10.7717/peerj.4794.
- HEALY, T. M. & SCHULTE, P. M. 2012. Thermal acclimation is not necessary to maintain a wide thermal breadth of aerobic scope in the common killifish (*Fundulus heteroclitus*). *Physiological and Biochemical Zoology* 85:107–19.
- HELAOUËT, P. & BEAUGRAND, G. 2007. Macroecology of *Calanus finmarchicus* and *C. helgolandicus* in the North Atlantic Ocean and adjacent seas. *Marine Ecology Progress Series* 345:147–165.
- HELMUTH, B. 2009. From cells to coastlines : how can we use physiology to forecast the impacts of climate change ? *Journal of Experimental Biology* 212:753–760.
- HELSEY, T. E., LAI, H. L. & BLACK, B. A. 2012. Bayesian hierarchical modeling of Pacific geoduck growth increment data and climate indices. *Ecological Modelling* 247:210–220.
- HESSENAUER, J. M., VOKOUN, J. C., SUSKI, C. D., DAVIS, J., JACOBS, R. & O'DONNELL, E. 2015. Differences in the metabolic rates of exploited and unexploited fish populations: A signature of recreational fisheries induced evolution? *PLoS ONE* 10:doi: 10.1371/journal.pone.0128336.
- HIJMANS, R. J. 2016. Raster: Geographic data analysis and modeling. *R package*.
- HILBORN, R., WALTERS, C. J. & LUDWIG, D. 1995. Sustainable exploitation of renewable resources. *Annual Review of Ecology, Evolution, and Systematics* 26:45–67.
- HIXON, M. A., JOHNSON, D. W. & SOGARD, S. M. 2014. BOFFFFs: On the importance of conserving old-growth age structure in fishery populations. *ICES Journal of Marine Science* 71:2171–2185.
- HOBDAY, A. J., ALEXANDER, L. V., PERKINS, S. E., SMALE, D. A., STRAUB, S. C., OLIVER, E. C. J., BENTHUYSEN, J. A., BURROWS, M. T., DONAT, M. G., FENG, M.,

- HOLBROOK, N. J., MOORE, P. J., SCANNELL, H. A., SEN GUPTA, A. & WERNBERG, T. 2016. A hierarchical approach to defining marine heatwaves. *Progress in Oceanography* 141:227–238.
- HOBDAY, A. J. & PECL, G. T. 2014. Identification of global marine hotspots: Sentinels for change and vanguards for adaptation action. *Reviews in Fish Biology and Fisheries* 24:415–425.
- HODGSON, D., MCDONALD, J. L. & HOSKEN, D. J. 2015. What do you mean, ‘resilient’? *Trends in Ecology & Evolution* 30:503–506.
- HOEGH-GULDBERG, O. & BRUNO, J. F. 2010. The impact of climate change on the world’s marine ecosystems. *Science* 328:1523–1529.
- HOEY, A., HOWELLS, E., JOHANSEN, J., HOBBS, J.-P., MESSMER, V., MCCOWAN, D., WILSON, S. & PRATCHETT, M. 2016. Recent advances in understanding the effects of climate change on coral reefs. *Diversity* 8:doi: 10.3390/d8020012.
- HOFFMANN, A. A. & SGRÓ, C. M. 2011. Climate change and evolutionary adaptation. *Nature* 470:479–485.
- HOFMANN, G. E. & TODGHAM, A. E. 2010. Living in the now: Physiological mechanisms to tolerate a rapidly changing environment. *Annual Review of Physiology* 72:127–145.
- HOLLINS, J., THAMBITHURAI, D., KÖECK, B., CRESPEL, A., BAILEY, D. M., COOKE, S. J., LINDSTRÖM, J., PARSONS, K. J. & KILLEN, S. S. 2018. A physiological perspective on fisheries-induced evolution. *Evolutionary Applications* 11:561–576.
- HOLT, R. E. & JØRGENSEN, C. 2014. Climate warming causes life-history evolution in a model for Atlantic cod (*Gadus morhua*). *Conservation Physiology* 2:doi: doi: 10.1093/conphys/cou050.
- HORODYSKY, A. Z., COOKE, S. J. & BRILL, R. W. 2015. Physiology in the service of fisheries science: Why thinking mechanistically matters. *Reviews in Fish Biology and Fisheries*

25:425–447.

HOWES, E., JOOS, F., EAKIN, M. & GATTUSO, J. 2015. An updated synthesis of the observed and projected impacts of climate change on the chemical, physical and biological processes in the oceans. *Frontiers in Marine Science* 2:doi:10.3389/fmars.2015.00036 An.

HSIEH, C.-H., REISS, C. S., HUNTER, J. R., BEDDINGTON, J. R., MAY, R. M. & SUGIHARA, G. 2006. Fishing elevates variability in the abundance of exploited species. *Nature* 443:859–862.

HSIEH, C., REISS, C. S., HEWITT, R. P. & SUGIHARA, G. 2008. Spatial analysis shows that fishing enhances the climatic sensitivity of marine fishes. *Canadian Journal of Fisheries and Aquatic Sciences* 65:947–961.

HUEY, R. B., KEARNEY, M. R., KROCKENBERGER, A., HOLTUM, J. A. M., JESS, M. & WILLIAMS, S. E. 2012. Predicting organismal vulnerability to climate warming: roles of behaviour, physiology and adaptation. *Philosophical transactions of the Royal Society B* 367:1665–1679.

HULBERT, S. H. 1984. Pseudo replication and the design of ecological field experiments. *Ecological Monographs* 54:187–211.

HUTCHINGS, L., VAN DER LINGEN, C. D., SHANNON, L. J., CRAWFORD, R. J. M., VERHEYE, H. M. S., BARTHOLOMAE, C. H., VAN DER PLAS, A. K., LOUW, D., KREINER, A., OSTROWSKI, M., FIDEL, Q., BARLOW, R. G., LAMONT, T., COETZEE, J., SHILLINGTON, F., VEITCH, J., CURRIE, J. C. & MONTEIRO, P. M. S. 2009. The Benguela Current: An ecosystem of four components. *Progress in Oceanography* 83:15–32.

IFTIKAR, F. I. & HICKEY, A. J. R. 2013. Do mitochondria limit hot fish hearts? Understanding the role of mitochondrial function with heat stress in *Notolabrus celidotus*. *PLoS ONE*

8:doi: 10.1371/journal.pone.0064120.

- IPCC. 2014. *Climate Change 2014: Synthesis Report. Contribution of Working Groups I, II and III to the Fifth Assessment Report of the Intergovernmental Panel on Climate Change*. P. (Core Writing Team, R. K. Pachauri, and L. A. Meyer, Eds.). IPCC, Geneva, Switzerland. 151 pp.
- ISEMONGER, D. N. 2013. Modelling the spatial and genetic response of the endemic sparid : *Polysteganus praeorbitalis* (Pisces : Sparidae ) to climate change in the Agulhas Current system. Rhodes University, MSc thesis. 104 pp.
- ISHIMATSU, A., HAYASHI, M. & KIKKAWA, T. 2008. Fishes in high-CO<sub>2</sub>, acidified oceans. *Marine Ecology Progress Series* 373:295–302.
- ISHIMATSU, A., KIKKAWA, T., HAYASHI, M., LEE, K.-S. & KITA, J. 2004. Effects of CO<sub>2</sub> on marine fish: Larvae and adults. *Journal of Oceanography* 60:731–741.
- IZZO, C., DOUBLEDAY, Z. A., GRAMMER, G. L., BARNES, T. C., DELEAN, S., FERGUSON, G. J., YE, Q. & GILLANDERS, B. M. 2016. Multi-species response to rapid environmental change in a large estuary system: A biochronological approach. *Ecological Indicators* 69:739–748.
- JAMES, N. C., WHITFIELD, A. K. & COWLEY, P. D. 2008. Preliminary indications of climate-induced change in a warm-temperate South African estuarine fish community. *Journal of Fish Biology* 72:1855–1863.
- JOHANSEN, J. L., MESSMER, V., COKER, D. J., HOEY, A. S. & PRATCHETT, M. S. 2014. Increasing ocean temperatures reduce activity patterns of a large commercially important coral reef fish. *Global Change Biology* 20:1067–1074.
- JONES, K. R., WATSON, J. E. M., POSSINGHAM, H. P. & KLEIN, C. J. 2016. Incorporating climate change into spatial conservation prioritisation : A review. *Biological Conservation* 194:121–130.

- JØRGENSEN, C., ENBERG, K., DUNLOP, E. S., ARLINGHAUS, R., BOUKAL, D. S., BRANDER, K., ERNANDE, B., GÅRDMARK, A., JOHNSTON, F., MATSUMURA, S., PARDOE, H., RAAB, K., SILVA, A., VAINIKKA, A., DIECKMANN, U., HEINO, M., RIJNSDORP, A. D., JORGENSEN, C., ENBERG, K., DUNLOP, E. S., ARLINGHAUS, R., BOUKAL, D. S., BRANDER, K., ERNANDE, B., GARDMARK, A., JOHNSTON, F., MATSUMURA, S., PARDOE, H., RAAB, K., SILVA, A., VAINIKKA, A., DIECKMANN, U., HEINO, M. & RIJNSDORP, A. D. 2007. Managing evolving fish stocks. *Science* 318:1247–1248.
- JUTFELT, F., NORIN, T., ERN, R., OVERGAARD, J., WANG, T., MCKENZIE, D. J., LEFEVRE, S., NILSSON, E., METCALFE, N. B., HICKEY, A. J. R., BRIJS, J., SPEERS-ROESCH, B., ROCHE, D. G., GAMPERL, A. K., RABY, G. D., MORGAN, R., ESBAUGH, A. J., SANDBLOM, E., BINNING, S. A., HICKS, J. W., AXELSSON, M., EKSTRO, A., SEEBACHER, F., JØRGENSEN, C., KILLEN, S. S., SCHULTE, P. M. & CLARK, T. D. 2018. Oxygen- and capacity-limited thermal tolerance : blurring ecology and physiology. *Journal of Experimental Biology* 221:doi: 10.1242/jeb.169615.
- KATERSKY, R. S. & CARTER, C. G. 2007. High growth efficiency occurs over a wide temperature range for juvenile barramundi *Lates calcarifer* fed a balanced diet. *Aquaculture* 272:444–450.
- KEARNEY, M., PHILLIPS, B. L., TRACY, C. R., CHRISTIAN, K. A., BETTS, G. & PORTER, W. P. 2008. Modelling species distributions without using species distributions: the cane toad in Australia under current and future climates. *Ecography* 31:423–434.
- KEARNEY, M. & PORTER, W. 2009. Mechanistic niche modelling: Combining physiological and spatial data to predict species' ranges. *Ecology Letters* 12:334–350.
- KELLER, B. D., GLEASON, D. F., MCLEOD, E., WOODLEY, C. M., AIRAMÉ, S., CAUSEY, B. D., FRIEDLANDER, A. M., GROBER-DUNSMORE, R., JOHNSON, J. E., MILLER, S. L. & STENECK, R. S. 2009. Climate change, coral reef ecosystems, and management

- options for marine protected areas. *Environmental Management* 44:1069–1088.
- KERWATH, S. E., GÖTZ, A., ATTWOOD, C. G., COWLEY, P. D. & SAUER, W. H. H. 2007a. Movement pattern and home range of Roman *Chrysoblephus laticeps*. *African Journal of Marine Science* 29:93–103.
- KERWATH, S. E., GÖTZ, A., ATTWOOD, C. G., SAUER, W. H. H. & WILKE, C. G. 2007b. Area utilisation and activity patterns of roman *Chrysoblephus laticeps* (Sparidae) in a small marine protected area. *African Journal of Marine Science* 29:259–270.
- KERWATH, S. E., WILKE, C. G. & GOTZ, A. 2013a. The effects of barotrauma on five species of South African line-caught fish. *African Journal of Marine Science* 35:243–252.
- KERWATH, S. E., WINKER, H., GÖTZ, A. & ATTWOOD, C. G. 2013b. Marine protected area improves yield without disadvantaging fishers. *Nature Communications* 4:doi: 10.1038/ncomms3347.
- KERWATH, S., GÖTZ, A., WILKE, C., ATTWOOD, C. & SAUER, W. 2006. A comparative evaluation of three methods used to tag South African linefish. *African Journal of Marine Science* 28:637–643.
- KEYSER, F. M., BROOME, J. E., BRADFORD, R. G., SANDERSON, B. & REDDEN, A. M. 2016. Winter presence and temperature-related diel vertical migration of striped bass (*Morone saxatilis*) in an extreme high-flow passage in the inner Bay of Fundy. *Canadian Journal of Fisheries and Aquatic Sciences* 1786:1777–1786.
- KHAN, J. R., PETHER, S., BRUCE, M., WALKER, S. P. & HERBERT, N. A. 2014. Optimum temperatures for growth and feed conversion in cultured hapuku (*Polyprion oxygeneios*) - Is there a link to aerobic metabolic scope and final temperature preference? *Aquaculture* 430:107–113.
- KILLEN, S. S., MARRAS, S., RYAN, M. R., DOMENICI, P. & MCKENZIE, D. J. 2012. A relationship between metabolic rate and risk-taking behaviour is revealed during hypoxia

- in juvenile European sea bass. *Functional Ecology* 26:134–143.
- KILLEN, S. S., MITCHELL, M. D., RUMMER, J. L., CHIVERS, D. P., FERRARI, M. C. O., MEEKAN, M. G. & MCCORMICK, M. I. 2014. Aerobic scope predicts dominance during early life in a tropical damselfish. *Functional Ecology* 28:1367–1376.
- KILLEN, S. S., NORIN, T. & HALSEY, L. G. 2016. Do method and species lifestyle affect measures of maximum metabolic rate in fishes? *Journal of Fish Biology* 90:1037–1046.
- KILLEN, S. S., ESBAUGH, A. J., MARTINS, N. F., RANTIN, F. T. & MCKENZIE, D. J., 2018. Aggression superceded individual oxygen demand to drive group air-breathing in social catfish. *Journal of Animal Ecology* 87:223-234.
- KLEFOTH, T., SKOV, C., KUPARINEN, A. & ARLINGHAUS, R. 2017. Toward a mechanistic understanding of vulnerability to hook-and-line fishing: Boldness as the basic target of angling-induced selection. *Evolutionary Applications* 10:994–1006.
- KOOIJMAN, S. A. L. M. 2009. *Dynamic energy budget theory for metabolic organization* (3rd edition). Cambridge University Press, cambridge. 532 pp.
- KOZLOWSKI, J. 1996. Optimal allocation of resources explains interspecific life-history patterns in animals with indeterminate growth. *Proceedings of the Royal Society B* 263:559–566.
- KUHN, M. 2008. Building predictive models in R using the caret package. *Journal of Statistical Software* 28.
- KUPARINEN, A. & MERILÄ, J. 2007. Detecting and managing fisheries-induced evolution. *Trends in Ecology and Evolution* 22:652–659.
- LAPOINTE-GARANT, M.-P., HUANG, J.-G., GEA-IZQUIERDO, G., RAULIER, F., BERNIER, P. & BERNINGER, F. 2010. Use of tree rings to study the effect of climate change on trembling aspen in Quebec. *Global Change Biology* 16:2039–2051.

- LASRAM, F. B. R., GUILHAUMON, F., ALBOUY, C., SOMOT, S., THUILLER, W. & MOULLOT, D. 2010. The Mediterranean Sea as a 'cul-de-sac' for endemic fishes facing climate change. *Global Change Biology* 16:3233–3245.
- LAST, P. R., WHITE, W. T., GLEDHILL, D. C., HOBDAV, A. J., BROWN, R., EDGAR, G. J. & PECL, G. 2011. Long-term shifts in abundance and distribution of a temperate fish fauna: a response to climate change and fishing practices. *Global Ecology and Biogeography* 20:58–72.
- LAW, R. 2000. Fishing, selection, and phenotypic evolution. *ICES Journal of Marine Science* 57:659–668.
- LEE, Q., THORSON, J. T., GERTSEVA, V. V & PUNT, A. E. 2017. The benefits and risks of incorporating climate-driven growth variation into stock assessment models, with application to Splitnose Rockfish (*Sebastes diploproa*). *ICES Journal of Marine Science* 75:245–256.
- LEFEVRE, S. 2016. Are global warming and ocean acidification conspiring against marine ectotherms? A meta-analysis of the respiratory effects of elevated temperature, high CO<sub>2</sub> and their interaction. *Conservation Physiology* 4:doi: 10.1093/conphys/cow009.
- LENNOX, R., ALÓS, J., ARLINGHAUS, R., HORODYSKY, A., KLEFOTH, T., MONK, C. & COOKE, S. 2017. What makes fish vulnerable to capture by hooks? A conceptual framework and a review of key determinants. *Fish and Fisheries* 18:986–1010.
- LESTER, N. P., SHUTER, B. J. & ABRAMS, P. A. 2004. Interpreting the von Bertalanffy model of somatic growth in fishes : the cost of reproduction. *Proceedings of the Royal Society of London B* 271:1625–1631.
- LEVY, J. S. & BAN, N. C. 2013. A method for incorporating climate change modelling into marine conservation planning : An Indo-west Pacific example. *Marine Policy* 38:16–24.
- LIAW, A. & WEINER, M. 2002. Classification and regression by randomForest. *R News* 2:18–

22.

- LIMA, F. P. & WETHEY, D. S. 2012. Three decades of high-resolution coastal sea surface temperatures reveal more than warming. *Nature Communications* 3:doi: 10.1038/ncomms1713.
- LINK, J. S., NYE, J. A. & HARE, J. A. 2011. Guidelines for incorporating fish distribution shifts into a fisheries management context. *Fish and Fisheries* 12:461–469.
- LLOYD, P., PLAGANYI, E. E., WEEKS, S. J., MAGNO-CANTO, M. & PLAGANYI, G. 2012. Ocean warming alters species abundance patterns and increases species diversity in an African sub-tropical reef-fish community. *Fisheries Oceanography* 21:78–94.
- LUCEY, S. M. & NYE, J. A. 2010. Shifting species assemblages in the Northeast US Continental Shelf Large Marine Ecosystem. *Marine Ecology Progress Series* 415:23–33.
- LUTJEHARMS, J. R. E., COOPER, J. & ROBERTS, M. 2000. Upwelling at the inshore edge of the Agulhas Current. *Continental Shelf Research* 20:737–761.
- MADEC, G. 2008. *NEMO ocean engine*. Institut Pierre-Simon Laplace (IPSL), France. 396 pp.
- MADLIGER, C. L., LOVE, O. P., HULTINE, K. R. & COOKE, S. J. 2018. The conservation physiology toolbox: status and opportunities. *Conservation Physiology* 6:doi: 10.1093/conphys/coy029.
- MANDIC, M., TODGHAM, A. E. & RICHARDS, J. G. 2009. Mechanisms and evolution of hypoxia tolerance in fish. *Proceedings of the Royal Society B* 276:735–744.
- MANN, B. Q. 2013. *Southern African Marine Linefish Species Profiles*. (B. Q. Mann, Ed.) *Special Publication No.9*. Oceanographic Research Institute, Durban. 357 pp.
- MANTUA, N. J., HARE, S. R., ZHANG, Y., WALLACE, J. M. & FRANCIS, R. C. 1997. A Pacific interdecadal climate oscillation with impacts on salmon production. *Bulletin of the*

*American Meteorological Soc* 78:1069–1079.

MAYNARD, J. A., MARSHAL, P. A., JOHNSON, J. E. & HARMAN, S. 2010. Building resilience into practical conservation : identifying local management responses to global climate change in the southern Great Barrier Reef. *Coral Reefs* 29:381–391.

MAZEROLLE, M. J. 2017. AICcmoavg: Model selection and multimodel inference based on (Q)AIC(c). *R package*.

MAZLOUMI, N., BURCH, P., FOWLER, A. J., DOUBLEDAY, Z. A. & GILLANDERS, B. M. 2017. Determining climate-growth relationships in a temperate fish: A sclerochronological approach. *Fisheries Research* 186:319–327.

MCGILL, B. 2014. Is requiring replication statistical machismo? *Dynamic ecology* Blog Post:<https://dynamicecology.wordpress.com/>.

MCKENZIE, D. J., AXELSSON, M., CHABOT, D., CLAIREAUX, G., COOKE, S. J., CORNER, R. A., BOECK, G. DE, DOMENICI, P., GUERREIRO, P. M., HAMER, B., JØRGENSEN, C., KILLEN, S. S., LEFEVRE, S., MARRAS, S., MICHAELIDIS, B., NILSSON, G. E., PECK, M. A., PEREZ-RUZAFÁ, A., RIJNSDORP, A. D., SHIELS, H. A., STEFFENSEN, J. F., SVENDSEN, J. C., SVENDSEN, M. B. S., TEAL, L. R., MEER, J. VAN DER, WANG, T., WILSON, J. M., WILSON, R. W. & METCALFE, J. D. 2016. Conservation physiology of marine fishes: state of the art and prospects for policy. *Conservation Physiology* 4.

MCLEOD, E., SALM, R., GREEN, A. & ALMANY, J. 2009. Designing marine protected area networks to address the impacts of climate change. *Frontiers in Ecology and the Environment* 7:362–370.

MEEHL, G. A., COVEY, C., DELWORTH, T., LATIF, M., MCAVANEY, B., MITCHELL, J. F. B., STOUFFER, R. J. . & TAYLOR, K. E. 2007. The WCRP CMIP3 multi-model dataset: A new era in climate change research. *Bulletin of American Meteorological Society* 88:1383–1394.

- MELZNER, F., GÖBEL, S., LANGENBUCH, M., GUTOWSKA, M. A., PÖRTNER, H. & LUCASSEN, M. 2009a. Swimming performance in Atlantic cod (*Gadus morhua*) following long-term (4 – 12 months) acclimation to elevated seawater PCO<sub>2</sub>. *Aquatic Toxicology* 92:30–37.
- MELZNER, F., GUTOWSKA, M. A., LANGENBUCH, M., DUPONT, S., LUCASSEN, M., THORNDYKE, M. C., BLEICH, M., PORTNER, H.-O. & ORTNER<sup>4</sup>. 2009b. Physiological basis for high CO<sub>2</sub> tolerance in marine ectothermic animals: pre-adaptation through lifestyle and ontogeny? *Biogeosciences* 6:2313–1331.
- METCALFE, J. D., LE QUESNE, W. J. F., CHEUNG, W. W. L. & RIGHTON, D. A. 2012. Conservation physiology for applied management of marine fish: an overview with perspectives on the role and value of telemetry. *Philosophical Transactions of the Royal Society B* 367:1746–1756.
- METCALFE, N. B., BULL, C. D. & MANGEL, M. 2002. Seasonal variation in catch-up growth reveals state-dependent somatic allocations in salmon. *Evolutionary Ecology Research* 4:871–881.
- METCALFE, N. B., VAN LEEUWEN, T. E. & KILLEN, S. S. 2016. Does individual variation in metabolic phenotype predict fish behaviour and performance? *Journal of Fish Biology* 88:298–321.
- METHOT, R. D. & WETZEL, C. R. 2013. Stock synthesis: A biological and statistical framework for fish stock assessment and fishery management. *Fisheries Research* 142:86–99.
- MICHELI, F., SAENZ-ARROYO, A., GREENLEY, A., VAZQUEZ, L., ESPINOZA MONTES, J. A., ROSSETTO, M. & DE LEO, G. A. 2012. Evidence that marine reserves enhance resilience to climatic impacts. *PLoS ONE* 7:doi: 10.1371/journal.pone.0040832.
- MORASH, A. J., NEUFELD, C., MACCORMACK, T. J. & CURRIE, S. 2018. The importance

- of incorporating natural thermal variation when evaluating physiological performance in wild species. *The Journal of Experimental Biology* 221:doi: 10.1242/jeb.164673.
- MORRONGIELLO, J. R., THRESHER, R. E. & SMITH, D. C. 2012. Aquatic biochronologies and climate change. *Nature Climate Change* 2:849–857.
- MORRONGIELLO, J. R., WALSH, C. T., GRAY, C. A., STOCKS, J. R. & CROOK, D. A. 2014. Environmental change drives long-term recruitment and growth variation in an estuarine fish. *Global Change Biology* 20:1844–1860.
- MORRONGIELLO, J. & THRESHER, R. 2015. A statistical framework to explore ontogenetic growth variation among individuals and populations : a marine fish example. *Ecological Monographs* 85:93–115.
- MOTYKA, R., NORIN, T., PETERSEN, L. H., HUGGETT, D. B. & GAMPERL, A. K. 2017. Long-term hypoxia exposure alters the cardiorespiratory physiology of Steelhead Trout (*Oncorhynchus mykiss*), but does not affect their upper thermal tolerance. *Journal of Thermal Biology* 68:149–161.
- MUGGEO, V. M. R. 2003. Estimating regression models with unknown break-points. *Statistics in Medicine* 22:3055–3071.
- MUGGEO, V. M. R. 2008. segmented: An R package to fit regression models with broken-line relationships. *R News* 8:20–25.
- MUNDAY, P. L. 2014. Transgenerational acclimation of fishes to climate change and ocean acidification. *F1000Prime Reports* 6.
- MUNDAY, P. L., CRAWLEY, N. E. & NILSSON, G. E. 2009. Interacting effects of elevated temperature and ocean acidification on the aerobic performance of coral reef fishes. *Marine Ecology Progress Series* 388:235–242.
- MUNDAY, P. L., DIXSON, D. L., MCCORMICK, M. I., MEEKAN, M., FERRARI, M. C. O. & CHIVERS, D. P. 2010. Replenishment of fish populations is threatened by ocean

- acidification. *Proceedings of the National Academy of Sciences* 107:12930–12934.
- MUNDAY, P. L., GAGLIANO, M., DONELSON, J. M., DIXSON, D. L. & THORROLD, S. R. 2011. Ocean acidification does not affect the early life history development of a tropical marine fish. *Marine Ecology Progress Series* 423:211–221.
- MUNDAY, P. L., DONELSON, J. M. & DOMINGOS, J. A. 2017. Potential for adaptation to climate change in a coral reef fish. *Global Change Biology* 13:307–317.
- MUNOZ, N. J., FARRELL, A. P., HEATH, J. W. & NEFF, B. D. 2015. Adaptive potential of a Pacific salmon challenged by climate change. *Nature Climate Change* 5:163–166.
- NATIONAL PLANNING COMMISSION. 2011. Our future - make it work National Development Plan 2030. Republic of South Africa. 486 pp.
- NEILL, W. H., MILLER, J. M., VAN DER VEER, H. W. & WINEMILLER, K. O. 1994. Ecophysiology of marine fish recruitment: A conceptual framework for understanding interannual variability. *Netherlands Journal of Sea Research* 32:135–152.
- NEUHEIMER, A. B., THRESHER, R. E., LYLE, J. M. & SEMMENS, J. M. 2011. Tolerance limit for fish growth exceeded by warming waters. *Nature Climate Change* 1:110–113.
- NEWMAN, S. J., WILLIAMS, D. M. & RUSS, G. R. 1996. Age validation , growth and mortality rates of the tropical snappers (Pisces : Lutjanidae) *Lutjanus adetii* (Castelnau , 1873) and *L. quinquelineatus* (Bloch , 1790) from the central Great Barrier Reef, Australia. *Marine and Freshwater Research* 47:575–584.
- NORIN, T. & CLARK, T. D. 2016. Measurement and relevance of maximum metabolic rate in fishes. *Journal of Fish Biology* 88:122–151.
- NORIN, T., MALTE, H. & CLARK, T. D. 2014. Aerobic scope does not predict the performance of a tropical eurythermal fish at elevated temperatures. *Journal of Experimental Biology* 217:244–251.

- NORIN, T., MALTE, H. & CLARK, T. D. 2016. Differential plasticity of metabolic rate phenotypes in a tropical fish facing environmental change. *Functional Ecology* 30:369–378.
- OKSANEN, L. 2001. Logic of experiments in ecology: is pseudoreplication a pseudoissue? *Oikos* 94:27–38.
- OLIVER, E. C. J., DONAT, M. G., BURROWS, M. T., MOORE, P. J., SMALE, D. A., ALEXANDER, L. V., BENTHUYSEN, J. A., FENG, M., SEN GUPTA, A., HOBDAI, A. J., HOLBROOK, N. J., PERKINS-KIRKPATRICK, S. E., SCANNELL, H. A., STRAUB, S. C. & WERNBERG, T. 2018. Longer and more frequent marine heatwaves over the past century. *Nature Communications* 9:doi: 10.1038/s41467-018-03732-9.
- ONG, J. J. L., ROUNTREY, A. N., MARRIOTT, R. J., NEWMAN, S. J., MEEUWIG, J. J. & MEEKAN, M. G. 2017. Cross-continent comparisons reveal differing environmental drivers of growth of the coral reef fish, *Lutjanus bohar*. *Coral Reefs* 36:195–206.
- ORTEGA-CISNEROS, K., YOKWANA, S., SAUER, W., COCHRANE, K., COCKCROFT, A., JAMES, N. C., POTTS, W. M., SINGH, L., SMALE, M., WOOD, A. & PECL, G. 2018. Assessment of the likely sensitivity to climate change for the key marine species in the southern Benguela system. *African Journal of Marine Science* 40:179-292.
- OTTERSEN, G., HJERMANN, D. O. & STENSETH, N. C. 2006. Changes in spawning stock structure strengthen the link between climate and recruitment in a heavily fished cod (*Gadus morhua*) stock. *Fisheries Oceanography* 15:230–243.
- PACIFICI, M., FODEN, W. B., VISCONTI, P., WATSON, J. E. M., BUTCHART, S. H. M., KOVACS, K. M., SCHEFFERS, B. R., HOLE, D. G., MARTIN, T. G., AKÇAKAYA, H. R., CORLETT, R. T., HUNTLEY, B., BICKFORD, D., CARR, J. A., HOFFMANN, A. A., MIDGLEY, G. F., PEARCE-KELLY, P., PEARSON, R. G., WILLIAMS, S. E., WILLIS, S. G., YOUNG, B. & RONDININI, C. 2015. Assessing species vulnerability to climate change. *Nature Climate Change* 5:215–225.

- PALUMBI, S. R. 2004. Marine reserves and ocean neighborhoods: The spatial scale of marine populations and their management. *Annual Review of Environment and Resources* 29:31–68.
- PANKHURST, N. W. & MUNDAY, P. L. 2011. Effects of climate change on fish reproduction and early life history stages. *Marine and Freshwater Research* 62:1015–1026.
- PARKER, D., WINKER, H., ATTWOOD, C. G. & KERWATH, S. E. 2016. Dark times for Dageaad *Chrysoblephus cristiceps*: evidence for stock collapse. *African Journal of Marine Science* 38:341–349.
- PARMESAN, C. 2006. Ecological and evolutionary responses to recent climate change. *Annual Review of Ecology, Evolution, and Systematics* 37:637–671.
- PATTERSON, D. A., COOKE, S. J., HINCH, S. G., ROBINSON, K. A., YOUNG, N., FARRELL, A. P. & MILLER, K. M. 2016. A perspective on physiological studies supporting the provision of scientific advice for the management of Fraser River Sockeye Salmon (*Oncorhynchus nerka*). *Conservation Physiology* 4:doi: 10.1093/conphys/cow026.
- PAULY, D., CHRISTENSEN, V., WALTERS, C. J., WATSON, R., ZELLER, D., GUÉNETTE, S., PITCHER, T. J., SUMAILA, U. R., WALTERS, C. J., WATSON, R. & ZELLER, D. 2002. Towards sustainability in world fisheries. *Nature* 418:689–695.
- PAYNE, N. L., SMITH, J. A., VAN DER MEULEN, D. E., TAYLOR, M. D., WATANABE, Y. Y., TAKAHASHI, A., MARZULLO, T. A., GRAY, C. A., CADIOU, G. & SUTHERS, I. M. 2016. Temperature dependence of fish performance in the wild: Links with species biogeography and physiological thermal tolerance. *Functional Ecology* 30:903–912.
- PECK, M. A., ARVANITIDIS, C., BUTENSCHON, M., CANU, D. M., CHATZINIKOLAOU, E., CUCCO, A., DOMENICI, P., FERNANDES, J. A., GASCHÉ, L., HUEBERT, K. B., HUFNAGL, M., JONES, M. C., KEMPF, A., KEYL, F., MAAR, M., MAH??VAS, S., MARCHAL, P., NICOLAS, D., PINNEGAR, J. K., RIVOT, E., ROCHETTE, S., SELL, A.

- F., SINERCHIA, M., SOLIDORO, C., SOMERFIELD, P. J., TEAL, L. R., TRAVERS-TROLET, M. & VAN DE WOLFSHAAR, K. E. 2016. Projecting changes in the distribution and productivity of living marine resources: A critical review of the suite of modelling approaches used in the large European project VECTORS. *Estuarine, Coastal and Shelf Science* 201:40–55.
- PECL, G. T., ARAÚJO, M. B., BELL, J. D., BLANCHARD, J., BONEBRAKE, T. C., CHEN, I., CLARK, T. D., COLWELL, R. K., DANIELSEN, F., EVENGÅRD, B., FALCONI, L., FERRIER, S., FRUSHER, S., GARCIA, R. A., GRIFFIS, R. B., HOBDAJ, A. J., JANIONSCHEEPERS, C., JARZYNA, M. A., JENNINGS, S., LENOIR, J., LINNETVED, H. I., MARTIN, V. Y., MCCORMACK, P. C., MCDONALD, J., MITCHELL, N. J., MUSTONEN, T., PANDOLFI, J. M., PETTORELLI, N., POPOVA, E., ROBINSON, S. A., SCHEFFERS, B. R., SHAW, J. D., SORTE, C. J. B., STRUGNELL, J. M., SUNDAY, J. M. & TUANMU, M. 2017. Biodiversity redistribution under climate change: Impacts on ecosystems and human well-being. *Science* 355:doi: 10.1126/science.aai9214.
- PECL, G. T., WARD, T. M., DOUBLEDAY, Z. A., CLARKE, S., DAY, J., DIXON, C., FRUSHER, S., GIBBS, P., HOBDAJ, A. J., HUTCHINSON, N., JENNINGS, S., JONES, K., LI, X., SPOONER, D. & STOKLOSA, R. 2014. Rapid assessment of fisheries species sensitivity to climate change. *Climatic Change* 127:505–520.
- PERRY, A. L., LOW, P. J., ELLIS, J. R. & REYNOLDS, J. D. 2005. Climate change and distribution shifts in marine fishes. *Science* 308:1912–1915.
- PERRY, R. I., CURY, P., BRANDER, K., JENNINGS, S., MÖLLMANN, C. & PLANQUE, B. 2010. Sensitivity of marine systems to climate and fishing: Concepts, issues and management responses. *Journal of Marine systems* 79:427–435.
- PHILIPP, D. P., COOKE, S. J., CLAUSSEN, J. E., KOPPELMAN, J. B., SUSKI, C. D. & BURKETT, D. P. 2009. Selection for vulnerability to angling in largemouth bass. *Transactions of the American Fisheries Society* 138:189–199.

- PINHEIRO, J., BATES, D., DEBROY, S., SARKAR, D. & R CORE TEAM. 2017. nlme: Linear and nonlinear mixed effects models. *R package*.
- PLANQUE, B., FROMENTIN, J. M., CURY, P., DRINKWATER, K. F., JENNINGS, S., PERRY, R. I. & KIFANI, S. 2010. How does fishing alter marine populations and ecosystems sensitivity to climate? *Journal of Marine Systems* 79:403–417.
- POLOCZANSKA, E. S., BROWN, C. J., SYDEMAN, W. J., KIESSLING, W., SCHOEMAN, D. S., MOORE, P. J., BRANDER, K., BRUNO, J. F., BUCKLEY, L. B., BURROWS, M. T., DUARTE, C. M., HALPERN, B. S., HOLDING, J., KAPPEL, C. V., O'CONNOR, M. I., PANDOLFI, J. M., PARMESAN, C., SCHWING, F. & THOMPSON, SARAH ANN RICHARDSON, A. J. 2013. Global imprint of climate change on marine life. *Nature Climate Change* 3:919–925.
- POLOCZANSKA, E. S., BURROWS, M. T., BROWN, C. J., MOLINOS, J. G., HALPERN, B. S. & HOEGH-GULDBERG, O. 2016. Responses of marine organisms to climate change across oceans. *Frontiers in Marine Science* 3:doi: 10.3389/fmars.2016.00062.
- POPOVA, E., YOOL, A., BYFIELD, V., COCHRANE, K., COWARD, A. C., SALIM, S. S., GASALLA, M. A., HENSON, S. A., HOBDAY, A. J., PECL, G. T., SAUER, W. H. & ROBERTS, M. J. 2016. From global to regional and back again: common climate stressors of marine ecosystems relevant for adaptation across five ocean warming hotspots. *Global Change Biology* 22:2038–2053.
- LE PORT, A., MONTGOMERY, J. C., SMITH, A. N. H., CROUCHER, A. E., MCLEOD, I. M. & LAVERY, S. D. 2017. Temperate marine protected area provides recruitment subsidies to local fisheries. *Proceedings of the Royal Society B* 284:doi: 10.1098/rspb.2017.1300.
- PÖRTNER, H. O. 2012. Integrating climate-related stressor effects on marine organisms: Unifying principles linking molecule to ecosystem-level changes. *Marine Ecology Progress Series* 470:273–290.

- PÖRTNER, H. O., BERDAL, B., BLUST, R., BRIX, O., COLOSIMO, A., DE WACHTER, B., GIULIANI, A., JOHANSEN, T., FISCHER, T., KNUST, R., LANNIG, G., NAEVDAL, G., NEDENES, A., NYHAMMER, G., SARTORIS, F. J., SERENDERO, I., SIRABELLA, P., THORKILDSEN, S. & ZAKHARTSEV, M. 2001. Climate induced temperature effects on growth performance, fecundity and recruitment in marine fish: Developing a hypothesis for cause and effect relationships in Atlantic cod (*Gadus morhua*) and Common Eelpout (*Zoarces viviparus*). *Continental Shelf Research* 21:1975–1997.
- PÖRTNER, H. O., BOCK, C. & MARK, F. C. 2017. Oxygen- and capacity-limited thermal tolerance: bridging ecology and physiology. *The Journal of Experimental Biology* 220:2685–2696.
- PÖRTNER, H. O. & KNUST, R. 2007. Climate change affects marine fishes through the oxygen limitation of thermal tolerance. *Science* 315:95–97.
- POTTS, W. M., BOOTH, A. J., RICHARDSON, T. J. & SAUER, W. H. H. 2014. Ocean warming affects the distribution and abundance of resident fishes by changing their reproductive scope. *Reviews in Fish Biology and Fisheries* 24:493–504.
- POTTS, W. M., GÖTZ, A. & JAMES, N. 2015. Review of the projected impacts of climate change on coastal fishes in southern Africa. *Reviews in Fish Biology and Fisheries* 25:603–630.
- R CORE TEAM. 2017. R: A language and environment for statistical computing. R Foundation for Statistical Computing, Vienna.
- RAWLINGS, J. O., PANTULA, S. G. & DICKEY, D. A. 1998. *Applied Regression Analysis : A Research Tool* (2nd edition). Springer, New York. 671 pp.
- REDPATH, T. D., COOKE, S. J., SUSKI, C. D., ARLINGHAUS, R., COUTURE, P., WAHL, D. H. & PHILIPP, D. P. 2010. The metabolic and biochemical basis of vulnerability to recreational angling after three generations of angling-induced selection in a teleost fish.

*Canadian Journal of Fisheries and Aquatic Sciences* 67:1983–1992.

- REED, T. E., SCHINDLER, D. E. & WAPLES, R. S. 2011. Interacting effects of phenotypic plasticity and evolution on population persistence in a changing climate. *Conservation Biology* 25:56–63.
- REYNOLDS, R. W., RAYNER, N. A., SMITH, T. M., STOKES, D. M. & WANG, W. 2002. An improved in-situ and satellite SST analysis for climate. *Journal of Climate* 15:1609–1625.
- RIJNSDORP, A. D. 1990. The mechanisms of energy allocation over reproduction and somatic growth in female North Sea plaice, *Pleuronectes platessa* L. *Netherlands Journal of Sea Research* 25:279–289.
- RIJNSDORP, A. D., PECK, M. A., ENGELHARD, G. H., MOLLMANN, C. & PINNEGAR, J. K. 2009. Resolving the effect of climate change on fish populations. *ICES Journal of Marine Science* 66:1570–1583.
- ROBERTS, C. M., O'LEARY, B. C., MCCAULEY, D. J., CURY, P. M., DUARTE, C. M., LUBCHENCO, J., PAULY, D., SÁENZ-ARROYO, A., SUMAILA, U. R., WILSON, R. W., WORM, B. & CASTILLA, J. C. 2017. Marine reserves can mitigate and promote adaptation to climate change. *Proceedings of the National Academy of Sciences* 114:6167–6175.
- ROBERTS, M. J. 2005. Chokka squid (*Loligo vulgaris reynaudii*) abundance linked to changes in South Africa's Agulhas Bank ecosystem during spawning and the early life cycle. *ICES Journal of Marine Science* 62:33–55.
- ROCHE, D. G., BINNING, S. A, BOSIGER, Y., JOHANSEN, J. L. & RUMMER, J. L. 2013. Finding the best estimates of metabolic rates in a coral reef fish. *The Journal of Experimental Biology* 216:2103–2110.
- ROGERS, N. J., URBINA, M. A., REARDON, E. E., MCKENZIE, D. J. & WILSON, R. W. 2016. A new analysis of hypoxia tolerance in fishes using a database of critical oxygen level (P

- crit). *Conservation Physiology* 4:doi: 10.1093/conphys/cow012.
- ROUAULT, M., POHL, B. & PENVEN, P. 2010. Coastal oceanic climate change and variability from 1982 to 2009 around South Africa. *African Journal of Marine Science* 32:237–246.
- ROUNTREY, A. N., COULSON, P. G., MEEUWIG, J. J. & MEEKAN, M. 2014. Water temperature and fish growth: Otoliths predict growth patterns of a marine fish in a changing climate. *Global Change Biology* 20:2450–2458.
- ROY, C., VAN DER LINGEN, C., COETZEE, J. & LUTJEHARMS, J. 2007. Abrupt environmental shift associated with changes in the distribution of Cape anchovy *Engraulis encrasicolus* spawners in the southern Benguela. *African Journal of Marine Science* 29:309–319.
- RUMMER, J. L., COUTURIER, C. S. & STECYK, J. A. W. 2014. Life on the edge : thermal optima for aerobic scope of equatorial reef fishes are close to current day temperatures. *Global Change Biology* 20:1055–1066.
- RUPIA, E. J., BINNING, S. A., ROCHE, D. G., LU, W. & MORAND-FERRON, J. 2016. Fight-flight or freeze-hide? Personality and metabolic phenotype mediate physiological defence responses in flatfish. *Journal of Animal Ecology* 85:927–937.
- RYPEL, A. L. 2009. Climate-growth relationships for largemouth bass (*Micropterus salmoides*) across three southeastern USA states. *Ecology of Freshwater Fish* 18:620–628.
- SANDBLOM, E., CLARK, T. D., GRÄNS, A., EKSTRÖM, A., BRIJS, J., SUNDSTRÖM, L. F., ODELSTRÖM, A., ADILL, A., AHO, T. & JUTFELT, F. 2016. Physiological constraints to climate warming in fish follow principles of plastic floors and concrete ceilings. *Nature Communications* 7:doi: 10.1038/ncomms11447.
- SCHLEGEL, R. W., OLIVER, E. C. J., WERNBERG, T. & SMIT, A. J. 2017. Nearshore and offshore co-occurrences of marine heatwaves and cold-spells. *Progress in Oceanography* 151:189–205.

- SCHLEGEL, R. W. & SMIT, A. J. 2016. Climate change in coastal waters: Time series properties affecting trend estimation. *Journal of Climate* 29:9113–9124.
- SCHNEIDER, C. A., RASBAND, W. S. & ELICEIRI, K. W. 2017. NIH Image to ImageJ : 25 years of Image Analysis. *Nature methods* 9:671–675.
- SCHULTE, P. M. 2015. The effects of temperature on aerobic metabolism: towards a mechanistic understanding of the responses of ectotherms to a changing environment. *Journal of Experimental Biology* 218:1856–1866.
- SCHUMANN, E. H. 1999. Wind-driven mixed layer and coastal upwelling processes off the south coast of South Africa. *Journal of Marine Research* 57:671–691.
- SCHUMANN, E. H., COHEN, A. L. & JURY, M. R. 1995. Coastal sea surface temperature variability along the south coast of South Africa and the relationship to regional and global climate. *Journal of Marine Research* 53:231–248.
- SEEBACHER, F., WHITE, C. R. & FRANKLIN, C. E. 2015. Physiological plasticity increases resilience of ectothermic animals to climate change. *Nature Climate Change* 5:61–66.
- SHEAVES, M. 2006. Is the timing of spawning in sparid fishes a response to sea temperature regimes? *Coral Reefs* 25:655–669.
- SIMS, D. W., MOUTH, V. J. W., GENNER, M. J., SOUTHWARD, A. J. & HAWKINS, S. J. 2004. Low-temperature-driven early spawning migration of a temperate marine fish. *Journal of Animal Ecology* 73:333–341.
- SINCLAIR, B. J., MARSHALL, K. E., SEWELL, M. A., LEVESQUE, D. L., WILLET, C. S., SLOTSBO, S., DONG, Y., HARLEY, C. D. G., MARSHALL, D. J., HELMUTH, B. S. & HUEY, R. B. 2016. Can we predict ectotherm responses to climate change using thermal performance curves and body temperatures? *Ecology Letters* 19:1372–1385.
- SINK, K. 2016. The marine protected areas debate : Implications for the proposed Phakisa marine protected areas network. *South African Journal of Science* 112:doi:

10.17159/sajs.2016/a0179.

- VAN DER SLEEN, P., STRANSKY, C., MORRONGIELLO, J. R., HASLOB, H., PERHARDA, M. & BLACK, B. A. 2018. Otolith increments in European plaice (*Pleuronectes platessa*) reveal temperature and density-dependent effects on growth. *ICES Journal of Marine Science* 75:doi: 10.1093/icesjms/fsy011.
- SMIT, A. J., ROBERTS, M., ANDERSON, R. J., DUFOIS, F., DUDLEY, S. F. J., BORNMAN, T. G., OLBERS, J. & BOLTON, J. J. 2013. A coastal seawater temperature dataset for biogeographical studies: Large biases between in situ and remotely-sensed data sets around the coast of South Africa. *PLoS ONE* 8:doi: 10.1371/journal.pone.0081944.
- SNYDER, S., NADLER, L. E., BAYLEY, J. S., SVENDSEN, M. B. S., JOHANSEN, J. L., DOMENICI, P. & STEFFENSEN, J. F. 2016. Effect of closed v. intermittent-flow respirometry on hypoxia tolerance in the shiner perch *Cymatogaster aggregata*. *Journal of Fish Biology* 88:252–264.
- SOGARD, S. M. & OLLA, B. L. 2000. Endurance of simulated winter conditions by age-0 walleye pollock : effects of body size , water temperature and energy stores. *Journal of Fish Biology* 56:1–21.
- SOMERO, G. N. 2010. The physiology of climate change: how potentials for acclimatization and genetic adaptation will determine ‘ winners ’ and ‘ losers ’. *Journal of Experimental Biology* 213:912–920.
- SOUSA, L. L., QUEIROZ, N., MUCIENTES, G., HUMPHRIES, N. E. & SIMS, D. W. 2016. Environmental influence on the seasonal movements of satellite-tracked ocean sunfish *Mola mola* in the north-east Atlantic Environmental influence on the seasonal movements of satellite-tracked ocean sunfish *Mola mola* in the north-east Atlantic. *Animal Biotelemetry* 4:doi: 10.1186/s40317-016-0099-2.
- STEIN, B., EDELSON, P. & STAUDT, A. (Eds.). 2014. *Climate-Smart Conservation: Putting*

- Adaptation Principles into Practice*. National Wildlife Federation, Washington, D.C. 264 pp.
- STENSETH, N. C., MYSTERUD, A., OTTERSEN, G., HURRELL, J. W., CHAN, K.-S. & LIMA, M. 2002. Ecological effects of climate fluctuations. *Science* 297:1292–1297.
- STOESSEL, D. J., MORRONGIELLO, J. R., RAADIK, T. A., LYON, J. & FAIRBROTHER, P. 2018. Is climate change driving recruitment failure in Australian bass *Macquaria novemaculeata* in southern latitudes of the species range? *Marine and Freshwater Research* 69:24–36.
- STRAMMA, L., PRINCE, E. D., SCHMIDTKO, S., LUO, J., HOOLIHAN, J. P., VISBECK, M., WALLACE, D. W. R., BRANDT, P. & KÖRTZINGER, A. 2012. Expansion of oxygen minimum zones may reduce available habitat for tropical pelagic fishes. *Nature Climate Change* 2:33–37.
- STRAMMA, L., SCHMIDTKO, S., LEVIN, L. A. & JOHNSON, G. C. 2010. Ocean oxygen minima expansions and their biological impacts. *Deep-Sea Research I* 57:587–595.
- SUMAILA, U. R., CHEUNG, W. W. L., LAM, V. W. Y., PAULY, D. & HERRICK, S. 2011. Climate change impacts on the biophysics and economics of world fisheries. *Nature Climate Change* 1:449–456.
- SUNDAY, J. M., BATES, A. E. & DULVY, N. K. 2012. Thermal tolerance and the global redistribution of animals. *Nature Climate Change* 2:686–690.
- SUNDAY, J. M., PECL, G. T., FRUSHER, S., HOBDAV, A. J., HILL, N., HOLBROOK, N. J., EDGAR, G. J., STUART-SMITH, R., WERNBERG, T., WATSON, R. A., SMALE, D. A., SLAWINSKI, D. & FENG, M. 2015. Species traits and climate velocity explain geographic range shifts in an ocean-warming hotspot. *Ecology Letters* 18:944–953.
- SVENDSEN, M. B. S., BUSHNELL, P. G. & STEFFENSEN, J. F. 2016. Design and setup of intermittent-flow respirometry system for aquatic organisms. *Journal of Fish Biology*

88:26–50.

- SYDEMAN, W. J., GARCÍA-REYES, M., SCHOEMAN, D. S., RYKACZEWSKI, R. R., THOMPSON, S. A., BLACK, B. A. & BOGRAD, S. J. 2014. Climate change and wind intensification in coastal upwelling ecosystems. *Science* 345:77–80.
- SZEKERES, P., BROWNSCOMBE, J. W., CULL, F., DANYLCHUK, A. J., SHULTZ, A. D., SUSKI, C. D., MURCHIE, K. J. & COOKE, S. J. 2014. Physiological and behavioural consequences of cold shock on bonefish (*Albula vulpes*) in The Bahamas. *Journal of Experimental Marine Biology and Ecology* 459:1–7.
- SZEKERES, P., ELIASON, E. J., LAPOINTE, D., DONALDSON, M. R., BROWNSCOMBE, J. W. & COOKE, S. J. 2016. On the neglected cold side of climate change and what it means to fish. *Climate Research* 69:239–245.
- TAO, J., CHEN, Y., HE, D. & DING, C. 2015. Relationships between climate and growth of *Gymnocypris selincuoensis* in the Tibetan Plateau. *Ecology and Evolution* 5:1693–1701.
- TAPIA, F. J., NAVARRETE, S. A., CASTILLO, M., MENGE, B. A., CASTILLA, J. C., LARGIER, J., WIETERS, E. A., BROITMAN, B. L. & BARTH, J. A. 2009. Thermal indices of upwelling effects on inner-shelf habitats. *Progress in Oceanography* 83:278–287.
- TEAL, L. R., MARRAS, S., PECK, M. A. & DOMENICI, P. 2015. Physiology-based modelling approaches to characterize fish habitat suitability: Their usefulness and limitations. *Estuarine, Coastal and Shelf Science* 201:56–63.
- TESKE, P. R., FORGET, F. R. G., COWLEY, P. D., VON DER HEYDEN, S. & BEHEREGARAY, L. B. 2010. Connectivity between marine reserves and exploited areas in the philopatric reef fish *Chrysoblephus laticeps* (Teleostei: Sparidae). *Marine Biology* 157:2029–2042.
- THE GOVERNMENT OF THE REPUBLIC OF SOUTH AFRICA. 2012. National climate change response white paper. South Africa. 48 pp.

- THORNTON, P. K., ERICKSEN, P. J., HERRERO, M. & CHALLINOR, A. J. 2014. Climate variability and vulnerability to climate change: a review. *Global Change Biology* 20:3313–3328.
- THRESHER, R. E., KOSLOW, J. A, MORISON, A K. & SMITH, D. C. 2007. Depth-mediated reversal of the effects of climate change on long-term growth rates of exploited marine fish. *Proceedings of the National Academy of Sciences* 104:7461–7465.
- TILNEY, R. L. & BUXTON, C. D. 1994. A preliminary ichthyoplankton survey of the Tsitsikamma National Park. *South African Journal of Zoology* 29:204–211.
- TILNEY, R. L., NELSON, G., RADLOFF, S. E. & BUXTON, C. D. 1996. Ichthyoplankton distribution and dispersal in the Tsitsikamma National Park marine reserve, South Africa. *South African Journal of Marine Science* 17:1–14.
- TODGHAM, A. E. & STILLMAN, J. H. 2013. Physiological responses to shifts in multiple environmental stressors: Relevance in a changing world. *Integrative and Comparative Biology* 53:539–544.
- TOWNHILL, B. L., MOLEN, J. VAN DER, METCALFE, J. D., SIMPSON, S. D., FARCAS, A. & PINNEGAR, J. K. 2017. Consequences of climate-induced low oxygen conditions for commercially important fish. *Marine Ecology Progress Series* 580:191–204.
- TRAPLETTI, A. & HORNIK, K. 2017. tseries: Time Series Analysis and Computational Finance. *R package*.
- VAQUER-SUNYER, R. & DUARTE, C. M. 2008. Thresholds of hypoxia for marine biodiversity. *Proceedings of the National Academy of Sciences* 105:15452–15457.
- VASSEUR, D. A., DELONG, J. P., GILBERT, B., GREIG, H. S., HARLEY, C. D. G., MCCANN, K. S., SAVAGE, V., TUNNEY, T. D., CONNOR, M. I. O., VASSEUR, D. A., DELONG, J. P., GILBERT, B., GREIG, H. S., HARLEY, C. D. G., MCCANN, K. S., SAVAGE, V., TUNNEY, T. D. & CONNOR, M. I. O. 2018. Increased temperature variation poses a

- greater risk to species than climate warming. *Proceedings of the Royal Society B* 281:doi:10.1098/rspb.2013.2612.
- WALKER, S. P. W. & MCCORMICK, M. I. 2004. Otolith-check formation and accelerated growth associated with sex change in an annual protogynous tropical fish. *Marine Ecology Progress Series* 266:201–212.
- WALTHER, G., POST, E., CONVEY, P., MENZEL, A., PARMESAN, C., BEEBEE, T. J. C., FROMENTIN, J., I, O. H. & BAIRLEIN, F. 2002. Ecological responses to recent climate change. *Nature* 416:389–395.
- WANG, G., CAI, W., GAN, B., WU, L., SANTOSO, A., LIN, X., CHEN, Z. & MCPHADEN, M. J. 2017. Continued increase of extreme El Niño frequency long after 1.5 °C warming stabilization. *Nature Climate Change* 7:568–573.
- WANG, Q., TAN, X., JIAO, S., YOU, F. & ZHANG, P. J. 2014. Analyzing cold tolerance mechanism in transgenic zebrafish (*Danio rerio*). *PLoS ONE* 9:doi:10.1371/journal.pone.0102492.
- WARD, T. D., ALGERA, D. A., GALLAGHER, A. J., HAWKINS, E., HORODYSKY, A., JØRGENSEN, C., KILLEN, S. S., MCKENZIE, D. J., METCALFE, J. D., PECK, M. A., VU, M. & COOKE, S. J. 2016. Understanding the individual to implement the ecosystem approach to fisheries management. *Conservation Physiology* 4:doi:10.1093/conphys/cow005.
- WARE, D. M. & THOMSON, R. E. 1991. Link between long-term variability in upwelling and fish production in the northeast pacific ocean. *Canadian Journal of Fisheries and Aquatic Sciences* 48:2296–2306.
- WEISBERG, S., SPANGLER, G. & RICHMOND, L. S. 2010. Mixed effects models for fish growth. *Canadian Journal of Fisheries and Aquatic Sciences* 67:269–277.
- WELLING, S. H., REFSGAARD, H. H. F., BROCKHOFF, P. B. & LINE, H. 2016. Forest Floor

visualizations of random forests. *arXiv:1605.09196*.

WERNBERG, T., RUSSELL, B. D., MOORE, P. J., LING, S. D., SMALE, D. A., CAMPBELL, A., COLEMAN, M. A., STEINBERG, P. D., KENDRICK, G. A. & CONNELL, S. D. 2011. Impacts of climate change in a global hotspot for temperate marine biodiversity and ocean warming. *Journal of Experimental Marine Biology and Ecology* 400:7–16.

WERNBERG, T., SMALE, D. A., TUYA, F., THOMSEN, M. S., LANGLOIS, T. J., DE BETTIGNIES, T., BENNETT, S. & ROUSSEAU, C. S. 2012. An extreme climatic event alters marine ecosystem structure in a global biodiversity hotspot. *Nature Climate Change* 3:78–82.

WEST, G. B., BROWN, J. H. & ENQUIST, B. J. 2001. A general model for ontogenetic growth. *Nature* 413:628–63.

WHITFIELD, A. K., JAMES, N. C., LAMBERTH, S. J., ADAMS, J. B., PERISSINOTTO, R., RAJKARAN, A. & BORNMAN, T. G. 2016. The role of pioneers as indicators of biogeographic range expansion caused by global change in southern African coastal waters. *Estuarine, Coastal and Shelf Science* 172:138–153.

WHITNEY, J. E., AL-CHOKHACHY, R., BUNNELL, D. B., CALDWELL, C. A., COOKE, S. J., ELIASON, E. J., ROGERS, M., LYNCH, A. J. & PAUKERT, C. P. 2016. Physiological basis of climate change impacts on North American inland fishes. *Fisheries* 41:332–345.

WHITTEN, A. R., KLAER, N. L., TUCK, G. N. & DAY, R. W. 2013. Accounting for cohort-specific variable growth in fisheries stock assessments: A case study from south-eastern Australia. *Fisheries Research* 142:27–36.

WIKELSKI, M. & COOKE, S. J. 2006. Conservation physiology. *Trends in Ecology and Evolution* 21:38–46.

WILSON, A. D. M., BROWNSCOMBE, J. W., SULLIVAN, B., JAIN-SCHLAEPFER, S. & COOKE, S. J. 2015. Does angling technique selectively target fishes based on their

- behavioural type? *PLoS ONE* 10:doi: 10.1371/journal.pone.0135848.
- WONG, B. B. M. & CANDOLIN, U. 2015. Behavioral responses to changing environments. *Behavioral Ecology* 26:665–673.
- WOOD, S. N. 2011. Fast stable restricted maximum likelihood and marginal likelihood estimation of semiparametric generalized linear models. *Journal of the Royal Statistical Society* 73:3–36.
- WWF-SA. 2014. State of management of South Africa's Marine Protected Areas. Cape Town. 160 pp.
- VAN WYK, J. A. 2015. Defining the blue economy as a South African strategic priority: toward a sustainable 10th province? *Journal of the Indian Ocean Region* 11:153–169.
- YOOL, A., POPOVA, E. E. & ANDERSON, T. R. 2013. M EDUSA-2.0: an intermediate complexity biogeochemical model of the marine carbon cycle for climate change and ocean acidification studies. *Geoscientific Model Development* 6:1767–1811.
- YOOL, A., POPOVA, E. E. & COWARD, A. C. 2015. Future change in ocean productivity: Is the Arctic the new Atlantic. *Journal of Geophysical Research Oceans* 120:7771–7790.
- ZIMMERMANN, N. E., JR, T. C. E., GRAHAM, C. H., PEARMAN, P. B. & SVENNING, J. 2010. New trends in species distribution modelling. *Ecography* 33:985–989.
- ZUUR, A. F., IENO, E. N., WALKER, N. J., SAVELIEV, A. A., SMITH, G. M., WALKER, Z. I. & SMITH, S. 2009. Mixed Effects Models and Extensions in Ecology with R. *Ecology* 32:580. Springer-Verlag, New York.